Title	Spin-Wave Theory of Thermal Excitations and Inelastic Scattering in Heisenberg Magnets : New Developments in Compactification and Renormalization
Author(s)	乗木, 優作
Citation	北海道大学. 博士(理学) 甲第13128号
Issue Date	2018-03-22
DOI	10.14943/doctoral.k13128
Doc URL	http://hdl.handle.net/2115/73151
Type	theses (doctoral)
File Information	Yusaku_Noriki.pdf

Spin-Wave Theory of Thermal Excitations and Inelastic Scattering in Heisenberg Magnets: New Developments in Compactification and Renormalization

（Heisenberg 磁性体における熱励起と非弾性散乱のスピン波理論:
コンパクト化と繰り込みの新しい展開）

乗木 優作

北海道大学大学院理学院
物性物理学専攻

2018 年 3 月

Abstract

We propose a new scheme for modifying conventional spin waves so as to precisely describe low-dimensional Heisenberg magnets at finite temperatures. What is called the modified spin-wave theory was initiated by Takahashi, who intended to describe the low-dimensional ferromagnetic thermodynamics. There are various ways for modifying spin waves, especially, in ferrimagnets. Which magnetization should be kept zero, uniform, staggered, or both? One or more chemical potentials can be introduced so as to satisfy the relevant constraint condition either in diagonalizing the Hamiltonian or in minimizing the free energy. We can bring the thus-modified spin waves into interaction on the basis of the Hartree-Fock approximation or through the use of Wick's theorem in an attempt to refine their descriptions. Comparing various modification schemes, we eventually find an excellent bosonic language capable of describing heterogeneous quantum magnets on a variety of lattices over the whole temperature range—*Wick's-theorem-based interacting spin waves modified so as to keep every sublattice magnetization zero via the temperature-dependent Bogoliubov transformation.*

Contents

Chapter 1

Introduction

The concept of spin waves (SWs) initiated by Bloch[1] developed into what we call the SW theory.[2–4] The theory was applied not only to ferromagnets but also to ferrimagnets[5] and antiferromagnets[6,7] in order to describe ground-state properties and thermodynamic quantities. Bloch's $T^{\frac{3}{2}}$ law,[1,8] in three-dimensional ferromagnets, demonstrated by bulk magnetization measurements on iron-based alloys.[9] The nuclear spin-lattice relaxation time T_1 was systematically formulated in terms of SWs[10–13] and a complicated three-magnon relaxation mechanism[14,15] was experimentally visualized.[16]

However, all these achievements are fundamentally limited to sufficiently low temperatures. Even in three dimensions, the conventional SW (CSW) theory suffers from divergent magnetizations with increasing temperature (Fig. 1.1). In order to overcome this "thermal divergence", a magnon chemical potential was introduced[17] for ferromagnets and antiferromagnets. In ferrimagnets, similar Lagrange multipliers were introduced.[18,19] Indeed these developments were pioneering, but modifying CSW will be more effective in less than three dimensions.

What we call the modified SW (MSW) theory was initiated by Takahashi.[20,21] In one and two dimensions, magnetizations and susceptibilities diverge even at absolute zero within the CSW theory. When constrained to keep the uniform magnetization zero, SWs become capable of precisely describing the ferromagnetic thermodynamics[20–23] at sufficiently low temperatures. Especially, in one-dimensional ferromagnets, the MSW

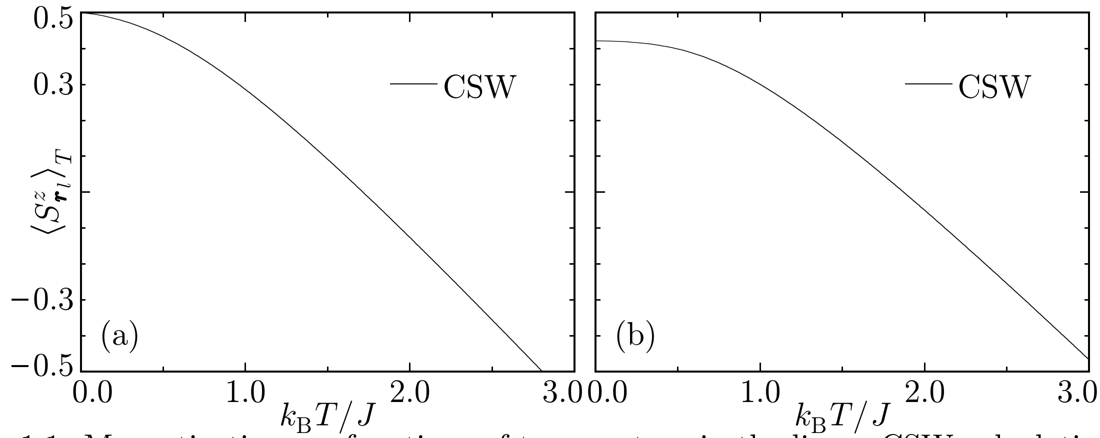

Fig. 1.1: Magnetizations as functions of temperature in the linear CSW calculation for ferromagnets (a) and antiferromagnets (b) on the simple-cubic lattice with $S = 1/2$.

theory reproduces results of Bethe-ansatz integral equations:[20, 21]

$$\frac{\chi J}{L\mu_{\rm B}^2}=0.1667\left(\frac{J}{k_{\rm B}T}\right)^2+0.5826\left(\frac{J}{k_{\rm B}T}\right)^{\frac{3}{2}}+0.6789\frac{J}{k_{\rm B}T}+O(T^{-\frac{1}{2}})\quad(\mathrm{MSW}),\quad(1.1)$$
$$\frac{\chi J}{L\mu_{\rm B}^2}=0.1667\left(\frac{J}{k_{\rm B}T}\right)^2+0.581\ \left(\frac{J}{k_{\rm B}T}\right)^{\frac{3}{2}}+0.68\ \ \frac{J}{k_{\rm B}T}+O(T^{-\frac{1}{2}})\quad(\text{Bethe-ansatz}).$$

The MSW theory further applied to antiferromagnets especially on the square lattice. Hirsch and coworkers first diagonalized a Hamiltonian, keeping the staggered magnetization zero, within the linear SW (LSW) formulation[24] and then refined such modified LSWs (MLSWs) into interacting SWs (ISWs) based on the Hartree–Fock (HF) approximation.[25] The thus modified-HF-ISW (MHFISW) theory makes the Bogoliubov transformation dependent on temperature and may therefore be referred to as a temperature-dependent-diagonalization (TDD)-MSW theory. This TDD-MHFISW theory[26, 27] reproduces quantum Monte Carlo (QMC) calculations[28] at sufficiently low temperatures [Fig. 1.2(b)], but this description deteriorates with increasing temperature [Fig. 1.2(a)] and ends in an artificial first-order phase transition.[25, 26] In order to overcome this thermal breakdown, Ohara and Yosida first minimized a free energy, keeping the sublattice magnetizations zero, within the LSW formulation[29] and then refined such MLSWs into ISWs based on HF approximation.[30] The thus MHFISW theory makes the Bogoliubov transformation independent on temperature and may therefore be referred to as a temperature-independent-diagonalization (TID)-MSW theory. This TID-MHFISW theory[30] overcomes thermal breakdown [Fig. 1.2(a)], but this description deteriorates at low temperature [Fig. 1.2(b)]. Frustrated square-lattice antiferromagnets were also investigated by means of MSWs.[31–39] There have been further attempts[40–44] at describing spin-gapped antiferromagnets in terms of MSWs.

In ferrimagnets, there are various constraint conditions. A uniform-magnetization constraint succeeds in precisely reproducing the specific heat and uniform susceptibility at sufficiently low temperatures[45] but completely fails to design a Schottky-like peak of the specific heat and a ferrimagnetic minimum of the susceptibility-temperature product.[46] A staggered-magnetization constraint combined with a perturbative treatment of SW interactions better reproduces not only the static properties[47, 48] but also the dynamic properties.[49, 50] There are further challenges in interpreting nuclear magnetic

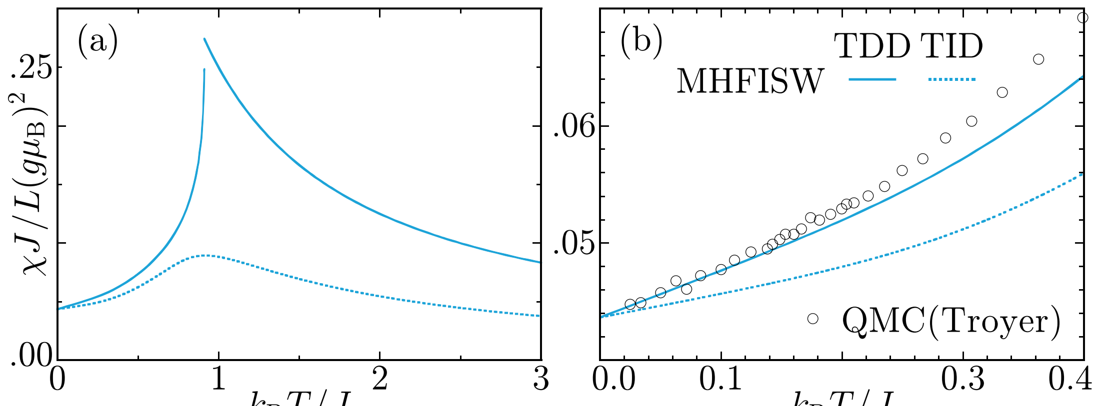

Fig. 1.2: Uniform susceptibility as functions of temperature in the MHFISW theory[26, 30] on the square lattice with $S = 1/2$, in comparison with QMC calculations.[28]

relaxation measurements on cluster[51] and chain[52,53] ferrimagnets in terms of such designed MSWs. A ferrimagnetic TID-MSW theory conditioned to keep the staggered magnetization zero was compared with its TDD version and an Schwinger-boson (SB) analog[54] in an attempt to demonstrate its superiority. However, singly constrained MSWs,[45–48] whether TDD or TID, misread the high-temperature properties.

In order to avoid thermal breakdown, we propose ISWs based on Wick decomposition (WD). The thus modified-WD-ISW (MWDISW) theory overcomes thermal breakdown and precisely describes thermodynamic properties at low temperature. When we constrain SWs to keep every magnetization zero, SWs describe thermodynamic properties over the whole temperature range. The MWDISW theory neglect the residual normal-ordered interaction. By taking into account the residual normal-ordered interaction, the theory also describes dynamic properties over the whole energy region.

Chapter 2

Diagonalization

2.1 Bosonic Hamiltonian

We consider Heisenberg magnets on a bipartite lattice whose sublattices have same geometry. N equivalent spins of magnitude S reside in sublattice A, while N equivalent spins of magnitude s reside in sublattice B. The generic Hamiltonian may be written as

$$\mathcal{H} = J \sum_{\langle mn \rangle} \boldsymbol{S}_{\boldsymbol{r}_m} \cdot \boldsymbol{s}_{\boldsymbol{r}_n} \qquad (J > 0), \tag{2.1}$$

where $\langle mn \rangle$ runs over nearest neighbors. We treat S and s as quantities of the same order and assume that $S \geq s$ without loss of generality. We denote the unique lattice spacing, the unique coordinate number of the lattice, and the number of sites in the lattice by a, z, and $L \equiv 2N$, respectively.

We introduce boson operators through the Holstein–Primakoff (HP) transformation[55]

$$\begin{cases} S_{\boldsymbol{r}_m}^{+} = \sqrt{2S}\mathcal{A}_{\boldsymbol{r}_m}(S) a_{\boldsymbol{r}_m}, \\ S_{\boldsymbol{r}_m}^{-} = \sqrt{2S} a_{\boldsymbol{r}_m}^{\dagger} \mathcal{A}_{\boldsymbol{r}_m}(S), \\ S_{\boldsymbol{r}_m}^{z} = S - a_{\boldsymbol{r}_m}^{\dagger} a_{\boldsymbol{r}_m}, \end{cases} \qquad \begin{cases} s_{\boldsymbol{r}_n}^{+} = \sqrt{2s} b_{\boldsymbol{r}_n}^{\dagger} \mathcal{B}_{\boldsymbol{r}_n}(s), \\ s_{\boldsymbol{r}_n}^{-} = \sqrt{2s} \mathcal{B}_{\boldsymbol{r}_n}(s) b_{\boldsymbol{r}_n}, \\ s_{\boldsymbol{r}_n}^{z} = -s + b_{\boldsymbol{r}_n}^{\dagger} b_{\boldsymbol{r}_n}, \end{cases} \tag{2.2}$$

and regard $\mathcal{A}_{\boldsymbol{r}_m}(S)$ and $\mathcal{B}_{\boldsymbol{r}_n}(s)$ as descending powers of S and s, respectively,

$$\mathcal{A}_{\boldsymbol{r}_m}(S) = \sqrt{1 - \frac{a_{\boldsymbol{r}_m}^{\dagger} a_{\boldsymbol{r}_m}}{2S}} = 1 - \sum_{\alpha=1}^{\infty} \frac{(2\alpha-3)!!}{\alpha!} \left(\frac{a_{\boldsymbol{r}_m}^{\dagger} a_{\boldsymbol{r}_m}}{4S} \right)^{\alpha}, \tag{2.3}$$

$$\mathcal{B}_{\boldsymbol{r}_n}(s) = \sqrt{1 - \frac{b_{\boldsymbol{r}_n}^{\dagger} b_{\boldsymbol{r}_n}}{2s}} = 1 - \sum_{\alpha=1}^{\infty} \frac{(2\alpha-3)!!}{\alpha!} \left(\frac{b_{\boldsymbol{r}_n}^{\dagger} b_{\boldsymbol{r}_n}}{4s} \right)^{\alpha}. \tag{2.4}$$

Via the HP transformation, the Hamiltonian (2.1) is expanded into the series

$$\mathcal{H} = \mathcal{H}^{(2)} + \mathcal{H}^{(1)} + \mathcal{H}^{(0)} + O(S^{-1}), \tag{2.5}$$

where $\mathcal{H}^{(l)}$, on the order of S^l, reads

$$\mathcal{H}^{(2)} = -NzJSs, \tag{2.6}$$

$$\mathcal{H}^{(1)} = J\sqrt{Ss} \sum_{\langle mn \rangle} \left(\sqrt{\frac{s}{S}} a_{\boldsymbol{r}_m}^{\dagger} a_{\boldsymbol{r}_m} + \sqrt{\frac{S}{s}} b_{\boldsymbol{r}_n}^{\dagger} b_{\boldsymbol{r}_n} + a_{\boldsymbol{r}_m}^{\dagger} b_{\boldsymbol{r}_n}^{\dagger} + a_{\boldsymbol{r}_m} b_{\boldsymbol{r}_n} \right), \tag{2.7}$$

$$\mathcal{H}^{(0)} = -\frac{J}{4}\sum_{\langle mn\rangle}\left[a^{\dagger}_{\boldsymbol{r}_m}\left(\sqrt[4]{\frac{s}{S}}a_{\boldsymbol{r}_m} + \sqrt[4]{\frac{S}{s}}b^{\dagger}_{\boldsymbol{r}_n}\right)^2 b_{\boldsymbol{r}_n}\right.$$
$$\left. + b^{\dagger}_{\boldsymbol{r}_n}\left(\sqrt[4]{\frac{s}{S}}a^{\dagger}_{\boldsymbol{r}_m} + \sqrt[4]{\frac{S}{s}}b_{\boldsymbol{r}_n}\right)^2 a_{\boldsymbol{r}_m}\right]. \tag{2.8}$$

In the HF approximation, the $O(S^0)$ quartic Hamiltonian (2.8) is approximated by quadratic terms,

$$\begin{aligned}\mathcal{H}^{(0)} \approx & NzJ(\sqrt{Ss} - \langle\mathcal{S}\rangle_T - \langle\mathcal{S}'\rangle_T)(\sqrt{Ss} - \langle\mathcal{S}\rangle_T + \langle\mathcal{S}'\rangle_T) \\ & + J\sum_{\langle mn\rangle}\Bigg[\left(\langle\mathcal{S}\rangle_T - \sqrt{Ss}\right)\left(a^{\dagger}_{\boldsymbol{r}_m}b^{\dagger}_{\boldsymbol{r}_n} + a_{\boldsymbol{r}_m}b_{\boldsymbol{r}_n}\right) + (\langle\mathcal{S}\rangle_T - \langle\mathcal{S}'\rangle_T - \sqrt{Ss})\sqrt{\frac{s}{S}}a^{\dagger}_{\boldsymbol{r}_m}a_{\boldsymbol{r}_m} \\ & + (\langle\mathcal{S}\rangle_T + \langle\mathcal{S}'\rangle_T - \sqrt{Ss})\sqrt{\frac{S}{s}}b^{\dagger}_{\boldsymbol{r}_n}b_{\boldsymbol{r}_n}\Bigg],\end{aligned} \tag{2.9}$$

where we introduce bosonic operators

$$\mathcal{S} \equiv \frac{s(S - a^{\dagger}_{\boldsymbol{r}_m}a_{\boldsymbol{r}_m}) + S(s - b^{\dagger}_{\boldsymbol{r}_m+\boldsymbol{\delta}_l}b_{\boldsymbol{r}_m+\boldsymbol{\delta}_l})}{2\sqrt{Ss}} - \frac{a^{\dagger}_{\boldsymbol{r}_m}b^{\dagger}_{\boldsymbol{r}_m+\boldsymbol{\delta}_l} + a_{\boldsymbol{r}_m}b_{\boldsymbol{r}_m+\boldsymbol{\delta}_l}}{2}, \tag{2.10}$$

$$\mathcal{S}' \equiv \frac{s(S - a^{\dagger}_{\boldsymbol{r}_m}a_{\boldsymbol{r}_m}) - S(s - b^{\dagger}_{\boldsymbol{r}_m+\boldsymbol{\delta}_l}b_{\boldsymbol{r}_m+\boldsymbol{\delta}_l})}{2\sqrt{Ss}}, \tag{2.11}$$

and denote a thermal average at temperature T by $\langle\cdots\rangle_T$. In the Wick theorem, the $O(S^0)$ quartic Hamiltonian (2.8) is decomposed into quadratic terms,

$$\begin{aligned}\mathcal{H}^{(0)} = & :\mathcal{H}^{(0)}: \\ & + NzJ(\sqrt{Ss} - \langle\mathcal{S}\rangle_0 - \langle\mathcal{S}'\rangle_0)(\sqrt{Ss} - \langle\mathcal{S}\rangle_0 + \langle\mathcal{S}'\rangle_0) \\ & + J\sum_{\langle mn\rangle}\Bigg[\left(\langle\mathcal{S}\rangle_0 - \sqrt{Ss}\right)\left(a^{\dagger}_{\boldsymbol{r}_m}b^{\dagger}_{\boldsymbol{r}_n} + a_{\boldsymbol{r}_m}b_{\boldsymbol{r}_n}\right) + (\langle\mathcal{S}\rangle_0 - \langle\mathcal{S}'\rangle_0 - \sqrt{Ss})\sqrt{\frac{s}{S}}a^{\dagger}_{\boldsymbol{r}_m}a_{\boldsymbol{r}_m} \\ & + (\langle\mathcal{S}\rangle_0 + \langle\mathcal{S}'\rangle_0 - \sqrt{Ss})\sqrt{\frac{S}{s}}b^{\dagger}_{\boldsymbol{r}_n}b_{\boldsymbol{r}_n}\Bigg],\end{aligned} \tag{2.12}$$

where we denote a quantum average in the magnon vacuum by $\langle\cdots\rangle_0$. If we neglect the residual normal-ordered interaction $:\mathcal{H}^{(0)}:$, the Hamiltonian (2.8) is approximated by [Eq. (2.9)] or decomposed into [Eq. (2.12)] the $O(S^0)$ bilinear Hamiltonian,

$$\begin{aligned}\mathcal{H}^{(0)}_{\mathrm{BL}} \equiv & NzJ(\sqrt{Ss} - \langle\!\langle\mathcal{S}\rangle\!\rangle - \langle\!\langle\mathcal{S}'\rangle\!\rangle)(\sqrt{Ss} - \langle\!\langle\mathcal{S}\rangle\!\rangle + \langle\!\langle\mathcal{S}'\rangle\!\rangle) \\ & + J\sum_{\langle mn\rangle}\Bigg[\left(\langle\!\langle\mathcal{S}\rangle\!\rangle - \sqrt{Ss}\right)\left(a^{\dagger}_{\boldsymbol{r}_m}b^{\dagger}_{\boldsymbol{r}_n} + a_{\boldsymbol{r}_m}b_{\boldsymbol{r}_n}\right) + (\langle\!\langle\mathcal{S}\rangle\!\rangle - \langle\!\langle\mathcal{S}'\rangle\!\rangle - \sqrt{Ss})\sqrt{\frac{s}{S}}a^{\dagger}_{\boldsymbol{r}_m}a_{\boldsymbol{r}_m} \\ & + (\langle\!\langle\mathcal{S}\rangle\!\rangle + \langle\!\langle\mathcal{S}'\rangle\!\rangle - \sqrt{Ss})\sqrt{\frac{S}{s}}b^{\dagger}_{\boldsymbol{r}_n}b_{\boldsymbol{r}_n}\Bigg],\end{aligned} \tag{2.13}$$

where we denote their certain expectation values by $\langle\!\langle\cdots\rangle\!\rangle$. If we read $\langle\!\langle\cdots\rangle\!\rangle$ as a quantum average in the HP-boson vacuum, denoted by $\langle\cdots\rangle_0'$, the $O(S^0)$ bilinear Hamiltonian $\mathcal{H}_{\mathrm{BL}}^{(0)}$ becomes zero. Depending on the approximation scheme adopted, we read $\langle\!\langle\cdots\rangle\!\rangle$ as a thermal average $\langle\cdots\rangle_T$ within the HF-ISW, a quantum average in the magnon vacuum $\langle\cdots\rangle_0$ within the WD-ISW, or a quantum average in the HP-boson vacuum $\langle\cdots\rangle_0'$ within the LSW.

The bosonic Hamiltonian (2.5) is approximated by or decomposed into the quadratic Hamiltonian

$$\begin{aligned}\mathcal{H}_{\mathrm{BL}} &\equiv \mathcal{H}^{(2)} + \mathcal{H}^{(1)} + \mathcal{H}_{\mathrm{BL}}^{(0)} \\ &= \mathcal{H}^{(2)} + NzJ(\sqrt{Ss} - \langle\!\langle\mathcal{S}\rangle\!\rangle - \langle\!\langle\mathcal{S}'\rangle\!\rangle)(\sqrt{Ss} - \langle\!\langle\mathcal{S}\rangle\!\rangle + \langle\!\langle\mathcal{S}'\rangle\!\rangle) \\ &\quad + J\langle\!\langle\mathcal{S}\rangle\!\rangle \sum_{\langle mn\rangle} \Bigg\{ a_{\boldsymbol{r}_m}^{\dagger} b_{\boldsymbol{r}_n}^{\dagger} + a_{\boldsymbol{r}_m} b_{\boldsymbol{r}_n} + \left[\sqrt{\frac{s}{S}}\left(1 - \frac{\langle\!\langle\mathcal{S}'\rangle\!\rangle}{\langle\!\langle\mathcal{S}\rangle\!\rangle}\right)\right] a_{\boldsymbol{r}_m}^{\dagger} a_{\boldsymbol{r}_m} \\ &\qquad + \left[\sqrt{\frac{S}{s}}\left(1 + \frac{\langle\!\langle\mathcal{S}'\rangle\!\rangle}{\langle\!\langle\mathcal{S}\rangle\!\rangle}\right)\right] b_{\boldsymbol{r}_n}^{\dagger} b_{\boldsymbol{r}_n} \Bigg\}.\end{aligned} \tag{2.14}$$

2.2 Temperature-Dependent Diagonalization

Our task is to control the number of HP bosons which is equivalent to the sublattice magnetizations

$$\mathcal{M}_{\mathrm{A}}^{z} \equiv \sum_{m=1}^{N} S_{\boldsymbol{r}_m}^{z} = N\left[S - \frac{1}{N}\sum_{m=1}^{N} a_{\boldsymbol{r}_m}^{\dagger} a_{\boldsymbol{r}_m}\right], \tag{2.15}$$

$$\mathcal{M}_{\mathrm{B}}^{z} \equiv \sum_{n=1}^{N} s_{\boldsymbol{r}_n}^{z} = -N\left[s - \frac{1}{N}\sum_{n=1}^{N} b_{\boldsymbol{r}_n}^{\dagger} b_{\boldsymbol{r}_n}\right]. \tag{2.16}$$

2.2.1 Effective Hamiltonian

In order to control the sublattice magnetizations, we introduce an effective Hamiltonian

$$\begin{aligned}\widetilde{\mathcal{H}}_{\mathrm{BL}} &\equiv \mathcal{H}_{\mathrm{BL}} + \mu_{\mathrm{A}}\mathcal{M}_{\mathrm{A}}^{z} + \mu_{\mathrm{B}}\mathcal{M}_{\mathrm{B}}^{z} \\ &= \mathcal{H}^{(2)} + NzJ(\sqrt{Ss} - \langle\!\langle\mathcal{S}\rangle\!\rangle - \langle\!\langle\mathcal{S}'\rangle\!\rangle)(\sqrt{Ss} - \langle\!\langle\mathcal{S}\rangle\!\rangle + \langle\!\langle\mathcal{S}'\rangle\!\rangle) + N(\mu_{\mathrm{A}}S - \mu_{\mathrm{B}}s) \\ &\quad + J\langle\!\langle\mathcal{S}\rangle\!\rangle \sum_{\langle mn\rangle} \Bigg\{ a_{\boldsymbol{r}_m}^{\dagger} b_{\boldsymbol{r}_n}^{\dagger} + a_{\boldsymbol{r}_m} b_{\boldsymbol{r}_n} + \left[\sqrt{\frac{s}{S}}\left(1 - \frac{\langle\!\langle\mathcal{S}'\rangle\!\rangle}{\langle\!\langle\mathcal{S}\rangle\!\rangle}\right) - \frac{\mu_{\mathrm{A}}}{zJ\langle\!\langle\mathcal{S}\rangle\!\rangle}\right] a_{\boldsymbol{r}_m}^{\dagger} a_{\boldsymbol{r}_m} \\ &\qquad + \left[\sqrt{\frac{S}{s}}\left(1 + \frac{\langle\!\langle\mathcal{S}'\rangle\!\rangle}{\langle\!\langle\mathcal{S}\rangle\!\rangle}\right) + \frac{\mu_{\mathrm{B}}}{zJ\langle\!\langle\mathcal{S}\rangle\!\rangle}\right] b_{\boldsymbol{r}_n}^{\dagger} b_{\boldsymbol{r}_n} \Bigg\},\end{aligned} \tag{2.17}$$

where μ_{A} and μ_{B} are Lagrange multipliers. We employ

$$\tilde{p} \equiv p + p'\frac{\langle\!\langle\mathcal{S}'\rangle\!\rangle}{\langle\!\langle\mathcal{S}\rangle\!\rangle} - \frac{\mu_{\mathrm{A}} - \mu_{\mathrm{B}}}{2zJ\langle\!\langle\mathcal{S}\rangle\!\rangle}, \quad \tilde{p}' \equiv p' + p\frac{\langle\!\langle\mathcal{S}'\rangle\!\rangle}{\langle\!\langle\mathcal{S}\rangle\!\rangle} + \frac{\mu_{\mathrm{A}} + \mu_{\mathrm{B}}}{2zJ\langle\!\langle\mathcal{S}\rangle\!\rangle}, \quad \tilde{q} \equiv \sqrt{\tilde{p}^2 - 1}, \tag{2.18}$$

instead of the Lagrange multipliers $\mu_{\rm A}$ and $\mu_{\rm B}$ in the calculation, where we introduce

$$p \equiv \frac{S+s}{2\sqrt{Ss}}, \qquad p' \equiv \frac{S-s}{2\sqrt{Ss}}, \qquad q \equiv \sqrt{p^2-1}, \tag{2.19}$$

instead of the spin magnitudes S and s. We also introduce some functions of $\tilde{p}$

$$\omega_{\boldsymbol{\kappa}_\nu}(\tilde{p}) \equiv \sqrt{\tilde{p}^2 - |\gamma_{\boldsymbol{\kappa}_\nu}|^2}, \qquad \gamma_{\boldsymbol{\kappa}_\nu} \equiv \frac{1}{z}\sum_{l=1}^{z} \mathrm{e}^{\mathrm{i}\boldsymbol{\kappa}_\nu\cdot\boldsymbol{\delta}_l}, \tag{2.20}$$

$$\epsilon(\tilde{p}) \equiv \frac{1}{2}\left[\tilde{p} - \frac{1}{N}\sum_{\nu=1}^{N}\omega_{\boldsymbol{\kappa}_\nu}(\tilde{p})\right], \tag{2.21}$$

$$\tau(\tilde{p}) \equiv \frac{1}{2}\left[\frac{1}{N}\sum_{\nu=1}^{N}\frac{\tilde{p}}{\omega_{\boldsymbol{\kappa}_\nu}(\tilde{p})} - 1\right], \tag{2.22}$$

where $\boldsymbol{\delta}_l$ is a vector connecting nearest neighbors. Via the Fourier transformation

$$\begin{aligned} a_{\boldsymbol{r}_m} &= \frac{1}{\sqrt{N}}\sum_{\nu=1}^{N}\mathrm{e}^{\mathrm{i}\boldsymbol{\kappa}_\nu\cdot\boldsymbol{r}_m}a_{\boldsymbol{\kappa}_\nu}, \quad b_{\boldsymbol{r}_n} = \frac{1}{\sqrt{N}}\sum_{\nu=1}^{N}\mathrm{e}^{-\mathrm{i}\boldsymbol{\kappa}_\nu\cdot\boldsymbol{r}_n}b_{\boldsymbol{\kappa}_\nu}, \\ a_{\boldsymbol{\kappa}_\nu} &= \frac{1}{\sqrt{N}}\sum_{m=1}^{N}\mathrm{e}^{-\mathrm{i}\boldsymbol{\kappa}_\nu\cdot\boldsymbol{r}_m}a_{\boldsymbol{r}_m}, \quad b_{\boldsymbol{\kappa}_\nu} = \frac{1}{\sqrt{N}}\sum_{n=1}^{N}\mathrm{e}^{\mathrm{i}\boldsymbol{\kappa}_\nu\cdot\boldsymbol{r}_n}b_{\boldsymbol{r}_n}, \end{aligned} \tag{2.23}$$

we define SWs as

$$\begin{aligned} \begin{pmatrix} a_{\boldsymbol{\kappa}_\nu} \\ b^\dagger_{\boldsymbol{\kappa}_\nu} \end{pmatrix} &= \begin{pmatrix} \cosh\theta_{\boldsymbol{\kappa}_\nu} & -\mathrm{e}^{-\mathrm{i}\delta_{\boldsymbol{\kappa}_\nu}}\sinh\theta_{\boldsymbol{\kappa}_\nu} \\ -\mathrm{e}^{\mathrm{i}\delta_{\boldsymbol{\kappa}_\nu}}\sinh\theta_{\boldsymbol{\kappa}_\nu} & \cosh\theta_{\boldsymbol{\kappa}_\nu} \end{pmatrix} \begin{pmatrix} \alpha^-_{\boldsymbol{\kappa}_\nu} \\ \alpha^{+\dagger}_{\boldsymbol{\kappa}_\nu} \end{pmatrix}, \\ \begin{pmatrix} \alpha^-_{\boldsymbol{\kappa}_\nu} \\ \alpha^{+\dagger}_{\boldsymbol{\kappa}_\nu} \end{pmatrix} &= \begin{pmatrix} \cosh\theta_{\boldsymbol{\kappa}_\nu} & \mathrm{e}^{-\mathrm{i}\delta_{\boldsymbol{\kappa}_\nu}}\sinh\theta_{\boldsymbol{\kappa}_\nu} \\ \mathrm{e}^{\mathrm{i}\delta_{\boldsymbol{\kappa}_\nu}}\sinh\theta_{\boldsymbol{\kappa}_\nu} & \cosh\theta_{\boldsymbol{\kappa}_\nu} \end{pmatrix} \begin{pmatrix} a_{\boldsymbol{\kappa}_\nu} \\ b^\dagger_{\boldsymbol{\kappa}_\nu} \end{pmatrix}. \end{aligned} \tag{2.24}$$

The Fourier Transformation (2.23) and the Bogoliubov Transformation (2.24) with

$$\cosh 2\theta_{\boldsymbol{\kappa}_\nu} = \frac{\tilde{p}}{\omega_{\boldsymbol{\kappa}_\nu}(\tilde{p})}, \qquad \sinh 2\theta_{\boldsymbol{\kappa}_\nu} = \frac{|\gamma_{\boldsymbol{\kappa}_\nu}|}{\omega_{\boldsymbol{\kappa}_\nu}(\tilde{p})}, \qquad \mathrm{e}^{-\mathrm{i}\delta_{\boldsymbol{\kappa}_\nu}} = \frac{\gamma_{\boldsymbol{\kappa}_\nu}}{|\gamma_{\boldsymbol{\kappa}_\nu}|}, \tag{2.25}$$

diagonalizes the effective bilinear Hamiltonian (2.17) into

$$\begin{aligned} \widetilde{\mathcal{H}}_{\rm BL} = \sum_{l=0}^{2} E^{(l)}(\tilde{p}) + N(\mu_{\rm A}S - \mu_{\rm B}s) \\ + \sum_{\nu=1}^{N}\left[\varepsilon^-_{\boldsymbol{\kappa}_\nu}(\tilde{p},\tilde{p}')\alpha^{-\dagger}_{\boldsymbol{\kappa}_\nu}\alpha^-_{\boldsymbol{\kappa}_\nu} + \varepsilon^+_{\boldsymbol{\kappa}_\nu}(\tilde{p},\tilde{p}')\alpha^{+\dagger}_{\boldsymbol{\kappa}_\nu}\alpha^+_{\boldsymbol{\kappa}_\nu}\right], \end{aligned} \tag{2.26}$$

where $E^{(2)}(\tilde{p})$ is the classical ground-state energy, $E^{(l\leq 1)}(\tilde{p})$ is its $O(S^l)$ quantum correction,

$$E^{(2)}(\tilde{p}) = -NzJSs, \qquad E^{(1)}(\tilde{p}) = -2NzJ\sqrt{Ss}\,\epsilon(\tilde{p}), \tag{2.27}$$

$$E^{(0)}(\tilde{p}) = 2NzJ\left(\sqrt{Ss} - \langle\!\langle\mathcal{S}\rangle\!\rangle\right)\epsilon(\tilde{p}) + NzJ\left(\sqrt{Ss} - \langle\!\langle\mathcal{S}\rangle\!\rangle\right)^2 - NzJ\langle\!\langle\mathcal{S}'\rangle\!\rangle^2, \tag{2.28}$$

and $\varepsilon^{\sigma}_{\boldsymbol{\kappa}_\nu}(\tilde{p},\tilde{p}')$ is the dispersion relations

$$\varepsilon^{\sigma}_{\boldsymbol{\kappa}_\nu}(\tilde{p},\tilde{p}') = zJ\langle\!\langle \mathcal{S} \rangle\!\rangle \left[\omega_{\boldsymbol{\kappa}_\nu}(\tilde{p}) + \sigma\tilde{p}'\right]. \tag{2.29}$$

The branch $\varepsilon^{-}_{\boldsymbol{\kappa}_\nu}(\tilde{p},\tilde{p}')$ is consists of excitations reducing the ground-state magnetization and thus assuming a ferromagnetic aspect, whereas the branch $\varepsilon^{+}_{\boldsymbol{\kappa}_\nu}(\tilde{p},\tilde{p}')$ is consists of excitations enhancing the ground-state magnetization and thus assuming an antiferromagnetic aspect. The lower branch $\varepsilon^{-}_{\boldsymbol{\kappa}_\nu}(\tilde{p},\tilde{p}')$ is gapless at $T=0$, the upper branch $\varepsilon^{+}_{\boldsymbol{\kappa}_\nu}(\tilde{p},\tilde{p}')$ is always gapful in ferrimagnets ($S>s$), and both branches are degenerate in antiferromagnets ($S=s$).

We introduce the thermal average of the number of magnons

$$\bar{n}^{\sigma}_{\boldsymbol{\kappa}_\nu} \equiv \langle \alpha^{\sigma\dagger}_{\boldsymbol{\kappa}_\nu}\alpha^{\sigma}_{\boldsymbol{\kappa}_\nu}\rangle_T\,, \tag{2.30}$$

and some functions of $\bar{n}^{\pm}_{\boldsymbol{\kappa}_\nu}$ and $\tilde{p}$

$$\begin{gathered}
I_1(\bar{n}^{\pm}_{\boldsymbol{\kappa}_\nu};\tilde{p}) = \frac{1}{2N}\sum_{\nu=1}^{N}\sum_{\sigma=\pm}\omega_{\boldsymbol{\kappa}_\nu}(\tilde{p})\bar{n}^{\sigma}_{\boldsymbol{\kappa}_\nu}, \quad I_2(\bar{n}^{\pm}_{\boldsymbol{\kappa}_\nu};\tilde{p}) = \frac{1}{2N}\sum_{\nu=1}^{N}\sum_{\sigma=\pm}\frac{\tilde{p}}{\omega_{\boldsymbol{\kappa}_\nu}(\tilde{p})}\bar{n}^{\sigma}_{\boldsymbol{\kappa}_\nu}, \\
I_3(\bar{n}^{\pm}_{\boldsymbol{\kappa}_\nu}) = \frac{1}{2N}\sum_{\nu=1}^{N}\sum_{\sigma=\pm}\sigma\bar{n}^{-\sigma}_{\boldsymbol{\kappa}_\nu}, \quad I_4(\bar{n}^{\pm}_{\boldsymbol{\kappa}_\nu}) = \frac{1}{2N}\sum_{\nu=1}^{N}\sum_{\sigma=\pm}\bar{n}^{\sigma}_{\boldsymbol{\kappa}_\nu}(\bar{n}^{\sigma}_{\boldsymbol{\kappa}_\nu}+1).
\end{gathered} \tag{2.31}$$

The specific heat is obtained as the temperature derivative of the internal energy, $C=\partial E/\partial T$, where E is identified, unless otherwise noted, with $\sum_{l=1}^{2}\langle\mathcal{H}^{(l)}\rangle_T$ in the LSW theory and with $\sum_{l=0}^{2}\langle\mathcal{H}^{(l)}\rangle_T$ in any ISW theory. The static uniform susceptibility is obtained by averaging magnetization fluctuations, $\chi=(\chi^{xx}+\chi^{yy}+\chi^{zz})/3$, where

$$\chi^{\lambda\lambda} = \frac{(g\mu_{\mathrm{B}})^2}{k_{\mathrm{B}}T}\left[\langle(\mathcal{M}^z_{\mathrm{A}}+\mathcal{M}^z_{\mathrm{B}})^2\rangle_T - \langle\mathcal{M}^z_{\mathrm{A}}+\mathcal{M}^z_{\mathrm{B}}\rangle_T^2\right] \qquad (\lambda=x,y,z). \tag{2.32}$$

We can calculate the uniform magnetization, the staggered magnetization,

$$\langle\mathcal{M}^z_{\mathrm{A}}+\mathcal{M}^z_{\mathrm{B}}\rangle_T = N\left[S-s-2I_3(\bar{n}^{\pm}_{\boldsymbol{\kappa}_\nu})\right], \tag{2.33}$$

$$\langle\mathcal{M}^z_{\mathrm{A}}-\mathcal{M}^z_{\mathrm{B}}\rangle_T = N\left[S+s-2\tau(\tilde{p})-2I_2(\bar{n}^{\pm}_{\boldsymbol{\kappa}_\nu};\tilde{p})\right], \tag{2.34}$$

the $O(S^1)$ internal energy $\sum_{l=1}^{2}\langle\mathcal{H}^{(l)}\rangle_T$, the $O(S^0)$ internal energy $\sum_{l=0}^{2}\langle\mathcal{H}^{(l)}\rangle_T$,

$$\sum_{l=1}^{2}\langle\mathcal{H}^{(l)}\rangle_T = -NzJ\sqrt{Ss}(2\langle\mathcal{S}\rangle_T - \sqrt{Ss}), \tag{2.35}$$

$$\sum_{l=0}^{2}\langle\mathcal{H}^{(l)}\rangle_T = -NzJ\left[\langle\mathcal{S}\rangle_T^2 - \langle\mathcal{S}'\rangle_T^2\right], \tag{2.36}$$

where

$$\begin{aligned}
\langle\mathcal{S}\rangle_T = \sqrt{Ss} + \epsilon(\tilde{p}) &+ (\tilde{p}-p)[\tau(\tilde{p}) + I_2(\bar{n}^{\pm}_{\boldsymbol{\kappa}_\nu};\tilde{p})] \\
&-(\tilde{q}-q)I_3(\bar{n}^{\pm}_{\boldsymbol{\kappa}_\nu}) - [I_1(\bar{n}^{\pm}_{\boldsymbol{\kappa}_\nu};\tilde{p}) - \tilde{q}I_3(\bar{n}^{\pm}_{\boldsymbol{\kappa}_\nu})],
\end{aligned} \tag{2.37}$$

$$\langle\mathcal{S}'\rangle_T = q[\tau(\tilde{p}) + I_2(\bar{n}^{\pm}_{\boldsymbol{\kappa}_\nu};\tilde{p})] - pI_3(\bar{n}^{\pm}_{\boldsymbol{\kappa}_\nu}), \tag{2.38}$$

and the static uniform susceptibilities

$$\frac{\chi^{xx}k_{\rm B}T}{L(g\mu_{\rm B})^2}=\frac{\chi^{yy}k_{\rm B}T}{L(g\mu_{\rm B})^2}$$
$$=\sum_{\sigma=\pm}\left[\frac{\tilde{p}-p}{2\tilde{q}}\frac{\langle\mathcal{M}_{\rm A}^z-\mathcal{M}_{\rm B}^z\rangle_T}{2N}-\frac{\sigma\tilde{q}-q}{2\tilde{q}}\frac{\langle\mathcal{M}_{\rm A}^z+\mathcal{M}_{\rm B}^z\rangle_T}{2N}\right]\left(\bar{n}_{\boldsymbol{0}}^{\sigma}+\frac{1}{2}\right), \tag{2.39}$$

$$\frac{\chi^{zz}k_{\rm B}T}{L(g\mu_{\rm B})^2}=I_4(\bar{n}_{\boldsymbol{\kappa}_\nu}^{\pm}). \tag{2.40}$$

The quantum SWs follow the Bose-Einstein distribution

$$\bar{n}_{\boldsymbol{\kappa}_\nu}^{\sigma}=\left\{\exp\left[\frac{\varepsilon_{\boldsymbol{\kappa}_\nu}^{\sigma}(\tilde{p},\tilde{p}')}{k_{\rm B}T}\right]-1\right\}^{-1}\qquad\text{(TDD MSW)}. \tag{2.41}$$

Let us consider the static structure factor $[S^{xx}(\boldsymbol{q})+S^{yy}(\boldsymbol{q})+S^{zz}(\boldsymbol{q})]/3$, where

$$S^{\lambda\lambda}(\boldsymbol{q})=\frac{1}{L}\sum_{l=1}^{L}\sum_{l'=1}^{L}\mathrm{e}^{\mathrm{i}\boldsymbol{q}\cdot(\boldsymbol{r}_l-\boldsymbol{r}_{l'})}\left\langle\delta S_{\boldsymbol{r}_l}^{\lambda}\delta S_{\boldsymbol{r}_{l'}}^{\lambda}\right\rangle_T, \tag{2.42}$$

with $\delta S_{\boldsymbol{r}_l}^{\lambda}\equiv S_{\boldsymbol{r}_l}^{\lambda}-\langle S_{\boldsymbol{r}_l}^{\lambda}\rangle_T$. After some algebraic manipulations, we obtain

$$S^{zz}(\boldsymbol{q})=\frac{1}{4N}\sum_{\sigma=\pm}\sum_{\nu=1}^{N}[\cosh 2\theta_{\boldsymbol{\kappa}_\nu+\boldsymbol{q}}\cosh 2\theta_{\boldsymbol{\kappa}_\nu}-\cos(\delta_{\boldsymbol{\kappa}_\nu+\boldsymbol{q}}-\delta_{\boldsymbol{\kappa}_\nu})\sinh 2\theta_{\boldsymbol{\kappa}_\nu+\boldsymbol{q}}\sinh 2\theta_{\boldsymbol{\kappa}_\nu}+1]$$
$$\times\bar{n}_{\boldsymbol{\kappa}_\nu}^{\sigma}\left(\bar{n}_{\boldsymbol{\kappa}_\nu+\boldsymbol{q}}^{\sigma}+1\right)$$
$$+\frac{1}{4N}\sum_{\nu=1}^{N}[\cosh 2\theta_{\boldsymbol{\kappa}_\nu+\boldsymbol{q}}\cosh 2\theta_{\boldsymbol{\kappa}_\nu}-\cos(\delta_{\boldsymbol{\kappa}_\nu+\boldsymbol{q}}-\delta_{\boldsymbol{\kappa}_\nu})\sinh 2\theta_{\boldsymbol{\kappa}_\nu+\boldsymbol{q}}\sinh 2\theta_{\boldsymbol{\kappa}_\nu}-1]$$
$$\times\left[\bar{n}_{\boldsymbol{\kappa}_\nu}^{-}\bar{n}_{\boldsymbol{\kappa}_\nu+\boldsymbol{q}}^{+}+\left(\bar{n}_{\boldsymbol{\kappa}_\nu}^{-}+1\right)\left(\bar{n}_{\boldsymbol{\kappa}_\nu+\boldsymbol{q}}^{+}+1\right)\right],$$
$$S^{xx}(\boldsymbol{q})=S^{yy}(\boldsymbol{q})=\frac{1}{4}\sum_{\sigma=\pm}\left[\frac{\langle\mathcal{M}_{\rm A}^z\rangle_T}{N}\left(\cosh 2\theta_{\boldsymbol{q}}-\sqrt{\frac{s}{S}}\cos\delta_{\boldsymbol{q}}\sinh 2\theta_{\boldsymbol{q}}-\sigma\right)\right. \tag{2.43}$$
$$\left.-\frac{\langle\mathcal{M}_{\rm B}^z\rangle_T}{N}\left(\cosh 2\theta_{\boldsymbol{q}}-\sqrt{\frac{S}{s}}\cos\delta_{\boldsymbol{q}}\sinh 2\theta_{\boldsymbol{q}}+\sigma\right)\right]\left(\bar{n}_{\boldsymbol{q}}^{\sigma}+\frac{1}{2}\right).$$

2.3 Temperature-Independent Diagonalization

If we set both $\mu_{\rm A}$ and $\mu_{\rm B}$ equal to zero, Eq. (2.25) becomes

$$\cosh 2\theta_{\boldsymbol{\kappa}_\nu}=\frac{\tilde{p}_{\rm csw}}{\omega_{\boldsymbol{\kappa}_\nu}(\tilde{p}_{\rm csw})},\qquad\sinh 2\theta_{\boldsymbol{\kappa}_\nu}=\frac{|\gamma_{\boldsymbol{\kappa}_\nu}|}{\omega_{\boldsymbol{\kappa}_\nu}(\tilde{p}_{\rm csw})},\qquad\mathrm{e}^{-\mathrm{i}\delta_{\boldsymbol{\kappa}_\nu}}=\frac{\gamma_{\boldsymbol{\kappa}_\nu}}{|\gamma_{\boldsymbol{\kappa}_\nu}|}, \tag{2.44}$$

where

$$\tilde{p}_{\rm csw}\equiv p+p'\frac{\langle\!\langle\mathcal{S}'\rangle\!\rangle}{\langle\!\langle\mathcal{S}\rangle\!\rangle},\qquad\tilde{p}'_{\rm csw}\equiv p'+p\frac{\langle\!\langle\mathcal{S}'\rangle\!\rangle}{\langle\!\langle\mathcal{S}\rangle\!\rangle},\qquad\tilde{q}_{\rm csw}\equiv\sqrt{\tilde{p}_{\rm csw}^2-1}. \tag{2.45}$$

The Bogoliubov Transformation (2.24) with Eq. (2.44) is no longer depend on temperature through the chemical potentials and diagonalizes the bilinear Hamiltonian (2.14) into

$$\mathcal{H}_{\mathrm{BL}} = \sum_{l=0}^{2} E^{(l)}\left(\tilde{p}_{\mathrm{csw}}\right) + \sum_{\nu=1}^{N}\left[\varepsilon^{-}_{\boldsymbol{\kappa}_\nu}(\tilde{p}_{\mathrm{csw}},\tilde{p}'_{\mathrm{csw}})\alpha^{-\dagger}_{\boldsymbol{\kappa}_\nu}\alpha^{-}_{\boldsymbol{\kappa}_\nu} + \varepsilon^{+}_{\boldsymbol{\kappa}_\nu}(\tilde{p}_{\mathrm{csw}},\tilde{p}'_{\mathrm{csw}})\alpha^{+\dagger}_{\boldsymbol{\kappa}_\nu}\alpha^{+}_{\boldsymbol{\kappa}_\nu}\right]. \quad (2.46)$$

The free energy is

$$\begin{aligned} F = \sum_{l=0}^{2} E^{(l)}\left(\tilde{p}_{\mathrm{csw}}\right) &+ \sum_{\nu=1}^{N}\sum_{\sigma=\pm}\varepsilon^{\sigma}_{\boldsymbol{\kappa}_\nu}(\tilde{p}_{\mathrm{csw}},\tilde{p}'_{\mathrm{csw}})\bar{n}^{\sigma}_{\boldsymbol{\kappa}_\nu} \\ &+ k_{\mathrm{B}}T\sum_{\nu=1}^{N}\sum_{n^-=0}^{\infty}\sum_{n^+=0}^{\infty} P_{\boldsymbol{\kappa}_\nu}(n^-,n^+)\ln P_{\boldsymbol{\kappa}_\nu}(n^-,n^+) \\ &+ \sum_{\nu=1}^{N}\mu_\nu\left[1-\sum_{n^-=0}^{\infty}\sum_{n^+=0}^{\infty} P_{\boldsymbol{\kappa}_\nu}(n^-,n^+)\right], \end{aligned} \quad (2.47)$$

where $\bar{n}^{\sigma}_{\boldsymbol{\kappa}_\nu}$ is the thermal average of the number of magnons

$$\bar{n}^{\sigma}_{\boldsymbol{\kappa}_\nu} = \sum_{n^-=0}^{\infty}\sum_{n^+=0}^{\infty} P_{\boldsymbol{\kappa}_\nu}(n^-,n^+)n^{\sigma}, \quad (2.48)$$

and $P_{\boldsymbol{\kappa}_\nu}(n^-,n^+)$ is the probability of n^- ferromagnetic and n^+ antiferromagnetic SWs of momentum $\boldsymbol{\kappa}_\nu$ appearing at temperature T and therefore satisfies

$$\sum_{n^-=0}^{\infty}\sum_{n^+=0}^{\infty} P_{\boldsymbol{\kappa}_\nu}(n^-,n^+) = 1 \qquad (\nu = 1,2,\ldots,N). \quad (2.49)$$

Our task is to control the number of HP bosons which is equivalent to the sublattice magnetizations

$$\langle \mathcal{M}^{z}_{\mathrm{A}}\rangle_T = N\left[S - \tau\left(\tilde{p}_{\mathrm{csw}}\right) - I_2(\bar{n}^{\pm}_{\boldsymbol{\kappa}_\nu};\tilde{p}_{\mathrm{csw}}) - I_3(\bar{n}^{\pm}_{\boldsymbol{\kappa}_\nu})\right], \quad (2.50)$$

$$\langle \mathcal{M}^{z}_{\mathrm{B}}\rangle_T = -N\left[s - \tau\left(\tilde{p}_{\mathrm{csw}}\right) - I_2(\bar{n}^{\pm}_{\boldsymbol{\kappa}_\nu};\tilde{p}_{\mathrm{csw}}) + I_3(\bar{n}^{\pm}_{\boldsymbol{\kappa}_\nu})\right]. \quad (2.51)$$

2.3.1 Effective free energy

In order to control the sublattice magnetizations, we introduce an effective free energy,

$$\widetilde{F} = F + \mu_{\mathrm{A}}\langle \mathcal{M}^{z}_{\mathrm{A}}\rangle_T + \mu_{\mathrm{B}}\langle \mathcal{M}^{z}_{\mathrm{B}}\rangle_T\,. \quad (2.52)$$

We minimize effective free energy $\widetilde{F}$

$$\begin{aligned} \frac{\partial \widetilde{F}}{\partial P_{\boldsymbol{\kappa}_\nu}(n^-,n^+)} = &\sum_{\sigma=\pm}\varepsilon^{\sigma}_{\boldsymbol{\kappa}_\nu}(\tilde{p}_{\mathrm{csw}},\tilde{p}'_{\mathrm{csw}})n^{\sigma} + k_{\mathrm{B}}T\ln P_{\boldsymbol{\kappa}_\nu}(n^-,n^+) + k_{\mathrm{B}}T - \mu_\nu \\ &- \frac{\mu_{\mathrm{A}}-\mu_{\mathrm{B}}}{2}\sum_{\sigma=\pm}\frac{\tilde{p}_{\mathrm{csw}}}{\omega_{\boldsymbol{\kappa}_\nu}(\tilde{p}_{\mathrm{csw}})}n^{\sigma} + \frac{\mu_{\mathrm{A}}+\mu_{\mathrm{B}}}{2}\sum_{\sigma=\pm}\sigma n^{\sigma} = 0, \end{aligned} \quad (2.53)$$

and then have

$$
\begin{aligned}
&P_{\boldsymbol{\kappa}_\nu}(n^-, n^+) \qquad (2.54)\\
&= \exp\left(\frac{\mu_\nu}{k_\mathrm{B}T} - 1\right) \prod_{\sigma=\pm} \exp\left[-\frac{\varepsilon^\sigma_{\boldsymbol{\kappa}_\nu}(\tilde{p}_\mathrm{csw}, \tilde{p}'_\mathrm{csw}) - \frac{\mu_\mathrm{A}-\mu_\mathrm{B}}{2}\frac{\tilde{p}_\mathrm{csw}}{\omega_{\boldsymbol{\kappa}_\nu}(\tilde{p}_\mathrm{csw})} + \sigma\frac{\mu_\mathrm{A}+\mu_\mathrm{B}}{2}}{k_\mathrm{B}T} n^\sigma\right].
\end{aligned}
$$

Substituting this into the normalization condition (2.49) yields

$$
\begin{aligned}
&P_{\boldsymbol{\kappa}_\nu}(n^-, n^+)\\
&= \prod_{\sigma=\pm}\left\{1 - \exp\left[-\frac{\varepsilon^\sigma_{\boldsymbol{\kappa}_\nu}(\tilde{p}_\mathrm{csw}, \tilde{p}'_\mathrm{csw}) - \frac{\mu_\mathrm{A}-\mu_\mathrm{B}}{2}\frac{\tilde{p}_\mathrm{csw}}{\omega_{\boldsymbol{\kappa}_\nu}(\tilde{p}_\mathrm{csw})} + \sigma\frac{\mu_\mathrm{A}+\mu_\mathrm{B}}{2}}{k_\mathrm{B}T}\right]\right\} \qquad (2.55)\\
&\qquad \times \exp\left[-\frac{\varepsilon^\sigma_{\boldsymbol{\kappa}_\nu}(\tilde{p}_\mathrm{csw}, \tilde{p}'_\mathrm{csw}) - \frac{\mu_\mathrm{A}-\mu_\mathrm{B}}{2}\frac{\tilde{p}_\mathrm{csw}}{\omega_{\boldsymbol{\kappa}_\nu}(\tilde{p}_\mathrm{csw})} + \sigma\frac{\mu_\mathrm{A}+\mu_\mathrm{B}}{2}}{k_\mathrm{B}T} n^\sigma\right],
\end{aligned}
$$

and then we can get the optimal distribution

$$
\begin{aligned}
&\bar{n}^\sigma_{\boldsymbol{\kappa}_\nu} \qquad (2.56)\\
&= \left\{\exp\left[\frac{\varepsilon^\sigma_{\boldsymbol{\kappa}_\nu}(\tilde{p}_\mathrm{csw}, \tilde{p}'_\mathrm{csw}) - \frac{\mu_\mathrm{A}-\mu_\mathrm{B}}{2}\frac{\tilde{p}_\mathrm{csw}}{\omega_{\boldsymbol{\kappa}_\nu}(\tilde{p}_\mathrm{csw})} + \sigma\frac{\mu_\mathrm{A}+\mu_\mathrm{B}}{2}}{k_\mathrm{B}T}\right] - 1\right\}^{-1} \qquad (\text{TID MSW}).
\end{aligned}
$$

The thermodynamic quantities are also given as Eqs. (2.33)–(2.43), provided that $\tilde{p}$, $\tilde{q}$ and $\bar{n}^\sigma_{\boldsymbol{\kappa}_\nu}$ are replaced by $\tilde{p}_\mathrm{csw}$, $\tilde{q}_\mathrm{csw}$ and Eq. (2.56), respectively. If we set both μ_A and μ_B equal to zero, both distribution Eqs. (2.41) and (2.56) become the CSW distribution

$$
\lim_{\mu_\mathrm{A},\mu_\mathrm{B}\to 0} \bar{n}^\sigma_{\boldsymbol{\kappa}_\nu} = \left\{\exp\left[\frac{\varepsilon^\sigma_{\boldsymbol{\kappa}_\nu}(\tilde{p}_\mathrm{csw}, \tilde{p}'_\mathrm{csw})}{k_\mathrm{B}T}\right] - 1\right\}^{-1} \qquad (\text{CSW}). \qquad (2.57)
$$

Chapter 3

Compactification

3.1 Modified Spin Waves in Antiferromagnets

In the antiferromagnetic limit $S=s$, Eqs. (2.19) and (2.45) become

$$p=1, \qquad p'=0, \qquad q=0, \tag{3.1}$$

$$\tilde{p}_{\text{csw}}=1, \qquad \tilde{p}'_{\text{csw}}=0, \qquad \tilde{q}_{\text{csw}}=0. \tag{3.2}$$

Also μ_{A} and $-\mu_{\text{B}}$ are set equal, and Eq. (2.18) becomes

$$\tilde{p}=1-\frac{\mu_{\text{A}}}{zJ\langle\!\langle\mathcal{S}\rangle\!\rangle}, \qquad \tilde{p}'=0, \qquad \tilde{q}=\sqrt{\tilde{p}^2-1}. \tag{3.3}$$

The chemical potential is determined so as to keep the thermal average of the staggered magnetization zero,

$$\langle\mathcal{M}^z_{\text{A}}-\mathcal{M}^z_{\text{B}}\rangle_T=2N\left[S-\tau\left(\tilde{p}\right)-I_2(\bar{n}^{\pm}_{\boldsymbol{\kappa}_\nu};\tilde{p})\right]=0. \tag{3.4}$$

The antiferromagnetic CSW theory[6,7] starts with a ground state consisting of two sublattices, one composed of spins pointing up and the other composed of spins pointing down. This ground state has neither sublattice symmetry nor up-down symmetry. In order to preserve these symmetries, what Hirsch and Tang call a sublattice-symmetric SW theory of antiferromagnets diagonalizes the Hamiltonian (2.17) under the condition of zero staggered magnetization (3.4),[24] where the two sublattices are no longer asymmetric and no longer assume an up-spin or down-spin character, having the same magnetization of zero,

$$\langle\mathcal{M}^z_{\text{A}}\rangle_T=\langle\mathcal{M}^z_{\text{B}}\rangle_T=-NI_3(\bar{n}^{\pm}_{\boldsymbol{\kappa}_\nu})=0. \tag{3.5}$$

If we read $\langle\!\langle\mathcal{S}\rangle\!\rangle$ and $\langle\!\langle\mathcal{S}'\rangle\!\rangle$ as the quantum averages in the HP-boson vacuum

$$\langle\mathcal{S}\rangle'_0=S, \qquad \langle\mathcal{S}'\rangle'_0=0, \tag{3.6}$$

respectively, the $O(S^0)$ quadratic Hamiltonian $\mathcal{H}^{(0)}_{\text{BL}}$ [Eq. (2.13)] and the consequent energy correction $E^{(0)}(\tilde{p})$ [Eq. (2.28)] vanish to fit in with the LSW formulation. We only have to solve Eq. (3.4) with a single unknown, $\tilde{p}$, in practice. This TDD-MLSW theory is insufficient to describe low-temperature antiferromagnetic thermodynamics precisely (cf. Figs. 3.1 and 3.2). If we apply TID-MLSW theory, we only have to solve Eq. (3.4) with a single unknown, μ_{A}, provided that $\tilde{p}$, $\tilde{q}$ and $\bar{n}^{\sigma}_{\boldsymbol{\kappa}_\nu}$ are replaced by $\tilde{p}_{\text{csw}}$, $\tilde{q}_{\text{csw}}$ and Eq. (2.56), respectively. This TDD to TID procedure is same in the MISWs.

3.1.1 Spin-wave interactions

In order to give a more accurate description of the thermodynamic properties, we consider bringing MLSWs into interaction. If we apply TDD-MHFISW theory, we read $\langle\!\langle \mathcal{S} \rangle\!\rangle$ and $\langle\!\langle \mathcal{S}' \rangle\!\rangle$ as the thermal average at temperature T

$$\langle \mathcal{S} \rangle_T = S + \epsilon\,(\tilde{p}) + (\tilde{p} - 1)\left[\tau\,(\tilde{p}) + I_2(\bar{n}^{\pm}_{\boldsymbol{\kappa}_\nu}; \tilde{p})\right] - I_1(\bar{n}^{\pm}_{\boldsymbol{\kappa}_\nu}; \tilde{p}), \qquad \langle \mathcal{S}' \rangle_T = 0, \qquad (3.7)$$

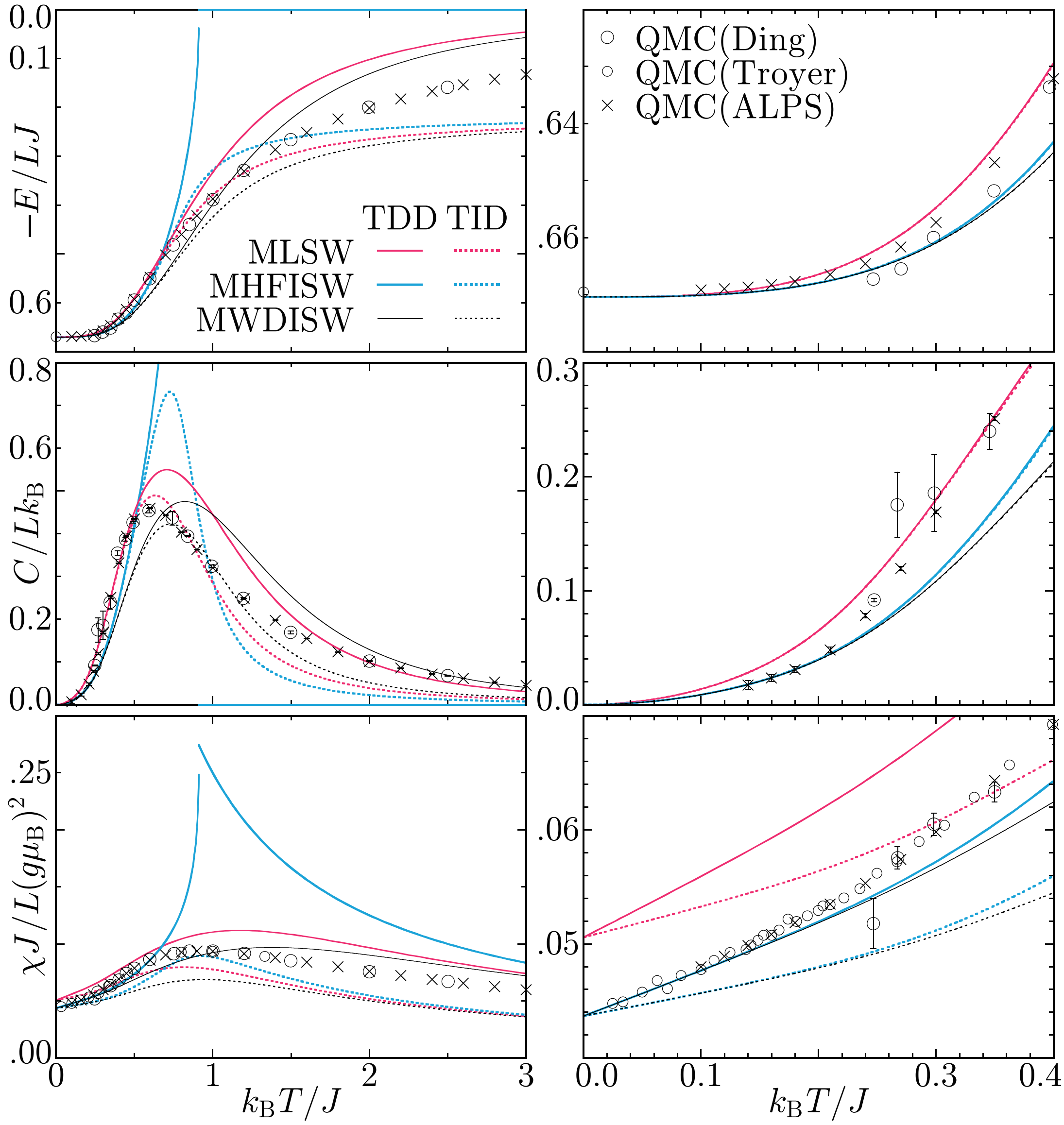

Fig. 3.1: MSW calculations of the internal energy E, specific heat C, and uniform susceptibility χ as functions of temperature for the Hamiltonian (2.1) on the square lattice with $(S, s) = (\frac{1}{2}, \frac{1}{2})$, the former two of which are defined with the up-to-$O(S^0)$ Hamiltonian. The findings with various approximation schemes are compared with QMC calculations.[28, 56, 57] The symbol of E at $T = 0$ indicates the ground-state energy (cf. Table 3.1).

respectively. We solve Eqs. (3.4) and (3.7) with two unknowns, $\langle \mathcal{S} \rangle_T$ and $\tilde{p}$, keeping in mind that $\langle \mathcal{S}' \rangle_T = 0$. We compare the MLSW and MHFISW descriptions of the antiferromagnetic thermodynamics in Figs. 3.1 and 3.2. Indeed the inclusion of SW interactions significantly improves TDD-MLSW description at sufficiently low temperature, but the TDD-MHFISW description deteriorates with increasing temperature and ends in an artificial first-order phase transition.[25,26] If we apply TID-MHFISW theory,[30] the description overcomes thermal breakdown, but deteriorates at low temperature [cf. Eqs. (3.36) and (3.58)].

In order to avoid thermal breakdown, we consider different treatment of the $O(S^0)$ interaction (2.8). We propose decomposing the $O(S^0)$ interaction (2.8) based on the

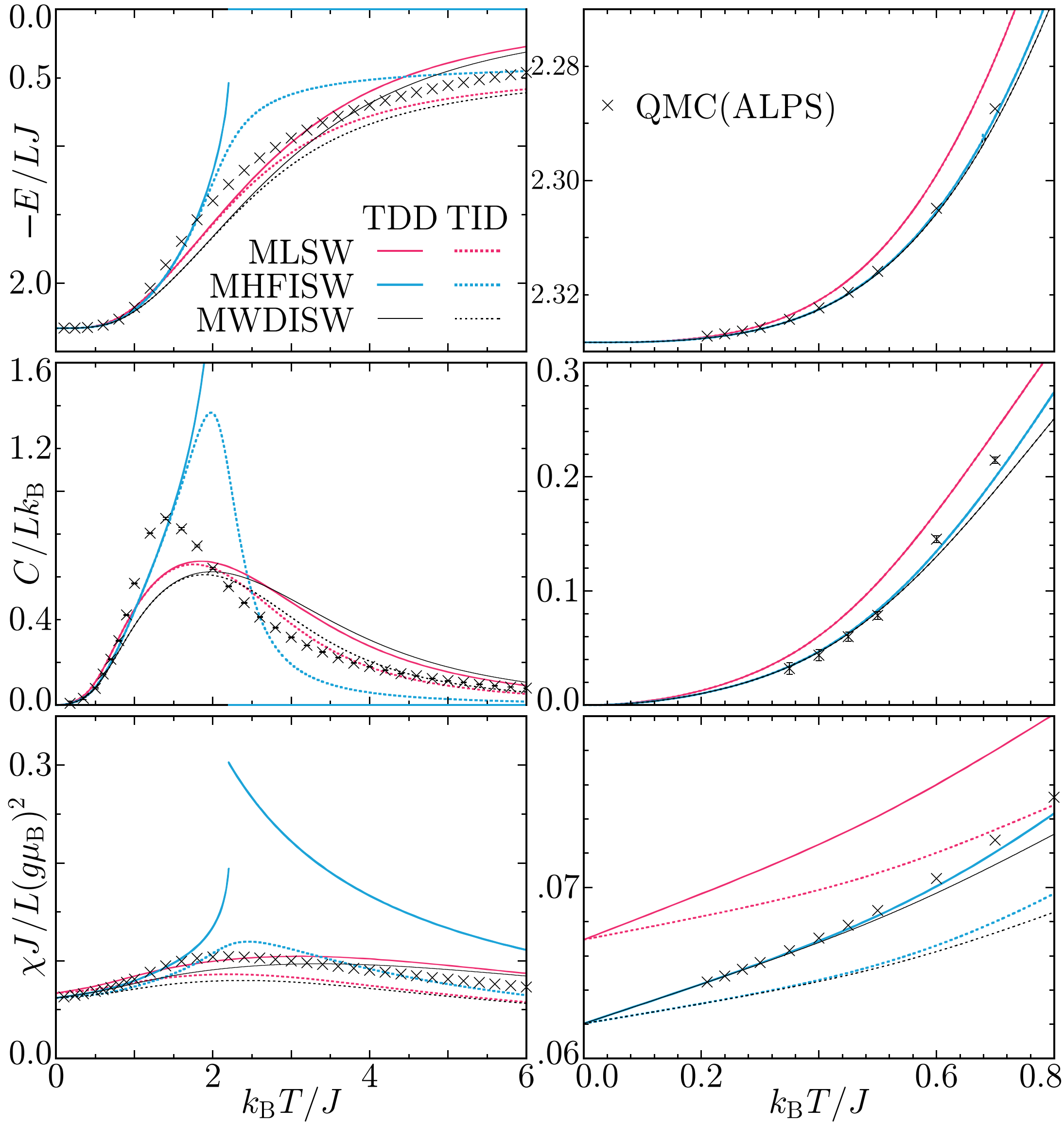

Fig. 3.2: MSW calculations of the internal energy E, specific heat C, and uniform susceptibility χ as functions of temperature for the Hamiltonian (2.1) on the square lattice with $(S, s) = (1, 1)$, the former two of which are defined with the up-to-$O(S^0)$ Hamiltonian. The findings with various approximation schemes are compared with QMC calculations.[57]

Wick Theorem. If we apply TDD-MWDISW theory, we read $\langle\!\langle \mathcal{S} \rangle\!\rangle$ and $\langle\!\langle \mathcal{S}' \rangle\!\rangle$ as the quantum average in the magnon vacuum

$$\langle \mathcal{S} \rangle_0 = S + \epsilon\left(\tilde{p}\right) + (\tilde{p}-1)\tau\left(\tilde{p}\right), \qquad\qquad \langle \mathcal{S}' \rangle_0 = 0, \tag{3.8}$$

respectively. We only have to solve Eq. (3.4) with a single unknown, $\tilde{p}$, in practice. The thus-obtained antiferromagnetic TDD-MWDISW thermodynamics is also shown in Figs. 3.1 and 3.2. It closely resembles the TDD-MHFISW thermodynamics at low temperatures but remains free from any thermal breakdown with increasing temperature. It is much better than the MLSW description in reproducing many thermal features. We can consider the TID-MWDISW theory, but the description deteriorates at low temperature as with TID-MHFISW one.

3.1.2 Low-temperature series expansion

The TDD-MWDISW thermodynamics closely resembles the TDD-MHFISW ones at low temperatures. We further analyze the thermodynamic quantities by expanding them into low-temperature series.

In the antiferromagnets, the dispersion relations (2.29) are degenerate,

$$\varepsilon_{\boldsymbol{\kappa}_\nu}(\tilde{p}) \equiv \varepsilon^{\sigma}_{\boldsymbol{\kappa}_\nu}(\tilde{p},0) = zJ\langle\!\langle \mathcal{S} \rangle\!\rangle \omega_{\boldsymbol{\kappa}_\nu}(\tilde{p}) = zJ\langle\!\langle \mathcal{S} \rangle\!\rangle\left[\omega_{\boldsymbol{\kappa}_\nu}(\tilde{p}) - \tilde{q}\right] + zJ\langle\!\langle \mathcal{S} \rangle\!\rangle\tilde{q}, \tag{3.9}$$

and $\omega_{\boldsymbol{\kappa}_\nu}(\tilde{p}) - \tilde{q}$ is always gapless. We define a state-density function as

$$\widetilde{w}(x) \equiv \frac{1}{N}\sum_{\nu=1}^{N}\delta\left[x - \omega_{\boldsymbol{\kappa}_\nu}(\tilde{p}) + \tilde{q}\right] \qquad\qquad (0 \leqq x \leqq \tilde{p} - \tilde{q}). \tag{3.10}$$

In the thermodynamic limit on the square lattice, this becomes

$$\lim_{N\to\infty}\widetilde{w}(x) = \left(\frac{2}{\pi}\right)^2 \frac{x+\tilde{q}}{\sqrt{\tilde{p}^2-(x+\tilde{q})^2}} K\left[\sqrt{x(x+2\tilde{q})}\right] \equiv 2\sum_{l=0}^{\infty}\widetilde{w}^{(2)}_{l}x^{l}, \tag{3.11}$$

$$\widetilde{w}^{(2)}_0 = \frac{\tilde{q}}{\pi}, \quad \widetilde{w}^{(2)}_1 = \frac{3\tilde{q}^2+2}{2\pi}, \quad \widetilde{w}^{(2)}_2 = \tilde{q}\frac{41\tilde{q}^2+36}{16\pi}, \quad \widetilde{w}^{(2)}_3 = \frac{147\tilde{q}^4+164\tilde{q}^2+24}{32\pi},$$
$$\widetilde{w}^{(2)}_4 = \tilde{q}\frac{8649\tilde{q}^4+11760\tilde{q}^2+3280}{1024\pi}, \quad \widetilde{w}^{(2)}_5 = \frac{32307\tilde{q}^6+51894\tilde{q}^4+21168\tilde{q}^2+1312}{2048\pi},$$

and converts a ν summation into an x integration, such as

$$I_1(\bar{n}^{\pm}_{\boldsymbol{\kappa}_\nu};\tilde{p}) = 2\tilde{q}\sum_{l'=0}^{1}\sum_{l=0}^{\infty}\frac{\widetilde{w}^{(2)}_l}{\tilde{q}^{l'}}F_{l+l'+1}\left(v,t\right), \tag{3.12}$$

$$I_2(\bar{n}^{\pm}_{\boldsymbol{\kappa}_\nu};\tilde{p}) = 2\frac{\tilde{p}}{\tilde{q}}\sum_{l'=0}^{\infty}\sum_{l=0}^{\infty}\frac{\widetilde{w}^{(2)}_l}{(-\tilde{q})^{l'}}F_{l+l'+1}\left(v,t\right), \tag{3.13}$$

$$I_4(\bar{n}^{\pm}_{\boldsymbol{\kappa}_\nu}) = 2\sum_{l=0}^{\infty}\widetilde{w}^{(2)}_l G_{l+1}\left(v,t\right), \tag{3.14}$$

$$\tau\left(\tilde{p}\right) = \frac{1}{2}\left[\frac{4}{\pi^2}K^2\left(\frac{\sqrt{1+1/\tilde{p}}-\sqrt{1-1/\tilde{p}}}{2}\right)-1\right], \tag{3.15}$$

$$\epsilon\left(\tilde{p}\right) = \frac{\tilde{p}}{2}\left[1 - {}_3F_2\left(\frac{1}{2},-\frac{1}{2},\frac{1}{2};1,1;\frac{1}{\tilde{p}}\right)\right], \tag{3.16}$$

where $K(k)$ is the complete elliptic integral of the first kind, ${}_3F_2(a_1,a_2,a_3;b_1,b_2;x)$ is the hypergeometric function, we introduce $F_\xi(v,t)$ and $G_\xi(v,t)$,

$$F_\xi(v,t) \equiv \int_0^{\tilde{p}-\tilde{q}} \frac{x^{\xi-1}}{\exp\left(\frac{x}{t}+v\right)-1}\mathrm{d}x, \tag{3.17}$$

$$G_\xi(v,t) \equiv \int_0^{\tilde{p}-\tilde{q}} \frac{x^{\xi-1}\exp\left(\frac{x}{t}+v\right)}{\left[\exp\left(\frac{x}{t}+v\right)-1\right]^2}\mathrm{d}x, \tag{3.18}$$

and we set the arguments t and v as

$$t \equiv \frac{k_\mathrm{B}T}{zJ\langle\!\langle \mathcal{S}\rangle\!\rangle}, \qquad v \equiv \frac{\tilde{q}}{t}. \tag{3.19}$$

With sufficiently small T, the Eqs. (3.17) and (3.18) can be expand in power of t and v

$$F_\xi(v,t) = t^\xi \int_0^\infty \frac{u^{\xi-1}}{\mathrm{e}^{u+v}-1}\mathrm{d}u = \Gamma(\xi)t^\xi f_\xi(v), \tag{3.20}$$

$$G_\xi(v,t) = t^\xi \int_0^\infty \frac{u^{\xi-1}\mathrm{e}^{u+v}}{(\mathrm{e}^{u+v}-1)^2}\mathrm{d}u = \Gamma(\xi)t^\xi f_{\xi-1}(v), \tag{3.21}$$

where we introduce the Bose–Einstein integral function $f_\xi(v)$

$$\begin{aligned} f_\xi(v) &\equiv \frac{1}{\Gamma(\xi)}\int_0^\infty \frac{u^{\xi-1}}{\mathrm{e}^{u+v}-1}\mathrm{d}u \\ &= \begin{cases} \Gamma(1-\xi)v^{\xi-1} + \displaystyle\sum_{n=0}^\infty \frac{(-v)^n\zeta(\xi-n)}{n!} & (\xi \neq 1,2,3,\ldots), \\ \dfrac{(-v)^{\xi-1}}{(\xi-1)!}\left(\displaystyle\sum_{r=1}^{\xi-1}\frac{1}{r} - \ln v\right) + \displaystyle\sum_{\substack{n=0\\ n\neq\xi-1}}^\infty \frac{(-v)^n\zeta(\xi-n)}{n!} & (\xi = 1,2,3,\ldots). \end{cases} \end{aligned} \tag{3.22}$$

In order to reveal how v depends on t, we expand Eq. (3.4)

$$\begin{aligned} S &= \tau(\tilde{p}) + I_2(\bar{n}^\pm_{\boldsymbol{\kappa}_\nu};\tilde{p}) = \tau(\tilde{p}) + 2\frac{\tilde{p}}{\tilde{q}}\sum_{l'=0}^\infty\sum_{l=0}^\infty \frac{\widetilde{w}_l^{(2)}}{(-\tilde{q})^{l'}}F_{l+l'+1}(v,t) \\ &= \tau(\tilde{p}) - 2\frac{\tilde{p}}{\pi}t\ln v + 2\zeta(2)\frac{3\tilde{p}\tilde{q}}{2\pi}t^2 + 4\zeta(3)\tilde{p}\frac{41\tilde{q}^2+12}{16\pi}t^3 + 12\zeta(4)\tilde{p}\tilde{q}\frac{147\tilde{q}^2+82}{32\pi}t^4 \\ &\qquad + 48\zeta(5)\tilde{p}\frac{8649\tilde{q}^4+7056\tilde{q}^2+656}{1024\pi}t^5 + \cdots. \end{aligned} \tag{3.23}$$

We solve Eq. (3.23) for v in an iterative manner, keeping in mind that $\tilde{q} = tv$,

$$v = \exp\left\{-\frac{\pi[S-\tau(1)]}{2t} + \frac{3\zeta(3)}{2}t^2 + \frac{123}{8}\zeta(5)t^4 + O(t^6)\right\}, \tag{3.24}$$

and then we have

$$\begin{aligned} \tilde{p} &= 1 + O(\mathrm{e}^{-1/t}), & \tilde{q} &= O(\mathrm{e}^{-1/t}), \\ \tau(\tilde{p}) &= \tau(1) + O(\mathrm{e}^{-1/t}), & \epsilon(\tilde{p}) &= \epsilon(1) + O(\mathrm{e}^{-1/t}). \end{aligned} \tag{3.25}$$

Inserting these t dependences into Eqs. (3.12) and (3.14) yields

$$
\begin{aligned}
I_1(\bar{n}^{\pm}_{\boldsymbol{\kappa}_\nu};\tilde{p}) &= 2\tilde{q}\sum_{l'=0}^{1}\sum_{l=0}^{\infty}\frac{\widetilde{w}_l^{(2)}}{\tilde{q}^{l'}}F_{l+l'+1}(v,t) = 2\tilde{q}\sum_{l=0}^{\infty}\widetilde{w}_l^{(2)}F_{l+1}(v,t) + 2\sum_{l=0}^{\infty}\widetilde{w}_l^{(2)}F_{l+2}(v,t) \\
&= 2\frac{\tilde{q}}{\pi}F_2(v,t) + 2\frac{3\tilde{q}^2+2}{2\pi}F_3(v,t) + 2\frac{\tilde{q}(41\tilde{q}^2+36)}{16\pi}F_4(v,t) \\
&\qquad + 2\frac{147\tilde{q}^4+164\tilde{q}^2+24}{32\pi}F_5(v,t) + 2\widetilde{w}_4^{(2)}F_6(v,t) + 2\widetilde{w}_5^{(2)}F_7(v,t) + \cdots \\
&= 4\frac{\zeta(3)}{\pi}t^3 + 36\frac{\zeta(5)}{\pi}t^5 + \frac{1845}{2}\frac{\zeta(7)}{\pi}t^7 + O(t^9), \qquad (3.26) \\
I_4(\bar{n}^{\pm}_{\boldsymbol{\kappa}_\nu}) &= 2\sum_{l=0}^{\infty}\widetilde{w}_l^{(2)}G_{l+1}(v,t) \\
&= 2\frac{\tilde{q}}{\pi}\frac{t}{v} + 2\frac{3\tilde{q}^2+2}{2\pi}\left(\ln\frac{1}{v}\right)t^2 + 2\frac{\tilde{q}(41\tilde{q}^2+36)}{16\pi}2\zeta(2)t^3 \\
&\qquad + 2\frac{147\tilde{q}^4+164\tilde{q}^2+24}{32\pi}6\zeta(3)t^4 + \cdots \\
&= \overbrace{\frac{2}{\pi}}^{\widetilde{w}_0^{(2)}}t^2 + \overbrace{\frac{2}{\pi}\left\{\frac{\pi[S-\tau(1)]}{2t} - \frac{3\zeta(3)}{2}t^2 - \frac{123}{8}\zeta(5)t^4 + O(t^6)\right\}}^{\widetilde{w}_1^{(2)}}t^2 \\
&\qquad + 9\overbrace{\frac{\zeta(3)}{\pi}}^{\widetilde{w}_3^{(2)}}t^4 + \overbrace{\frac{615}{4\pi}\zeta(5)}^{\widetilde{w}_5^{(2)}}t^6 + O(t^8) \\
&= [S-\tau(1)]t + \frac{2}{\pi}t^2 + 6\frac{\zeta(3)}{\pi}t^4 + 123\frac{\zeta(5)}{\pi}t^6 + O(t^8). \qquad (3.27)
\end{aligned}
$$

In antiferromagnets, thermodynamic quantities, Eqs. (2.36), (2.39) and (2.40), read

$$\sum_{l=0}^{2}\frac{\langle\mathcal{H}^{(l)}\rangle_T}{NzJ} = -\left[S+\epsilon(\tilde{p})+(\tilde{p}-1)S - I_1(\bar{n}^{\pm}_{\boldsymbol{\kappa}_\nu};\tilde{p})\right]^2, \qquad (3.28)$$

$$\frac{\chi^{xx}k_{\mathrm{B}}T}{L(g\mu_{\mathrm{B}})^2} = \frac{\chi^{yy}k_{\mathrm{B}}T}{L(g\mu_{\mathrm{B}})^2} = 0, \qquad (3.29)$$

$$\frac{\chi^{zz}k_{\mathrm{B}}T}{L(g\mu_{\mathrm{B}})^2} = I_4(\bar{n}^{\pm}_{\boldsymbol{\kappa}_\nu}). \qquad (3.30)$$

Substituting (3.25), (3.26) and (3.27) into these quantities yields

$$
\begin{aligned}
\sum_{l=0}^{2}\frac{\langle\mathcal{H}^{(l)}\rangle_T}{NzJ} &= -\left[S+\epsilon(1) - 4\frac{\zeta(3)}{\pi}t^3 - 36\frac{\zeta(5)}{\pi}t^5 + O(t^7)\right]^2 \qquad (3.31) \\
&= -[S+\epsilon(1)]^2 + 8[S+\epsilon(1)]\frac{\zeta(3)}{\pi}t^3 + 72[S+\epsilon(1)]\frac{\zeta(5)}{\pi}t^5 \\
&\qquad - 16\left[\frac{\zeta(3)}{\pi}\right]^2 t^6 + O(t^7),
\end{aligned}
$$

$$\frac{\chi k_{\rm B}T}{L(g\mu_{\rm B})^2} = \frac{1}{3}\frac{(\chi^{xx}+\chi^{yy}+\chi^{zz})k_{\rm B}T}{L(g\mu_{\rm B})^2} = \frac{1}{3}I_4(\bar{n}^{\pm}_{\boldsymbol{\kappa}_\nu}) \\ = \frac{S-\tau(1)}{3}t+\frac{2}{3\pi}t^2+2\frac{\zeta(3)}{\pi}t^4+41\frac{\zeta(5)}{\pi}t^6+O(t^8). \tag{3.32}$$

The dependence of the renormalized temperature $t=k_{\rm B}T/zJ\langle\!\langle\mathcal{S}\rangle\!\rangle$ on the bare temperature T is yet to be clarified. Since $\langle\!\langle\mathcal{S}\rangle\!\rangle$ varies depending on the formulation as

$$\langle\!\langle\mathcal{S}\rangle\!\rangle = \begin{cases} \langle\mathcal{S}\rangle'_0 = S & \text{(TDD MLSW)}, \\ \langle\mathcal{S}\rangle_0 = S+\epsilon(1)+O(\mathrm{e}^{-1/t}) & \text{(TDD MWDISW)}, \\ \langle\mathcal{S}\rangle_T = S+\epsilon(1)-4\dfrac{\zeta(3)}{\pi}t^3+O(t^5) & \text{(TDD MHFISW)}, \end{cases} \tag{3.33}$$

renormalized temperature t also depends on the formulation,

$$t = \begin{cases} \dfrac{k_{\rm B}T}{zJ\langle\mathcal{S}\rangle'_0} = \dfrac{k_{\rm B}T}{z\varsigma_0 J} & \text{(TDD MLSW)}, \\ \dfrac{k_{\rm B}T}{zJ\langle\mathcal{S}\rangle_0} = \dfrac{k_{\rm B}T}{z\varsigma_0 J}\left[1+O(\mathrm{e}^{-1/T})\right] & \text{(TDD MWDISW)}, \\ \dfrac{k_{\rm B}T}{zJ\langle\mathcal{S}\rangle_T} = \dfrac{k_{\rm B}T}{z\varsigma_0 J}\left[1+4\dfrac{\zeta(3)}{\pi\varsigma_0}\left(\dfrac{k_{\rm B}T}{z\varsigma_0 J}\right)^3+O(T^5)\right] & \text{(TDD MHFISW)}, \end{cases} \tag{3.34}$$

where $\varsigma_0 \equiv \lim_{T\to 0}\langle\!\langle\mathcal{S}\rangle\!\rangle$. We eventually have

$$\sum_{l=0}^{2}\frac{\langle\mathcal{H}^{(l)}\rangle_T}{NzJ} = -\left[S+\epsilon(1)\right]^2+8\left[S+\epsilon(1)\right]\frac{\zeta(3)}{\pi}\left(\frac{k_{\rm B}T}{z\varsigma_0 J}\right)^3+72\left[S+\epsilon(1)\right]\frac{\zeta(5)}{\pi}\left(\frac{k_{\rm B}T}{z\varsigma_0 J}\right)^5 \\ +\begin{cases} -16\left[\dfrac{\zeta(3)}{\pi}\right]^2\left(\dfrac{k_{\rm B}T}{z\varsigma_0 J}\right)^6+O(T^7) & \text{(TDD MLSW)}, \\ -16\left[\dfrac{\zeta(3)}{\pi}\right]^2\left(\dfrac{k_{\rm B}T}{z\varsigma_0 J}\right)^6+O(T^7) & \text{(TDD MWDISW)}, \\ 80\left[\dfrac{\zeta(3)}{\pi}\right]^2\left(\dfrac{k_{\rm B}T}{z\varsigma_0 J}\right)^6+O(T^7) & \text{(TDD MHFISW)}, \end{cases} \tag{3.35}$$

$$\frac{\chi J}{L(g\mu_{\rm B})^2} = \frac{S-\tau(1)}{3z\varsigma_0}+\frac{2}{3z\pi\varsigma_0}\left(\frac{k_{\rm B}T}{z\varsigma_0 J}\right) \\ +\begin{cases} 2\dfrac{\zeta(3)}{z\pi\varsigma_0}\left(\dfrac{k_{\rm B}T}{z\varsigma_0 J}\right)^3+O(T^5) & \text{(TDD MLSW)}, \\ 2\dfrac{\zeta(3)}{z\pi\varsigma_0}\left(\dfrac{k_{\rm B}T}{z\varsigma_0 J}\right)^3+O(T^5) & \text{(TDD MWDISW)}, \\ 2\left[\dfrac{2}{3}\dfrac{S-\tau(1)}{\varsigma_0}+1\right]\dfrac{\zeta(3)}{z\pi\varsigma_0}\left(\dfrac{k_{\rm B}T}{z\varsigma_0 J}\right)^3+O(T^4) & \text{(TDD MHFISW)}. \end{cases} \tag{3.36}$$

The leading bare-temperature series expansion coefficients for C and χ in the TDD-MHFISW and TDD-MWDISW are exactly the same within the first two terms.

The TID-MSW theory expands the thermodynamic quantities into low-temperature series similar to the TDD-MSW one. We define a state-density function as

$$w(x) \equiv \frac{1}{N}\sum_{\nu=1}^{N}\delta[x-\omega_{\boldsymbol{\kappa}_\nu}(\tilde{p}_{\mathrm{csw}})+\tilde{q}_{\mathrm{csw}}] \qquad (0 \leqq x \leqq \tilde{p}_{\mathrm{csw}}-\tilde{q}_{\mathrm{csw}}=1). \tag{3.37}$$

In the thermodynamic limit on the square lattice, this becomes

$$\lim_{N\to\infty} w(x) = \left(\frac{2}{\pi}\right)^2 \frac{x}{\sqrt{1-x^2}}K(x) \equiv 2\sum_{l=0}^{\infty} w_l^{(2)} x^l, \tag{3.38}$$

$$w_0^{(2)}=0,\quad w_1^{(2)}=\frac{1}{\pi},\quad w_2^{(2)}=0,\quad w_3^{(2)}=\frac{3}{4\pi},\quad w_4^{(2)}=0,\quad w_5^{(2)}=\frac{41}{64\pi},$$

and converts a ν summation into an x integration, such as

$$I_1(\bar{n}_{\boldsymbol{\kappa}_\nu};\tilde{p}_{\mathrm{csw}}) = 2\sum_{l=1}^{\infty} w_{2l-1}^{(2)}\mathcal{F}_{2l+1}(v,t), \tag{3.39}$$

$$I_2(\bar{n}_{\boldsymbol{\kappa}_\nu};\tilde{p}_{\mathrm{csw}}) = 2\sum_{l=1}^{\infty} w_{2l-1}^{(2)}\mathcal{F}_{2l-1}(v,t), \tag{3.40}$$

$$I_4(\bar{n}_{\boldsymbol{\kappa}_\nu}) = 2\sum_{l=1}^{\infty} w_{2l-1}^{(2)}\mathcal{G}_{2l}(v,t), \tag{3.41}$$

where we introduce

$$\mathcal{F}_\xi(v,t) \equiv \int_0^1 \frac{x^{\xi-1}}{\exp\left(\frac{x}{t}+\frac{v}{x}\right)-1}\mathrm{d}x, \tag{3.42}$$

$$\mathcal{G}_\xi(v,t) \equiv \int_0^1 \frac{x^{\xi-1}\exp\left(\frac{x}{t}+\frac{v}{x}\right)}{\left[\exp\left(\frac{x}{t}+\frac{v}{x}\right)-1\right]^2}\mathrm{d}x = -\frac{\partial}{\partial v}\mathcal{F}_{\xi+1}(v,t), \tag{3.43}$$

and we set the arguments t and v as

$$t \equiv \frac{k_{\mathrm{B}}T}{zJ\langle\!\langle \mathcal{S}\rangle\!\rangle}, \qquad\qquad v \equiv -\frac{\mu}{k_{\mathrm{B}}T}. \tag{3.44}$$

With sufficiently small T, the Eqs. (3.42) and (3.43) can be expand in power of t and v

$$\begin{aligned}
&\mathcal{F}_{2m+1}(v,t) \qquad\qquad (m=0,1,2,\ldots)\\
&\quad = t^{2m+1}\Biggl\{\frac{(-1)^m}{2}\left(\frac{v}{t}\right)^m\left[2\sum_{k=1}^{m}\frac{1}{k}-\ln\frac{v}{t}\right]\\
&\qquad + \sum_{\substack{n=0\\ n\neq m}}^{2m}\frac{(-1)^n}{n!}\Gamma(2m+1-n)\zeta(2m+1-2n)\left(\frac{v}{t}\right)^n\\
&\qquad - \sum_{n=1}^{\infty}\frac{\zeta(-2m-2n+1)}{(2m+n)!(n-1)!}\left(\frac{v}{t}\right)^{2m+n}\\
&\qquad\quad \times\left[-2\gamma+\sum_{k=1}^{2m+n}\frac{1}{k}+\sum_{k=1}^{n-1}\frac{1}{k}+\frac{\zeta'(-2m-2n+1)}{\zeta(-2m-2n+1)}-\ln\frac{v}{t}\right]\Biggr\}.
\end{aligned} \tag{3.45}$$

In order to reveal how v depends on t, we expand Eq. (3.4)

$$\begin{aligned}S &= \tau\left(\tilde{p}_{\rm csw}\right) + I_2(\bar{n}_{\boldsymbol{\kappa}_\nu};\tilde{p}_{\rm csw}) = \tau\left(\tilde{p}_{\rm csw}\right) + 2\sum_{l=1}^{\infty} w_{2l-1}^{(2)}\mathcal{F}_{2l-1}\left(v,t\right) \\ &= \tau\left(\tilde{p}_{\rm csw}\right) - \frac{t}{\pi}\ln\frac{v}{t} + \frac{3}{\pi}\zeta(3)t^3 + \frac{123}{4\pi}\zeta(5)t^5 + \cdots. \qquad (3.46)\end{aligned}$$

We solve Eq. (3.46) for v in an iterative manner

$$\sqrt{\frac{v}{t}} = \exp\left\{-\frac{\pi[S-\tau\left(1\right)]}{2t} + \frac{3\zeta(3)}{2}t^2 + \frac{123}{8}\zeta(5)t^4 + O(t^6)\right\}. \qquad (3.47)$$

Inserting this t dependences into Eqs. (3.39) and (3.41) yields

$$\begin{aligned}I_1(\bar{n}_{\boldsymbol{\kappa}_\nu};\tilde{p}_{\rm csw}) &= 2\sum_{l=1}^{\infty} w_{2l-1}^{(2)}\mathcal{F}_{2l+1}\left(v,t\right) \\ &= 4\frac{\zeta(3)}{\pi}t^3 + 36\frac{\zeta(5)}{\pi}t^5 + \frac{1845}{2}\frac{\zeta(7)}{\pi}t^7 + O(t^9), \qquad (3.48)\\ I_4(\bar{n}_{\boldsymbol{\kappa}_\nu}) &= 2\sum_{l=1}^{\infty} w_{2l-1}^{(2)}\mathcal{G}_{2l}\left(v,t\right) \\ &= \frac{2}{\pi}\left(-\frac{t^2}{2}\ln\frac{v}{t} + \frac{1}{2}t^2\right) + 9\frac{\zeta(3)}{\pi}t^4 + \frac{615}{4\pi}\zeta(5)t^6 + \cdots \\ &= \overbrace{\frac{2}{\pi}\left\{\frac{\pi[S-\tau\left(1\right)]}{2t} - \frac{3\zeta(3)}{2}t^2 - \frac{123}{8}\zeta(5)t^4 + O(t^6)\right\}t^2 + \frac{2}{\pi}\frac{1}{2}t^2}^{w_1^{(2)}} \\ &\qquad + \overbrace{9\frac{\zeta(3)}{\pi}t^4}^{w_3^{(2)}} + \overbrace{\frac{615}{4\pi}\zeta(5)t^6}^{w_5^{(2)}} + O(t^8) \\ &= [S-\tau\left(1\right)]t + \frac{2}{\pi}\frac{1}{2}t^2 + 6\frac{\zeta(3)}{\pi}t^4 + 123\frac{\zeta(5)}{\pi}t^6 + O(t^8). \qquad (3.49)\end{aligned}$$

In antiferromagnets, thermodynamic quantities, Eqs. (2.36), (2.39) and (2.40), read

$$\sum_{l=0}^{2}\frac{\langle\mathcal{H}^{(l)}\rangle_T}{NzJ} = -\left\{S + \epsilon\left(\tilde{p}_{\rm csw}\right) + (\tilde{p}_{\rm csw}-1)S - I_1(\bar{n}_{\boldsymbol{\kappa}_\nu}^{\pm};\tilde{p}_{\rm csw})\right\}^2, \qquad (3.50)$$

$$\frac{\chi^{xx}k_{\rm B}T}{L(g\mu_{\rm B})^2} = \frac{\chi^{yy}k_{\rm B}T}{L(g\mu_{\rm B})^2} = 0, \qquad (3.51)$$

$$\frac{\chi^{zz}k_{\rm B}T}{L(g\mu_{\rm B})^2} = I_4(\bar{n}_{\boldsymbol{\kappa}_\nu}^{\pm}). \qquad (3.52)$$

Substituting (3.48) and (3.49) into these quantities yields

$$\begin{aligned}\sum_{l=0}^{2}\frac{\langle\mathcal{H}^{(l)}\rangle_T}{NzJ} &= -\left[S + \epsilon\left(1\right) - 4\frac{\zeta(3)}{\pi}t^3 - 36\frac{\zeta(5)}{\pi}t^5 + O(t^7)\right]^2 \\ &= -\left[S+\epsilon\left(1\right)\right]^2 + 8\left[S+\epsilon\left(1\right)\right]\frac{\zeta(3)}{\pi}t^3 + 72\left[S+\epsilon\left(1\right)\right]\frac{\zeta(5)}{\pi}t^5 \\ &\qquad - 16\left[\frac{\zeta(3)}{\pi}\right]^2 t^6 + O(t^7), \qquad (3.53)\end{aligned}$$

$$\frac{\chi k_{\mathrm{B}}T}{L(g\mu_{\mathrm{B}})^2} = \frac{1}{3}\frac{(\chi^{xx}+\chi^{yy}+\chi^{zz})k_{\mathrm{B}}T}{L(g\mu_{\mathrm{B}})^2} = \frac{1}{3}I_4(\bar{n}_{\boldsymbol{\kappa}_\nu})$$
$$= \frac{S-\tau(1)}{3}t + \frac{2}{3\pi}\frac{1}{2}t^2 + 2\frac{\zeta(3)}{\pi}t^4 + 41\frac{\zeta(5)}{\pi}t^6 + O(t^8). \tag{3.54}$$

The dependence of the renormalized temperature $t = k_{\mathrm{B}}T/zJ\langle\!\langle\mathcal{S}\rangle\!\rangle$ on the bare temperature T is yet to be clarified. Since $\langle\!\langle\mathcal{S}\rangle\!\rangle$ varies depending on the formulation as

$$\langle\!\langle\mathcal{S}\rangle\!\rangle = \begin{cases} \langle\mathcal{S}\rangle_0' = S & \text{(TID MLSW)}, \\ \langle\mathcal{S}\rangle_0 = S + \epsilon(1) & \text{(TID MWDISW)}, \\ \langle\mathcal{S}\rangle_T = S + \epsilon(1) - 4\dfrac{\zeta(3)}{\pi}t^3 + O(t^5) & \text{(TID MHFISW)}, \end{cases} \tag{3.55}$$

renormalized temperature t also depends on the formulation,

$$t = \begin{cases} \dfrac{k_{\mathrm{B}}T}{zJ\langle\mathcal{S}\rangle_0'} = \dfrac{k_{\mathrm{B}}T}{z\varsigma_0 J}, & \text{(TID MLSW)}, \\ \dfrac{k_{\mathrm{B}}T}{zJ\langle\mathcal{S}\rangle_0} = \dfrac{k_{\mathrm{B}}T}{z\varsigma_0 J}, & \text{(TID MWDISW)}, \\ \dfrac{k_{\mathrm{B}}T}{zJ\langle\mathcal{S}\rangle_T} = \dfrac{k_{\mathrm{B}}T}{z\varsigma_0 J}\left[1 + 4\dfrac{\zeta(3)}{\pi\varsigma_0}\left(\dfrac{k_{\mathrm{B}}T}{z\varsigma_0 J}\right)^3 + O(T^5)\right] & \text{(TID MHFISW)}, \end{cases} \tag{3.56}$$

where $\varsigma_0 \equiv \lim_{T\to 0}\langle\!\langle\mathcal{S}\rangle\!\rangle$. We eventually have

$$\sum_{l=0}^{2}\frac{\langle\mathcal{H}^{(l)}\rangle_T}{NzJ} = -[S+\epsilon(1)]^2 + 8[S+\epsilon(1)]\frac{\zeta(3)}{\pi}\left(\frac{k_{\mathrm{B}}T}{z\varsigma_0 J}\right)^3 + 72[S+\epsilon(1)]\frac{\zeta(5)}{\pi}\left(\frac{k_{\mathrm{B}}T}{z\varsigma_0 J}\right)^5$$
$$+\begin{cases} -16\left[\dfrac{\zeta(3)}{\pi}\right]^2\left(\dfrac{k_{\mathrm{B}}T}{z\varsigma_0 J}\right)^6 + O(T^7) & \text{(TID MLSW)}, \\ -16\left[\dfrac{\zeta(3)}{\pi}\right]^2\left(\dfrac{k_{\mathrm{B}}T}{z\varsigma_0 J}\right)^6 + O(T^7) & \text{(TID MWDISW)}, \\ 80\left[\dfrac{\zeta(3)}{\pi}\right]^2\left(\dfrac{k_{\mathrm{B}}T}{z\varsigma_0 J}\right)^6 + O(T^7) & \text{(TID MHFISW)}, \end{cases} \tag{3.57}$$

$$\frac{\chi J}{L(g\mu_{\mathrm{B}})^2} = \frac{S-\tau(1)}{3z\varsigma_0} + \frac{1}{3z\pi\varsigma_0}\left(\frac{k_{\mathrm{B}}T}{z\varsigma_0 J}\right) \tag{3.58}$$
$$+\begin{cases} 2\dfrac{\zeta(3)}{z\pi\varsigma_0}\left(\dfrac{k_{\mathrm{B}}T}{z\varsigma_0 J}\right)^3 + O(T^5) & \text{(TID MLSW)}, \\ 2\dfrac{\zeta(3)}{z\pi\varsigma_0}\left(\dfrac{k_{\mathrm{B}}T}{z\varsigma_0 J}\right)^3 + O(T^5) & \text{(TID MWDISW)}, \\ 2\left[\dfrac{2}{3}\dfrac{S-\tau(1)}{\varsigma_0} + 1\right]\dfrac{\zeta(3)}{z\pi\varsigma_0}\left(\dfrac{k_{\mathrm{B}}T}{z\varsigma_0 J}\right)^3 + O(T^4) & \text{(TID MHFISW)}. \end{cases}$$

The leading bare-temperature series expansion coefficients in the TDD-MSW and TID-MSW are the same except the second term of χ. This difference is visible in Figs. 3.1 and 3.2 at low temperature.

3.1.3 Dynamic structure factor

The TDD-MISW theory reproduces not only the static properties but also the dynamic properties. The TDD-MHFISW description is equivalent to the rotationally invariant SB mean-field theory constructed by Arovas and Auerbach.[58, 59] In antiferromagnets, the TDD-MHFISW and TDD-MWDISW are degenerate at $T = 0$. Let us consider the dynamic structure factor $S(\boldsymbol{q},\omega) = [S^{xx}(\boldsymbol{q},\omega) + S^{yy}(\boldsymbol{q},\omega) + S^{zz}(\boldsymbol{q},\omega)]/3$, where

$$\begin{aligned} &S^{\lambda\lambda}(\boldsymbol{q},\omega) \\ &\quad = \frac{1}{2\pi\hbar}\int_{-\infty}^{\infty}\frac{1}{L}\sum_{l=1}^{L}\sum_{l'=1}^{L} \mathrm{e}^{\mathrm{i}\boldsymbol{q}\cdot(\boldsymbol{r}_l-\boldsymbol{r}_{l'})}\left\langle \delta S^{\lambda}_{\boldsymbol{r}_l}(t)\delta S^{\lambda}_{\boldsymbol{r}_{l'}}(0)\right\rangle_T \mathrm{e}^{\mathrm{i}\omega t}\mathrm{d}t \quad (\lambda = z, y, z), \end{aligned} \tag{3.59}$$

with

$$\delta S^{\lambda}_{\boldsymbol{r}_l}(t) = \mathrm{e}^{\mathrm{i}\widetilde{\mathcal{H}}_{\mathrm{BL}}t/\hbar} S^{\lambda}_{\boldsymbol{r}_l}\mathrm{e}^{-\mathrm{i}\widetilde{\mathcal{H}}_{\mathrm{BL}}t/\hbar} - \langle S^{\lambda}_{\boldsymbol{r}_l}\rangle_T\,. \tag{3.60}$$

After some algebraic manipulations, we obtain

$$\begin{aligned} &S^{zz}(\boldsymbol{q},\omega) \\ &= \frac{1}{2N}\sum_{\nu=1}^{N}\left[\cosh 2\theta_{\boldsymbol{\kappa}_\nu+\boldsymbol{q}}\cosh 2\theta_{\boldsymbol{\kappa}_\nu} - \cos\left(\delta_{\boldsymbol{\kappa}_\nu+\boldsymbol{q}} - \delta_{\boldsymbol{\kappa}_\nu}\right)\sinh 2\theta_{\boldsymbol{\kappa}_\nu+\boldsymbol{q}}\sinh 2\theta_{\boldsymbol{\kappa}_\nu} + 1\right] \\ &\qquad\qquad \times \bar{n}_{\boldsymbol{\kappa}_\nu}(\bar{n}_{\boldsymbol{\kappa}_\nu+\boldsymbol{q}} + 1)\delta[\hbar\omega + \varepsilon_{\boldsymbol{\kappa}_\nu}(\tilde{p}) - \varepsilon_{\boldsymbol{\kappa}_\nu+\boldsymbol{q}}(\tilde{p})] \\ &+ \frac{1}{4N}\sum_{\nu=1}^{N}\left[\cosh 2\theta_{\boldsymbol{\kappa}_\nu+\boldsymbol{q}}\cosh 2\theta_{\boldsymbol{\kappa}_\nu} - \cos\left(\delta_{\boldsymbol{\kappa}_\nu+\boldsymbol{q}} - \delta_{\boldsymbol{\kappa}_\nu}\right)\sinh 2\theta_{\boldsymbol{\kappa}_\nu+\boldsymbol{q}}\sinh 2\theta_{\boldsymbol{\kappa}_\nu} - 1\right] \\ &\qquad\qquad \times\big\{\bar{n}_{\boldsymbol{\kappa}_\nu}\bar{n}_{\boldsymbol{\kappa}_\nu+\boldsymbol{q}}\delta[\hbar\omega + \varepsilon_{\boldsymbol{\kappa}_\nu}(\tilde{p}) + \varepsilon_{\boldsymbol{\kappa}_\nu+\boldsymbol{q}}(\tilde{p})] \\ &\qquad\qquad\quad + (\bar{n}_{\boldsymbol{\kappa}_\nu} + 1)(\bar{n}_{\boldsymbol{\kappa}_\nu+\boldsymbol{q}} + 1)\delta[\hbar\omega - \varepsilon_{\boldsymbol{\kappa}_\nu}(\tilde{p}) - \varepsilon_{\boldsymbol{\kappa}_\nu+\boldsymbol{q}}(\tilde{p})]\big\}, \end{aligned} \tag{3.61}$$

$$\begin{aligned} S^{xx}(\boldsymbol{q},\omega) &= S^{yy}(\boldsymbol{q},\omega) \\ &= \frac{\langle\mathcal{M}^z_{\mathrm{A}}\rangle_T - \langle\mathcal{M}^z_{\mathrm{B}}\rangle_T}{2N}\left(\cosh 2\theta_{\boldsymbol{q}} - \cos\delta_{\boldsymbol{q}}\sinh 2\theta_{\boldsymbol{q}}\right) \\ &\qquad \times\left\{\frac{\bar{n}_{\boldsymbol{q}}}{2}\delta[\hbar\omega + \varepsilon_{\boldsymbol{q}}(\tilde{p})] + \frac{\bar{n}_{\boldsymbol{q}} + 1}{2}\delta[\hbar\omega - \varepsilon_{\boldsymbol{q}}(\tilde{p})]\right\}, \end{aligned} \tag{3.62}$$

where $\bar{n}_{\boldsymbol{\kappa}_\nu} \equiv \bar{n}^{\sigma}_{\boldsymbol{\kappa}_\nu}$. $\bar{n}^{+}_{\boldsymbol{\kappa}_\nu}$ and $\bar{n}^{-}_{\boldsymbol{\kappa}_\nu}$ are degenerate in the antiferromagnets. We show the TDD-MISW calculations of the dynamic structure factor together with exact-diagonalization (ED) calculations in Fig. 3.3. The TDD-MISW description reproduces dynamic properties and becomes more precisely with increasing spin magnitude S. The description is equivalent to the rotationally invariant SB mean-field theory.[60]

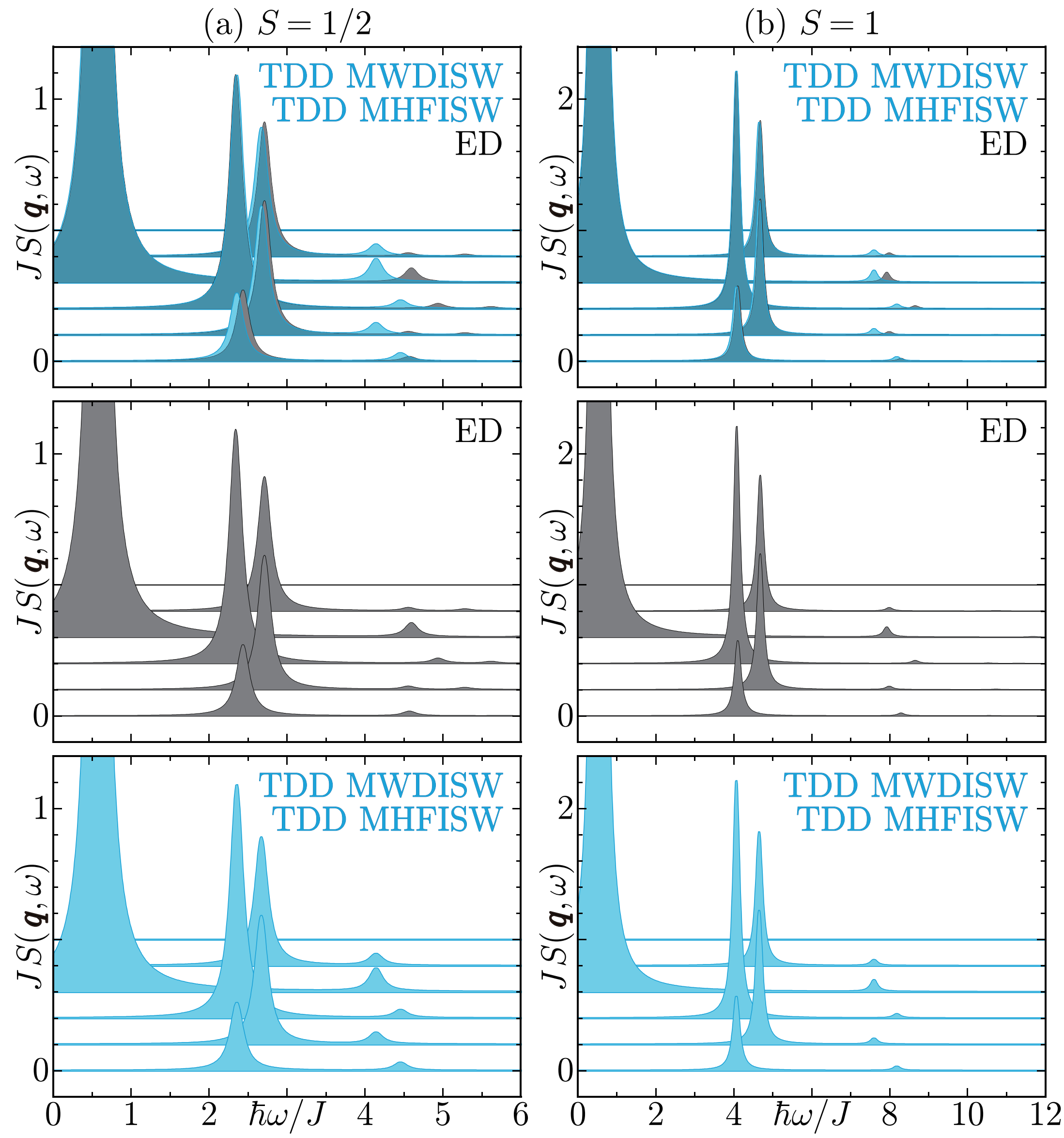

Fig. 3.3: TDD-MISW calculations of the dynamic structure factor $S(\boldsymbol{q}, \omega)$ at $T = 0$ as functions of ω for the Hamiltonian (2.1) on the 4×4 square lattice with $(S, s) = (\frac{1}{2}, \frac{1}{2})$ (a) and $(S, s) = (1, 1)$ (b). The findings with various momentum [bottom to top: $a\boldsymbol{q}/\pi = (0, 1/2), (0, 1), (1/2, 1), (1, 1), (1/2, 1/2), (0, 0)$] are compared with ED calculations. Note that all curves are shifted by $0.2S$ with respect to each other for better visibility.

3.2 Modified Spin Waves in Ferrimagnets

In ferrimagnets, there are various constraint constraint.[61] Which magnetization should be kept zero, uniform, staggered, or both? Let us start by following the earliest antiferromagnetic MLSW theory,[24] where μ_{A} and $-\mu_{\mathrm{B}}$ are set equal and determined so as to keep the thermal average of the staggered magnetization zero,

$$\langle \mathcal{M}_{\mathrm{A}}^{z} - \mathcal{M}_{\mathrm{B}}^{z} \rangle_T = N\left[S + s - 2\tau(\tilde{p}) - 2I_2(\bar{n}_{\boldsymbol{\kappa}_\nu}^{\pm};\tilde{p})\right] = 0. \tag{3.63}$$

We only have to solve Eq. (3.63) with a single unknown, $\tilde{p}$, in practice. If we read $\langle\!\langle \mathcal{S} \rangle\!\rangle$ and $\langle\!\langle \mathcal{S}' \rangle\!\rangle$ as the quantum averages in the HP-boson vacuum

$$\langle \mathcal{S} \rangle_0' = \sqrt{Ss}, \qquad \langle \mathcal{S}' \rangle_0' = 0, \tag{3.64}$$

respectively, the $O(S^0)$ quadratic Hamiltonian $\mathcal{H}_{\mathrm{BL}}^{(0)}$ [Eq. (2.13)] and the consequent energy correction $E^{(0)}(\tilde{p})$ [Eq. (2.28)] vanish to fit in with the LSW formulation.

We show the TDD-MLSW calculations of thermodynamic quantities under the single-constraint (SC) condition (3.63) together with QMC,[47] density-matrix renormalization group (DMRG),[47] and ED[48] calculations in Fig. 3.4. Considering that the antiferromagnetic SW excitations are far apart in energy from the ferromagnetic ones,[62] the ferromagnetic dispersion relation $\varepsilon_{\boldsymbol{\kappa}_\nu}^{-}(\tilde{p},\tilde{p}')$, especially that at small momenta, has a decisive effect on the low-temperature thermodynamics, in a close analogy with the ferromagnetic MSW findings.[20,21] The SC-TDD-MLSW calculations show us the $\sqrt{T}$ vanishing behavior of C and the $1/T^2$ diverging behavior of χ with $T \to 0$, which are characteristic of one-dimensional Heisenberg ferromagnets,[63,64] as will later be shown rigorously. They successfully reproduce the Schottky-like peak of C and the ferrimagnetic minimum of χT as well. We find, however, that the SC-TDD-MLSW theory misread the high-temperature properties. Under the SC condition for antiferromagnets, the sublattice magnetizations (3.5) vanish, and both sublattice symmetry and up-down symmetry preserve. Unless $S = s$, however, the sublattice magnetizations

$$\langle \mathcal{M}_{\mathrm{A}}^{z} \rangle_T = \langle \mathcal{M}_{\mathrm{B}}^{z} \rangle_T = N\left[\frac{S-s}{2} - I_3(\bar{n}_{\boldsymbol{\kappa}_\nu}^{\pm})\right], \tag{3.65}$$

Table 3.1: SC-TDD-MLSW and DC-TDD-MLSW calculations of the up-to-$O(S^1)$ and up-to-$O(S^0)$ ground-state energies $\lim_{T\to 0} E$ for the Hamiltonian (2.1) on the single-chain (1D) and square (2D) lattices in comparison with QMC[28] and ED[48] calculations.

(S,s)	$\lim_{T\to 0} E/LJ$				
	QMC / ED	MLSW $\left(E \equiv \sum_{l=1}^{2} \langle \mathcal{H}^{(l)} \rangle_T\right)$ SC	MLSW $\left(E \equiv \sum_{l=1}^{2} \langle \mathcal{H}^{(l)} \rangle_T\right)$ DC	MLSW $\left(E \equiv \sum_{l=0}^{2} \langle \mathcal{H}^{(l)} \rangle_T\right)$ SC	MLSW $\left(E \equiv \sum_{l=0}^{2} \langle \mathcal{H}^{(l)} \rangle_T\right)$ DC
2D-$(\frac{1}{2},\frac{1}{2})$	$-0.66953(4)$[28]	-0.65795	-0.65795	-0.67042	-0.67042
1D-$(1,\frac{1}{2})$	$-0.72705(5)$[48]	-0.71823	-0.70634	-0.73042	-0.72763
1D-$(\frac{3}{2},\frac{1}{2})$	$-0.98360(5)$	-0.97902	-0.96794	-0.98491	-0.98378
1D-$(\frac{3}{2},1)$	$-1.9305(5)$	-1.9140	-1.9041	-1.9338	-1.9314
1D-$(2,1)$	$-2.4465(5)$	-2.4365	-2.4246	-2.4486	-2.4471

Table 3.2: SC-TDD-MLSW and DC-TDD-MLSW calculations of the ground-state spin reduction $\lim_{T\to 0}\tau(\tilde{p})$ on the single-chain (1D) and square (2D) lattices in comparison with QMC[66] and ED[48] calculations.

(S,s)	$\lim_{T\to 0}\tau(\tilde{p})$		
	QMC	MLSW	
	ED	SC	DC
2D-$(\frac{1}{2},\frac{1}{2})$	0.1930(3)[66]	0.19660	0.19660
1D-$(1,\frac{1}{2})$	0.2073(3)[48]	0.30489	0.20902
1D-$(\frac{3}{2},\frac{1}{2})$	0.1410(2)	0.18644	0.14294
1D-$(\frac{3}{2},1)$	0.3513(3)	0.46006	0.35723
1D-$(2,1)$	0.2394(3)	0.30489	0.25079

are generally finite and up-down symmetry is left broken. This is the very reason why the ferrimagnetic SC-TDD-MSW theory fails to reproduce the paramagnetic behavior[65] correctly.

Let us further constrain the uniform magnetization to be zero,

$$\langle \mathcal{M}_{\mathrm{A}}^{z}+\mathcal{M}_{\mathrm{B}}^{z}\rangle_{T}=N\left[S-s-2I_{3}(\bar{n}_{\boldsymbol{\kappa}_{\nu}}^{\pm})\right]=0. \tag{3.66}$$

We solve Eqs. (3.63) and (3.66) with two unknowns, $\tilde{p}$ and $\tilde{p}'$. Under the double-constraint (DC) condition, sublattice magnetizations vanish, and both sublattice symmetry and up-down symmetry preserve even in ferrimagnets. The DC-TDD-MSW theory reproduces the paramagnetic behavior correctly. Tables 3.1 and 3.2 demonstrate that the DC condition gives fine estimates of the ground-state properties as well. We evaluate the quantum averages in the magnon vacuum for the sublattice magnetizations,

$$\lim_{T\to 0}\frac{\langle \mathcal{M}_{\mathrm{A}}^{z}\rangle_{0}}{N}=S-\lim_{T\to 0}\langle a_{\boldsymbol{r}_m}^{\dagger}a_{\boldsymbol{r}_m}\rangle_{0}=S-\lim_{T\to 0}\tau\left(\tilde{p}\right), \tag{3.67}$$

$$\lim_{T\to 0}\frac{\langle \mathcal{M}_{\mathrm{B}}^{z}\rangle_{0}}{N}=-s+\lim_{T\to 0}\langle b_{\boldsymbol{r}_n}^{\dagger}b_{\boldsymbol{r}_n}\rangle_{0}=-s+\lim_{T\to 0}\tau\left(\tilde{p}\right), \tag{3.68}$$

and calculate the ground-state energy $\sum_{l}\langle\mathcal{H}^{(l)}\rangle_{T=0}$ in two ways, up to $O(S^1)$ and up to $O(S^0)$, in terms of SC and DC MLSWs. The internal energy, regardless of whether up to $O(S^1)$ or up to $O(S^0)$, is a function of $\tilde{p}$ in the $T\to 0$ limit [cf. Eq. (3.99)]. This is the case with the sublattice magnetizations as well [cf. Eqs. (3.67) and (3.68)]. Under the DC condition, $\tilde{p}$ in the ground state does not depend on whether or not $\mathcal{H}_{\mathrm{BL}}^{(0)}$ is included in the TDD-modified Hamiltonian $\widetilde{\mathcal{H}}_{\mathrm{BL}}$, as will be shown later. The DC-MLSW findings for the quantum spin reduction $\lim_{T\to 0}\tau(\tilde{p})$ and the ground-state energy $\sum_{l=0}^{2}\langle\mathcal{H}^{(l)}\rangle_{T=0}$ are thus exactly the same as the DC-MISW ones and indeed turn out to be highly satisfactory as shown in Tables 3.1 and 3.2.

3.2.1 High-temperature limit

The SC-TDD-MSW theory states that

$$\frac{\langle \mathcal{M}_{\mathrm{A}}^{z}\rangle_{T\to\infty}}{N}=\frac{\langle \mathcal{M}_{\mathrm{B}}^{z}\rangle_{T\to\infty}}{N}=\frac{S-s}{2}, \tag{3.69}$$

where $\bar{n}^{\pm}_{\boldsymbol{\kappa}_\nu} = (S+s)/2$ with $\tilde{p}$ diverging but $\tilde{p}'$ remaining finite, while the DC-TDD-MSW theory corrects these findings into

$$\frac{\langle \mathcal{M}^z_{\mathrm{A}} \rangle_{T\to\infty}}{N} = \frac{\langle \mathcal{M}^z_{\mathrm{B}} \rangle_{T\to\infty}}{N} = 0, \tag{3.70}$$

where $\bar{n}^{+}_{k_\nu} = s$ but $\bar{n}^{-}_{k_\nu} = S$ with $\tilde{p}$ and $\tilde{p}'$ both diverging.

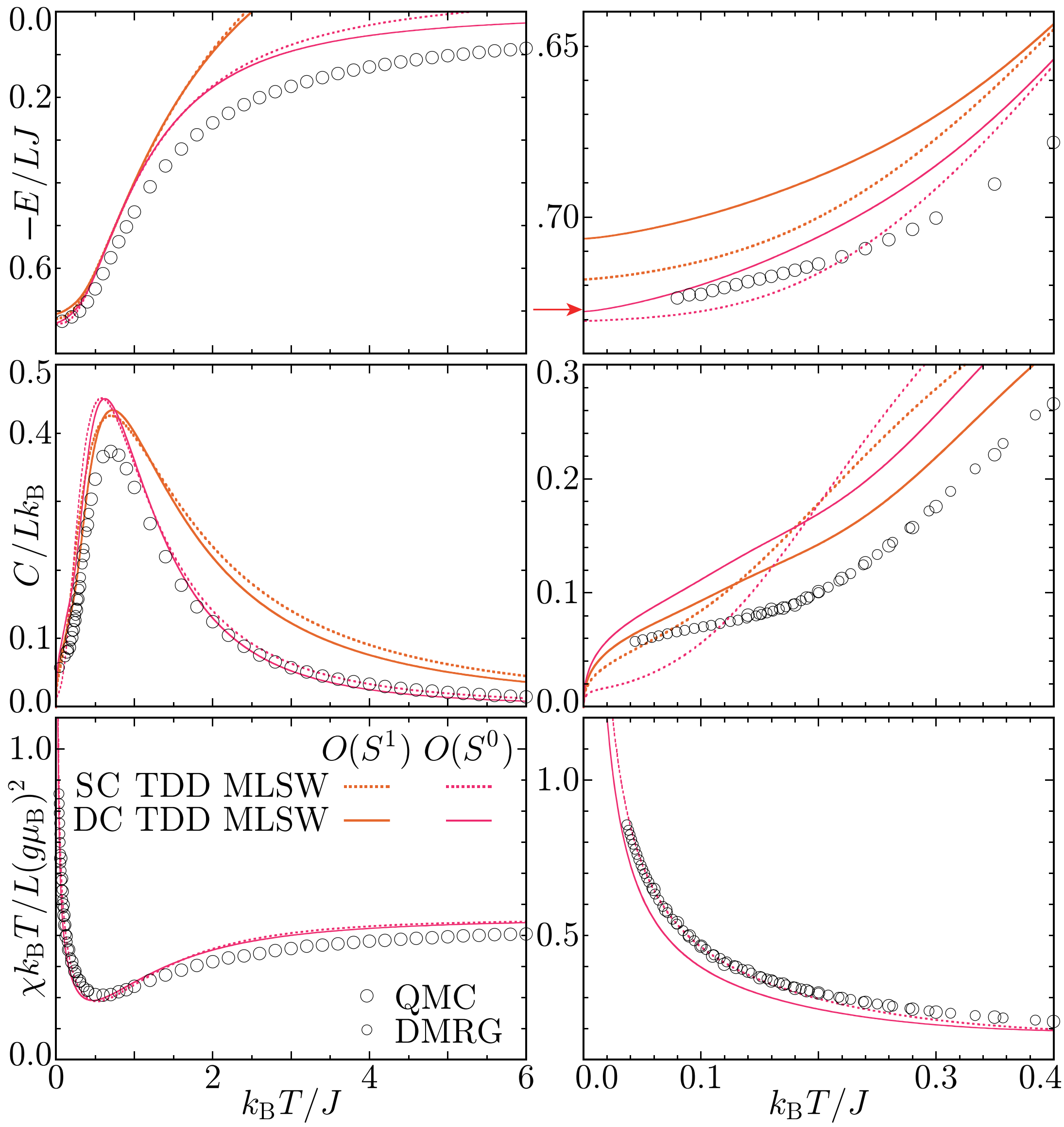

Fig. 3.4: TDD-MLSW calculations of the internal energy E, specific heat C, and uniform susceptibility χ as functions of temperature for the Hamiltonian (2.1) on the single-chain lattice with $(S,s) = (1, \frac{1}{2})$, the former two of which are defined in two ways, up to $O(S^1)$ and up to $O(S^0)$. The findings with various constraint constraint are compared with QMC and DMRG calculations.[47)] The arrow to E at $T=0$ indicates the ED estimate[48)] of the ground-state energy (cf. Table 3.1).

The $O(S^1)$ paramagnetic internal energy within the TDD-MSW theory reads

$$\sum_{l=1}^{2} \frac{\langle \mathcal{H}^{(l)} \rangle_{T\to\infty}}{NzJ} = Ss + S\frac{\langle \mathcal{M}_{\mathrm{B}}^{z} \rangle_{T\to\infty}}{N} - s\frac{\langle \mathcal{M}_{\mathrm{A}}^{z} \rangle_{T\to\infty}}{N}, \tag{3.71}$$

which deviates from the correct value by Ss even under the DC condition (3.63) plus (3.66). The persistent error Ss is merely due to the definition $E = \langle \sum_{l=1}^{2} \mathcal{H}^{(l)} \rangle_T$ and is therefore canceled out by the $O(S^0)$ Hamiltonian,

$$\sum_{l=0}^{2} \frac{\langle \mathcal{H}^{(l)} \rangle_{T\to\infty}}{NzJ} = \frac{\langle \mathcal{M}_{\mathrm{A}}^{z} \rangle_{T\to\infty}}{N} \frac{\langle \mathcal{M}_{\mathrm{B}}^{z} \rangle_{T\to\infty}}{N}. \tag{3.72}$$

The paramagnetic static structure factor within the TDD-MSW theory reads

$$\lim_{T\to\infty} S(\boldsymbol{q}) = \frac{S(S+1)+s(s+1)}{2} - \frac{1}{2}\left[\left(\frac{\langle \mathcal{M}_{\mathrm{A}}^{z} \rangle_{T\to\infty}}{N}\right)^2 + \left(\frac{\langle \mathcal{M}_{\mathrm{B}}^{z} \rangle_{T\to\infty}}{N}\right)^2\right]. \tag{3.73}$$

In the TDD-MSW theory, $\lim_{T\to\infty} S(\boldsymbol{q})$ no longer depends on $\boldsymbol{q}$ [Fig. 3.5(a)]. In contrast, the TID-MSW theory completely fails to describe $\lim_{T\to\infty} S(\boldsymbol{q})$, as illustrated in Fig. 3.5(b). None of its variations can reproduce $S(\boldsymbol{q})$ without any dispersion, where the MISW findings are less dispersive than the MLSW findings and those under the SC condition are better than those under the DC condition. We can further improve the SC-TID-MSW theory by perturbatively treating the quartic interaction (2.8),[47, 48] but this artifact, even though much less significant, still remains.

The MSW description of the paramagnetic behavior remains unsatisfactory under the SC condition. The DC modification scheme is thus superior to the SC one at both low and high temperatures. Since the DC condition (3.63) plus (3.66) reads $\langle \mathcal{M}_{\mathrm{A}}^{z} \rangle_T = \langle \mathcal{M}_{\mathrm{B}}^{z} \rangle_T = 0$, the general principle of modifying CSWs in heterogeneous[18, 19, 67] or random[68] magnets is such that every sublattice magnetization be zero.

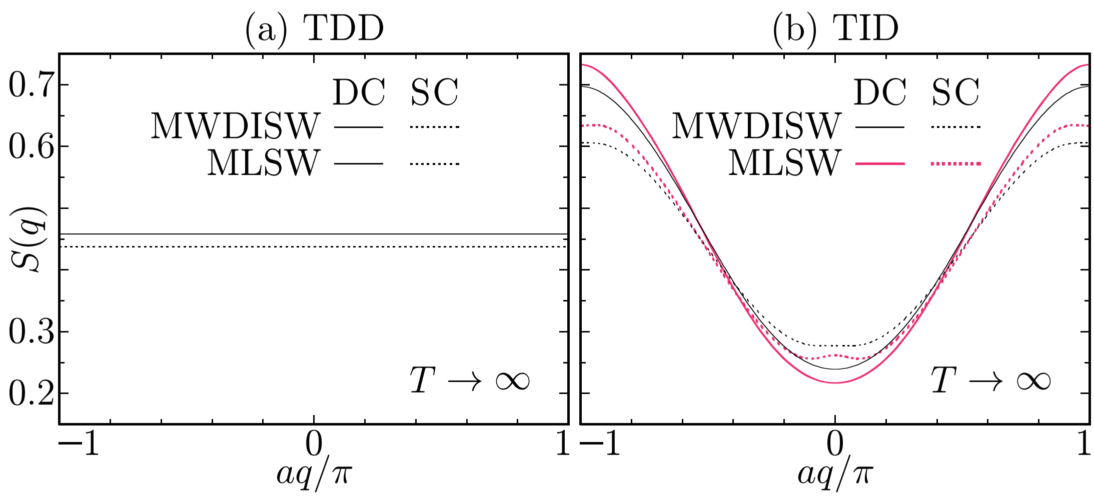

Fig. 3.5: TDD-MSW (a) and TID-MSW (b) calculations of the static structure factor $S(q)$ in the high-temperature limit for the Hamiltonian (2.1) on the single-chain lattice with $(S, s) = (1, \frac{1}{2})$.

3.2.2 Spin-wave interactions

In order to give a more accurate description of the thermodynamic properties, we consider bringing DC MLSWs into interaction. If we apply DC-TDD-MHFISW theory, we read $\langle\!\langle \mathcal{S} \rangle\!\rangle$ and $\langle\!\langle \mathcal{S}' \rangle\!\rangle$ as the thermal average at temperature T

$$\langle \mathcal{S} \rangle_T = \sqrt{Ss} + \epsilon(\tilde{p}) + (\tilde{p} - p)[\tau(\tilde{p}) + I_2(\bar{n}^{\pm}_{\boldsymbol{\kappa}_\nu}; \tilde{p})] \\ -(\tilde{q} - q) I_3(\bar{n}^{\pm}_{\boldsymbol{\kappa}_\nu}) - [I_1(\bar{n}^{\pm}_{\boldsymbol{\kappa}_\nu}; \tilde{p}) - \tilde{q} I_3(\bar{n}^{\pm}_{\boldsymbol{\kappa}_\nu})], \tag{3.74}$$

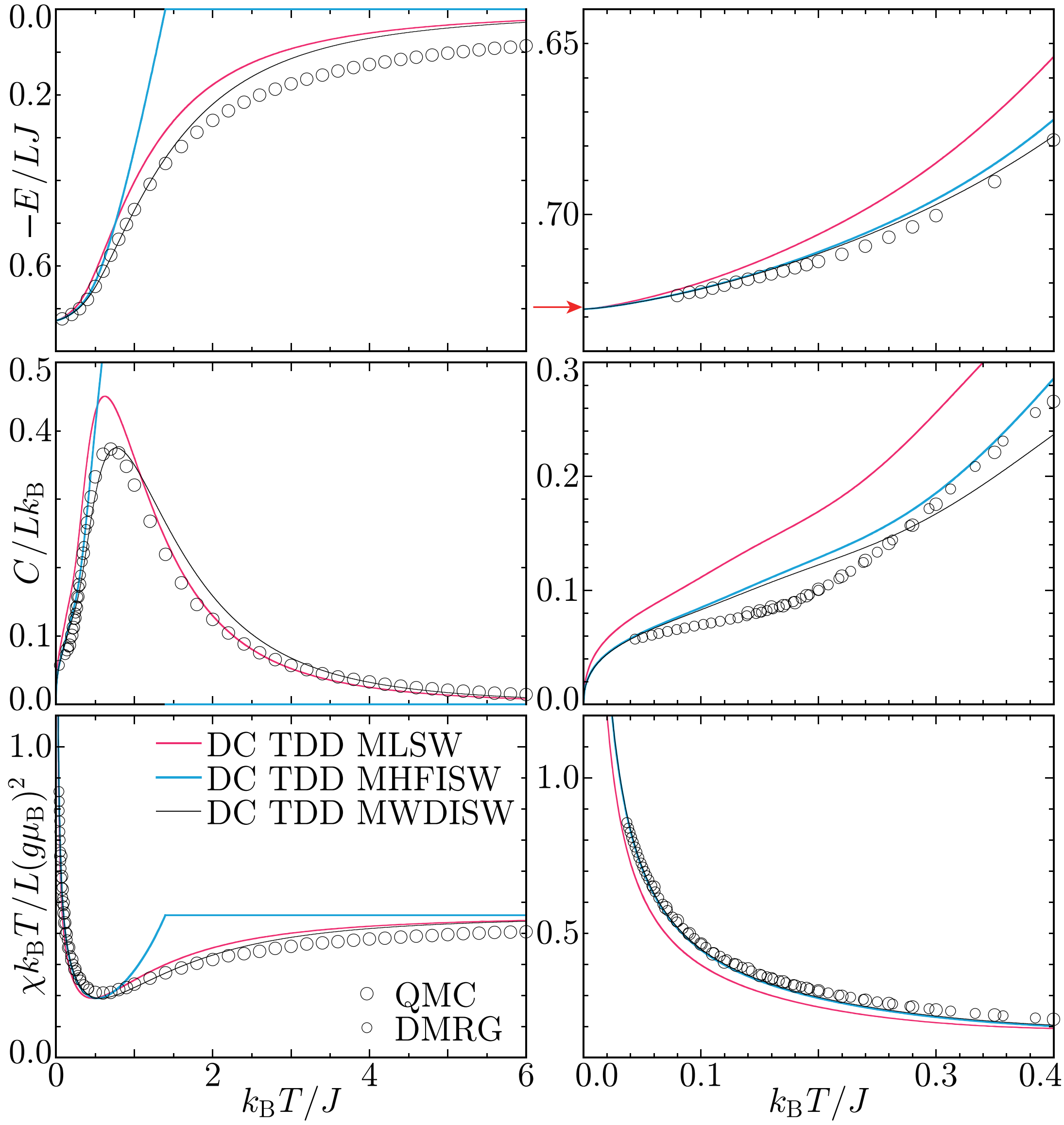

Fig. 3.6: DC-TDD-MSW calculations of the internal energy E, specific heat C, and uniform susceptibility χ as functions of temperature for the Hamiltonian (2.1) on the single-chain lattice with $(S, s) = (1, \frac{1}{2})$, the former two of which are defined with the up-to-$O(S^0)$ Hamiltonian. The findings with various approximation schemes are compared with QMC and DMRG calculations.[47] The arrow to E at $T = 0$ indicates the ED estimate[48] of the ground-state energy (cf. Table 3.1).

$$\langle \mathcal{S}' \rangle_T = q[\tau(\tilde{p}) + I_2(\bar{n}^{\pm}_{\boldsymbol{\kappa}_\nu}; \tilde{p})] - pI_3(\bar{n}^{\pm}_{\boldsymbol{\kappa}_\nu}),$$

respectively. We solve Eqs. (3.63), (3.66) and (3.74) with three unknowns, $\langle \mathcal{S} \rangle_T$, $\tilde{p}$ and $\tilde{p}'$, keeping in mind that $\langle \mathcal{S}' \rangle_T = 0$.

We compare in Fig. 3.6 the DC-TDD-MHFISW and DC-TDD-MLSW descriptions of the ferrimagnetic thermodynamics on the single-chain lattice. Indeed the inclusion of SW interactions significantly improves the MLSW description at sufficiently low temperatures, but the MHFISW description deteriorates with increasing temperature and ends in a phase transition to the trivial solution of paramagnetic aspect, $\tilde{p}\,\langle \mathcal{S} \rangle_T = (k_{\mathrm{B}}T/2zJ)\ln[(S+1)(s+1)/Ss]$ and $\tilde{p}'\,\langle \mathcal{S} \rangle_T = (k_{\mathrm{B}}T/2zJ)\ln[S(s+1)/s(S+1)]$

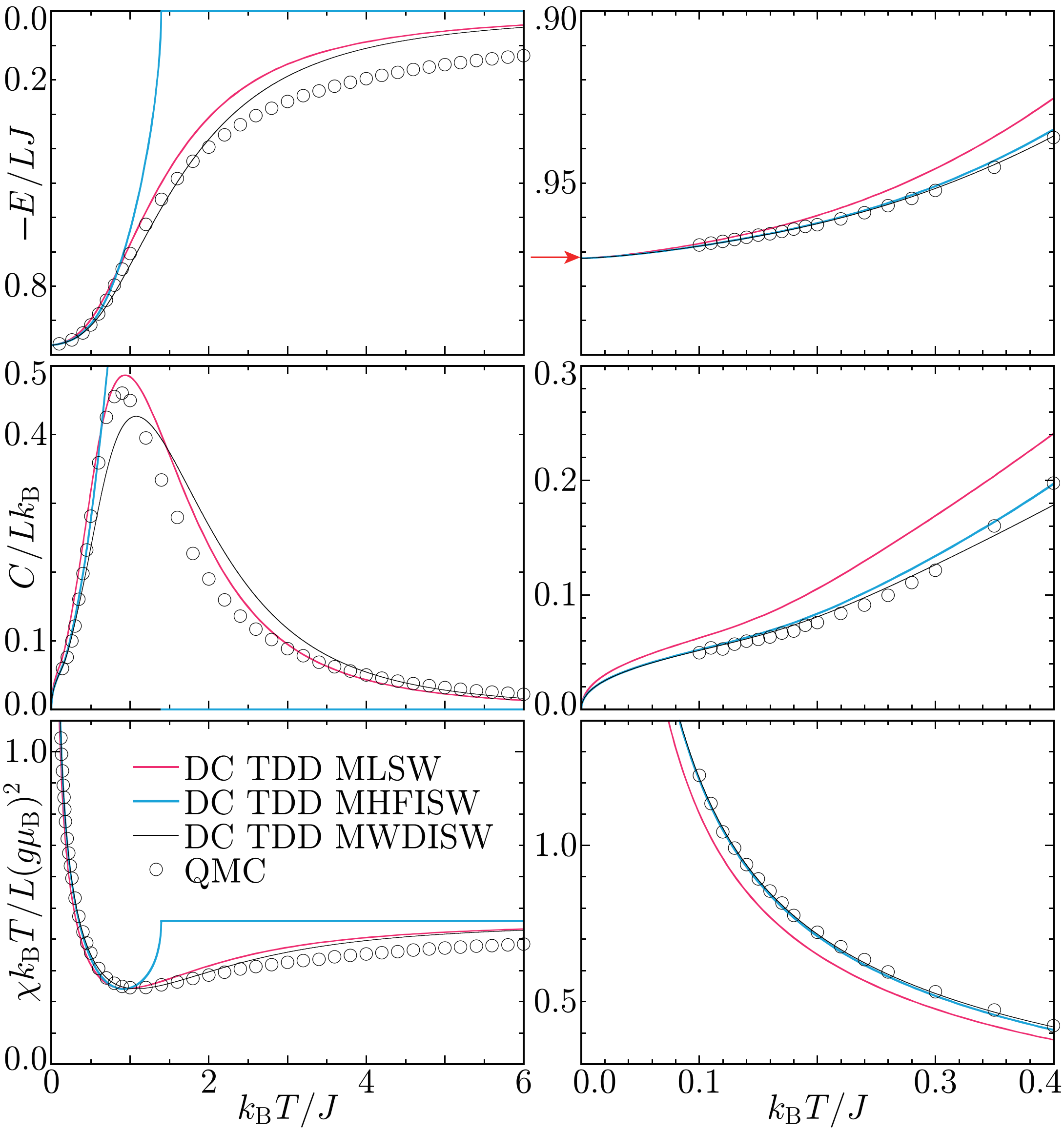

Fig. 3.7: DC-TDD-MSW calculations of the internal energy E, specific heat C, and uniform susceptibility χ as functions of temperature for the Hamiltonian (2.1) on the two-leg-ladder lattice with $(S, s) = (1, \frac{1}{2})$, the former two of which are defined with the up-to-$O(S^0)$ Hamiltonian. The findings with various approximation schemes are compared with QMC calculations. The arrow to E at $T = 0$ indicates the ED estimates[69, 70] of the ground-state energy.

Table 3.3: Scaled ferrimagnetic (antiferromagnetic)-to-paramagnetic transition temperature $k_{\rm B}T/J\sqrt{Ss}$ in the DC-TDD-MHFISW theory for the Hamiltonian (2.1) on various lattices for various S and s.

(S,s)	Single chain	2-leg ladder	4-leg ladder	Square
$(\frac{1}{2},\frac{1}{2})$	1.820	1.820	1.820	1.822
$(1,\frac{1}{2})$	1.973	1.973	1.977	1.984
$(\frac{3}{2},\frac{1}{2})$	2.152	2.152	2.160	2.170
$(1,1)$	2.164	2.167	2.184	2.202
$(\frac{3}{2},1)$	2.374	2.378	2.402	2.427
$(2,1)$	2.575	2.581	2.610	2.639
$(\frac{3}{2},\frac{3}{2})$	2.610	2.619	2.652	2.684

with vanishing $\langle\mathcal{S}\rangle_T$ and diverging $\tilde{p}$ and $\tilde{p}'$. This artificial transition is a defect inherent in the HF self-consistent calculation and commonly occurs in antiferromagnetic cases as well (cf. Table 3.3), which is of the first order in the square lattice[25, 26] but seems to be of the second order in the single-chain lattice.

In order to avoid thermal breakdown, we consider different treatment of the $O(S^0)$ interaction (2.8). We propose decomposing the $O(S^0)$ interaction (2.8) based on the Wick Theorem. If we apply TDD-MWDISW theory, we read $\langle\!\langle\mathcal{S}\rangle\!\rangle$ and $\langle\!\langle\mathcal{S}'\rangle\!\rangle$ as the quantum average in the magnon vacuum

$$\langle\mathcal{S}\rangle_0=\sqrt{Ss}+\epsilon\,(\tilde{p})+(\tilde{p}-p)\tau\,(\tilde{p})\,,\qquad\qquad \langle\mathcal{S}'\rangle_0=q\tau\,(\tilde{p})\,, \tag{3.75}$$

respectively. We only have to solve Eqs. (3.63) and (3.66) with two unknowns, $\tilde{p}$ and $\tilde{p}'$. The thus-obtained ferrimagnetic DC-TDD-MWDISW thermodynamics is also shown in Fig. 3.6. It closely resembles the DC-TDD-MHFISW thermodynamics at low temperatures but remains free from any thermal breakdown with increasing temperature. It is much better than the MLSW description in reproducing many thermal features including the Schottky-like peak of C. We show in Fig. 3.7 the DC-TDD-MSW calculations of thermodynamic quantities for the ferrimagnetic Hamiltonian (2.1) on the two-leg-ladder lattice in comparison with QMC estimates.

3.2.3 Low-temperature series expansion

We further analyze the thermodynamic quantities by expanding them into low-temperature series. Keeping in mind that the gapful antiferromagnetic excitations $\bar{n}^{+}_{k_\nu}$ are all irrelevant to the low-temperature thermodynamics. The lower branch

$$\varepsilon^{-}_{\boldsymbol{\kappa}_\nu}(\tilde{p},\tilde{p}')=zJ\langle\!\langle\mathcal{S}\rangle\!\rangle\left[\omega_{\boldsymbol{\kappa}_\nu}(\tilde{p})-\tilde{p}'\right]=zJ\langle\!\langle\mathcal{S}\rangle\!\rangle\left[\omega_{\boldsymbol{\kappa}_\nu}(\tilde{p})-\tilde{q}-(\tilde{p}'-\tilde{q})\right], \tag{3.76}$$

has always gapless part $\omega_{\boldsymbol{\kappa}_\nu}(\tilde{p})-\tilde{q}$.

In the thermodynamic limit on the single-chain lattice, a state-density function (3.10) becomes

$$\lim_{N\to\infty}\widetilde{w}(x)=\frac{2}{\pi}\frac{x+\tilde{q}}{\sqrt{\tilde{p}^2-(x+\tilde{q})^2}}\frac{1}{\sqrt{x(x+2\tilde{q})}}\equiv 2\sum_{l=0}^{\infty}\widetilde{w}_l^{(1)}x^{l-\frac{1}{2}}, \tag{3.77}$$

$$\widetilde{w}_0^{(1)} = \frac{\tilde{q}}{\pi\sqrt{2\tilde{q}}}, \quad \widetilde{w}_1^{(1)} = \frac{1}{\pi\sqrt{2\tilde{q}}}\left(\tilde{p}^2 - \frac{1}{4}\right), \quad \widetilde{w}_2^{(1)} = \frac{1}{\pi\sqrt{2\tilde{q}}}\frac{48\tilde{p}^4 - 56\tilde{p}^2 + 3}{32\tilde{q}}, \tag{3.78}$$

and converts a ν summation into an x integration, such as

$$I_1(\bar{n}^{\pm}_{\boldsymbol{\kappa}_\nu};\tilde{p}) = \tilde{q}\sum_{l=0}^{\infty}\sum_{l'=0}^{1}\frac{\widetilde{w}_l^{(1)}}{\tilde{q}^{l'}}F_{l+l'+\frac{1}{2}}\left(v,t\right), \tag{3.79}$$

$$I_2(\bar{n}^{\pm}_{\boldsymbol{\kappa}_\nu};\tilde{p}) = \frac{\tilde{p}}{\tilde{q}}\sum_{l=0}^{\infty}\sum_{l'=0}^{\infty}\frac{\widetilde{w}_l^{(1)}}{(-\tilde{q})^{l'}}F_{l+l'+\frac{1}{2}}\left(v,t\right), \tag{3.80}$$

$$I_3(\bar{n}^{\pm}_{\boldsymbol{\kappa}_\nu}) = \sum_{l=0}^{\infty}\widetilde{w}_l^{(1)}F_{l+\frac{1}{2}}\left(v,t\right), \tag{3.81}$$

$$I_4(\bar{n}^{\pm}_{\boldsymbol{\kappa}_\nu}) = \sum_{l=0}^{\infty}\widetilde{w}_l^{(1)}G_{l+\frac{1}{2}}\left(v,t\right), \tag{3.82}$$

$$\tau\left(\tilde{p}\right) = \frac{1}{2}\left[\frac{2}{\pi}K\left(\frac{1}{\tilde{p}}\right) - 1\right], \tag{3.83}$$

$$\epsilon\left(\tilde{p}\right) = \frac{\tilde{p}}{2}\left[1 - \frac{2}{\pi}E\left(\frac{1}{\tilde{p}}\right)\right], \tag{3.84}$$

where $E(k)$ is the complete elliptic integral of the second kind, and we set the arguments t and v as

$$t \equiv \frac{k_{\mathrm{B}}T}{zJ\langle\!\langle\mathcal{S}\rangle\!\rangle}, \qquad v \equiv -\frac{\tilde{p}' - \tilde{q}}{t}. \tag{3.85}$$

In order to reveal how v and $\tilde{p}$ depend on t, we expand Eq. (3.66)

$$\begin{aligned}\frac{S-s}{2} &= I_3(\bar{n}^{\pm}_{\boldsymbol{\kappa}_\nu}) = \sum_{l=0}^{\infty}\widetilde{w}_l^{(1)}F_{l+\frac{1}{2}}\left(v,t\right)\\ &= \frac{(4\tilde{q}t)^{\frac{1}{2}}}{2\sqrt{2\pi}}\left[\sqrt{\pi}v^{-\frac{1}{2}} + \zeta\left(\frac{1}{2}\right) - \zeta\left(-\frac{1}{2}\right)v + \left(\tilde{p}^2 - \frac{1}{4}\right)\frac{t}{2\tilde{q}}\zeta\left(\frac{3}{2}\right) + \cdots\right].\end{aligned} \tag{3.86}$$

We solve Eq. (3.86) for v in an iterative manner,

$$v^{\frac{1}{2}} = \frac{\sqrt{2\tilde{q}t}}{S-s}\left\{1 + \frac{\zeta\left(\frac{1}{2}\right)}{\sqrt{2\pi}}\frac{2\sqrt{\tilde{q}t}}{S-s} + \left[\frac{\zeta\left(\frac{1}{2}\right)}{\sqrt{2\pi}}\frac{2\sqrt{\tilde{q}t}}{S-s}\right]^2 + \cdots\right\}. \tag{3.87}$$

Inserting this t dependence into Eqs. (3.79), (3.80) and (3.82) yields

$$\begin{aligned}I_1(\bar{n}^{\pm}_{\boldsymbol{\kappa}_\nu};\tilde{p}) = \tilde{q}\frac{S-s}{2} &+ \frac{1}{2\tilde{q}}\frac{\zeta\left(\frac{3}{2}\right)}{\sqrt{2\pi}}(\tilde{q}t)^{\frac{3}{2}} - \frac{1}{(S-s)\tilde{q}}(\tilde{q}t)^2\\ &- \frac{3}{4\tilde{q}}\left[\frac{4}{(S-s)^2}\frac{\zeta\left(\frac{1}{2}\right)}{\sqrt{2\pi}} - \left(1 + \frac{3}{4\tilde{q}^2}\right)\frac{\zeta\left(\frac{5}{2}\right)}{\sqrt{2\pi}}\right](\tilde{q}t)^{\frac{5}{2}} + \cdots,\end{aligned} \tag{3.88}$$

$$I_2(\bar{n}^{\pm}_{\boldsymbol{\kappa}_\nu};\tilde{p}) = \frac{(S-s)\tilde{p}}{2\tilde{q}} - \frac{\zeta\left(\frac{3}{2}\right)}{\sqrt{2\pi}}\frac{\tilde{p}t^{\frac{3}{2}}}{2\tilde{q}^{\frac{3}{2}}} + \frac{\tilde{p}t^2}{(S-s)\tilde{q}} + \cdots, \tag{3.89}$$

Table 3.4: Leading coefficients of the up-to-$O(S^0)$ internal energy E/NzJ expanded in powers of $(k_{\mathrm{B}}T/J)^{\frac{1}{2}}$ in the DC-TDD-MSW theory for the Hamiltonian (2.1) on the single-chain lattice with various S and s [cf. Eq. (3.105)].

(S,s)	Scheme	$-\phi(\tilde{p}_0)^2$	$e_{\frac{3}{2}}\left(\frac{\tilde{q}_0}{2\varsigma_0}\right)^{\frac{3}{2}}$	$e_2\left(\frac{\tilde{q}_0}{2\varsigma_0}\right)^2$	$e_{\frac{5}{2}}\left(\frac{\tilde{q}_0}{2\varsigma_0}\right)^{\frac{5}{2}}$
	DC TDD MLSW	-0.72763	0.38158	-0.88902	2.2938
$(1,\frac{1}{2})$	DC TDD MHFISW	-0.72763	0.28800	-0.61090	1.4351
	DC TDD MWDISW	-0.72763	0.28515	-0.60288	1.4116
	DC TDD MLSW	-0.98378	0.38433	-0.47496	0.83581
$(\frac{3}{2},\frac{1}{2})$	DC TDD MHFISW	-0.98378	0.31356	-0.36209	0.59541
	DC TDD MWDISW	-0.98378	0.31127	-0.35856	0.58815
	DC TDD MLSW	-1.9314	0.20405	-0.27025	0.50969
$(\frac{3}{2},1)$	DC TDD MHFISW	-1.9314	0.16881	-0.20989	0.37162
	DC TDD MWDISW	-1.9314	0.16825	-0.20896	0.36956
	DC TDD MLSW	-2.4471	0.22651	-0.17081	0.25018
$(2,1)$	DC TDD MHFISW	-2.4471	0.19470	-0.13960	0.19441
	DC TDD MWDISW	-2.4471	0.19406	-0.13899	0.19335

$$I_4(\bar{n}^{\pm}_{\boldsymbol{\kappa}_\nu}) = \frac{(S-s)^3}{8}(\tilde{q}t)^{-1} - \frac{3(S-s)^2}{4}\frac{\zeta\left(\frac{1}{2}\right)}{\sqrt{2\pi}}(\tilde{q}t)^{-\frac{1}{2}} + \frac{3(S-s)}{2}\left[\frac{\zeta\left(\frac{1}{2}\right)}{\sqrt{2\pi}}\right]^2 + \cdots . \tag{3.90}$$

In order to reveal how $\tilde{p}$ depends on t, we expand Eq. (3.63)

$$\begin{aligned}\frac{S+s}{2} &= \tau\left(\tilde{p}\right) + I_2(\bar{n}^{\pm}_{\boldsymbol{\kappa}_\nu};\tilde{p}) \\ &= \tau\left(\tilde{p}\right) + \frac{(S-s)\tilde{p}}{2\tilde{q}} - \frac{\zeta\left(\frac{3}{2}\right)}{\sqrt{2\pi}}\frac{\tilde{p}t^{\frac{3}{2}}}{2\tilde{q}^{\frac{3}{2}}} + \frac{\tilde{p}t^2}{(S-s)\tilde{q}} + \cdots ,\end{aligned} \tag{3.91}$$

and then we have

$$\tilde{p} = \tilde{p}_0 + O(t^{\frac{3}{2}}), \quad \tilde{q} = \tilde{q}_0 + O(t^{\frac{3}{2}}), \tag{3.92}$$

$$\epsilon\left(\tilde{p}\right) = \epsilon\left(\tilde{p}_0\right) + O(t^{\frac{3}{2}}), \quad \tau\left(\tilde{p}\right) = \tau\left(\tilde{p}_0\right) + O(t^{\frac{3}{2}}), \tag{3.93}$$

$$\phi\left(\tilde{p}\right) = \phi\left(\tilde{p}_0\right) + O(t^3), \tag{3.94}$$

where we introduce

$$\phi\left(\tilde{p}\right) \equiv \sqrt{Ss} + \epsilon\left(\tilde{p}\right) + (\tilde{p}-p)\frac{S+s}{2} - (\tilde{q}-q)\frac{S-s}{2}, \tag{3.95}$$

and $\tilde{q}_0 \equiv \sqrt{\tilde{p}_0^2 - 1}$ is determined by solving

$$S + s - \frac{\tilde{p}_0}{\tilde{q}_0}(S-s) = 2\tau\left(\tilde{p}_0\right) = \frac{2}{\pi}K\left(\frac{1}{\tilde{p}_0}\right) - 1. \tag{3.96}$$

Table 3.5: Leading coefficients of susceptibility-temperature product $\chi k_{\mathrm{B}}T/L(g\mu_{\mathrm{B}})^2$ expanded in powers of $(k_{\mathrm{B}}T/J)^{\frac{1}{2}}$ in the DC-TDD-MSW theory for the Hamiltonian (2.1) on the single-chain lattice with various S and s [cf. Eq. (3.106)].

(S,s)	Scheme	$c_{-1}\left(\frac{\tilde{q}_0}{2\varsigma_0}\right)^{-1}$	$c_{-\frac{1}{2}}\left(\frac{\tilde{q}_0}{2\varsigma_0}\right)^{-\frac{1}{2}}$	$c_0\left(\frac{\tilde{q}_0}{2\varsigma_0}\right)^{0}$
	DC TDD MLSW	0.014135	0.059985	0.084855
$(1,\frac{1}{2})$	DC TDD MHFISW	0.017051	0.065884	0.084855
	DC TDD MWDISW	0.017164	0.066102	0.084855
	DC TDD MLSW	0.10047	0.22617	0.16971
$(\frac{3}{2},\frac{1}{2})$	DC TDD MHFISW	0.11507	0.24205	0.16971
	DC TDD MWDISW	0.11564	0.24264	0.16971
	DC TDD MLSW	0.043737	0.10552	0.084855
$(\frac{3}{2},1)$	DC TDD MHFISW	0.049628	0.11240	0.084855
	DC TDD MWDISW	0.049739	0.11252	0.084855
	DC TDD MLSW	0.26983	0.37064	0.16971
$(2,1)$	DC TDD MHFISW	0.29847	0.38982	0.16971
	DC TDD MWDISW	0.29912	0.39025	0.16971

Inserting these t dependences into Eqs. (3.88) and (3.90) yields

$$I_1(\bar{n}^{\pm}_{\boldsymbol{\kappa}_\nu};\tilde{p})-\tilde{q}\frac{S-s}{2}=\frac{1}{2\tilde{q}_0}\frac{\zeta\left(\frac{3}{2}\right)}{\sqrt{2\pi}}(\tilde{q}_0t)^{\frac{3}{2}}-\frac{1}{(S-s)\tilde{q}_0}(\tilde{q}_0t)^2 -\frac{3}{4\tilde{q}_0}\left[\frac{4}{(S-s)^2}\frac{\zeta\left(\frac{1}{2}\right)}{\sqrt{2\pi}}-\left(1+\frac{3}{4\tilde{q}_0^2}\right)\frac{\zeta\left(\frac{5}{2}\right)}{\sqrt{2\pi}}\right](\tilde{q}_0t)^{\frac{5}{2}}+O(t^3), \tag{3.97}$$

$$I_4(\bar{n}^{\pm}_{\boldsymbol{\kappa}_\nu})=\frac{(S-s)^3}{8}(\tilde{q}_0t)^{-1}-\frac{3(S-s)^2}{4}\frac{\zeta\left(\frac{1}{2}\right)}{\sqrt{2\pi}}(\tilde{q}_0t)^{-\frac{1}{2}} +\frac{3(S-s)}{2}\left[\frac{\zeta\left(\frac{1}{2}\right)}{\sqrt{2\pi}}\right]^2+O(t^{\frac{1}{2}}). \tag{3.98}$$

In ferrimagnets, thermodynamic quantities, Eqs. (2.36), (2.39) and (2.40), read

$$\sum_{l=0}^{2}\frac{\langle\mathcal{H}^{(l)}\rangle_T}{NzJ}=-\left\{\phi(\tilde{p})-\left[I_1(\bar{n}^{\pm}_{\boldsymbol{\kappa}_\nu};\tilde{p})-\tilde{q}\frac{S-s}{2}\right]\right\}^2, \tag{3.99}$$

$$\frac{\chi^{xx}k_{\mathrm{B}}T}{L(g\mu_{\mathrm{B}})^2}=\frac{\chi^{yy}k_{\mathrm{B}}T}{L(g\mu_{\mathrm{B}})^2}=0,\quad \frac{\chi^{zz}k_{\mathrm{B}}T}{L(g\mu_{\mathrm{B}})^2}=I_4(\bar{n}^{\pm}_{\boldsymbol{\kappa}_\nu}). \tag{3.100}$$

Substituting (3.94), (3.97) and (3.98) into these quantities yields

$$\sum_{l=0}^{2}\frac{\langle\mathcal{H}^{(l)}\rangle_T}{NzJ}=-\phi(\tilde{p}_0)^2+\sum_{l=3}^{5}e_{\frac{l}{2}}(\tilde{q}_0t)^{\frac{l}{2}}+O(t^3); \tag{3.101}$$

$$e_{\frac{3}{2}}=\frac{\phi(\tilde{p}_0)}{\tilde{q}_0}\frac{\zeta\left(\frac{3}{2}\right)}{\sqrt{2\pi}},\ e_2=-\frac{2\phi(\tilde{p}_0)}{(S-s)\tilde{q}_0},\ e_{\frac{5}{2}}=-\frac{3\phi(\tilde{p}_0)}{2\tilde{q}_0}\left[\frac{4}{(S-s)^2}\frac{\zeta\left(\frac{1}{2}\right)}{\sqrt{2\pi}}-\left(1+\frac{3}{4\tilde{q}_0^2}\right)\frac{\zeta\left(\frac{5}{2}\right)}{\sqrt{2\pi}}\right],$$

$$\frac{\chi k_{\mathrm{B}} T}{L(g\mu_{\mathrm{B}})^2} = \sum_{l=-2}^{0} c_{\frac{l}{2}} (\tilde{q}_0 t)^{\frac{l}{2}} + O(t^{\frac{1}{2}}); \tag{3.102}$$

$$c_{-1} = \frac{(S-s)^3}{24},\ c_{-\frac{1}{2}} = -\frac{(S-s)^2}{4} \frac{\zeta\left(\frac{1}{2}\right)}{\sqrt{2\pi}},\ c_0 = \frac{S-s}{2} \left[\frac{\zeta\left(\frac{1}{2}\right)}{\sqrt{2\pi}}\right]^2.$$

The dependence of the renormalized temperature $t = k_{\mathrm{B}} T / zJ \langle\!\langle \mathcal{S} \rangle\!\rangle$ on the bare temperature T is yet to be clarified. While $\langle\!\langle \mathcal{S} \rangle\!\rangle$ varies depending on the formulation as

$$\langle\!\langle \mathcal{S} \rangle\!\rangle = \begin{cases} \langle \mathcal{S} \rangle_0' = \sqrt{Ss} & \text{(DC TDD MLSW)}, \\ \langle \mathcal{S} \rangle_T = \sqrt{Ss} + \epsilon(\tilde{p}_0) + (\tilde{p}_0 - p)\dfrac{S+s}{2} \\ \qquad\qquad - (\tilde{q}_0 - q)\dfrac{S-s}{2} + O(t^{\frac{3}{2}}) & \text{(DC TDD MHFISW)}, \\ \langle \mathcal{S} \rangle_0 = \sqrt{Ss} + \epsilon(\tilde{p}_0) + (\tilde{p}_0 - p)\tau(\tilde{p}_0) + O(t^{\frac{3}{2}}) & \text{(DC TDD MWDISW)}, \end{cases} \tag{3.103}$$

the nonlinearity of t as a function of T, if any, is not so high as to affect the leading expansion coefficients in Eqs. (3.101) and (3.102) in any case,

$$t = \frac{k_{\mathrm{B}} T}{z\varsigma_0 J} \left[1 + O(T^{\frac{3}{2}})\right], \tag{3.104}$$

where $\varsigma_0 \equiv \lim_{T\to 0} \langle\!\langle \mathcal{S} \rangle\!\rangle$. We eventually have

$$\sum_{l=0}^{2} \frac{\langle \mathcal{H}^{(l)} \rangle_T}{NzJ} = -\phi(\tilde{p}_0)^2 + \sum_{l=3}^{5} e_{\frac{l}{2}} \left(\frac{\tilde{q}_0}{z\varsigma_0} \frac{k_{\mathrm{B}} T}{J}\right)^{\frac{l}{2}} + O(T^3), \tag{3.105}$$

$$\frac{\chi k_{\mathrm{B}} T}{L(g\mu_{\mathrm{B}})^2} = \sum_{l=-2}^{0} c_{\frac{l}{2}} \left(\frac{\tilde{q}_0}{z\varsigma_0} \frac{k_{\mathrm{B}} T}{J}\right)^{\frac{l}{2}} + O(T^{\frac{1}{2}}). \tag{3.106}$$

Numerical calculations of the low-temperature series expansion coefficients are listed in Tables 3.4 and 3.5. The leading bare-temperature series expansion coefficients for C and χ in the DC-TDD-MHFISW and DC-TDD-MWDISW descriptions coincide with each other within an error of about one percent and such a small difference is invisible in Figs. 3.6 and 3.7. In the antiferromagnetic cases, they are exactly the same within the first two terms. However, the DC-TDD-MHFISW theory rapidly deviates from the DC-TDD-MWDISW theory with increasing temperature and soon loses its validity.

The TID-MSW thermodynamics on the single-chain lattice is shown in Fig. 3.8. We are fully convinced that the DC condition is a key requirement for precisely reproducing the thermodynamic properties in the TDD-MSW theory. We are hence surprised to find that TID MSWs under the DC condition, regardless of whether linear or interacting, completely fail to reproduce any thermal features. They misinterpret the specific heat as double-peaked. Such behavior does not occur in the SC-TID-MSW theory. We introduce some functions of $\tilde{p}_{\mathrm{csw}}$

$$\begin{aligned} \varphi(\tilde{p}_{\mathrm{csw}}) &= \sqrt{Ss} + \epsilon(\tilde{p}_{\mathrm{csw}}) + (\tilde{p}_{\mathrm{csw}} - p)\frac{S+s}{2} \\ &\qquad - (\tilde{q}_{\mathrm{csw}} - q)\frac{\tilde{q}_{\mathrm{csw}}[S+s-2\tau(\tilde{p}_{\mathrm{csw}})]}{2\tilde{p}_{\mathrm{csw}}}, \end{aligned} \tag{3.107}$$

$$\varphi'(\tilde{p}_{\mathrm{csw}}) = q\frac{S+s}{2} - p\frac{\tilde{q}_{\mathrm{csw}}[S+s-2\tau(\tilde{p}_{\mathrm{csw}})]}{2\tilde{p}_{\mathrm{csw}}}, \tag{3.108}$$

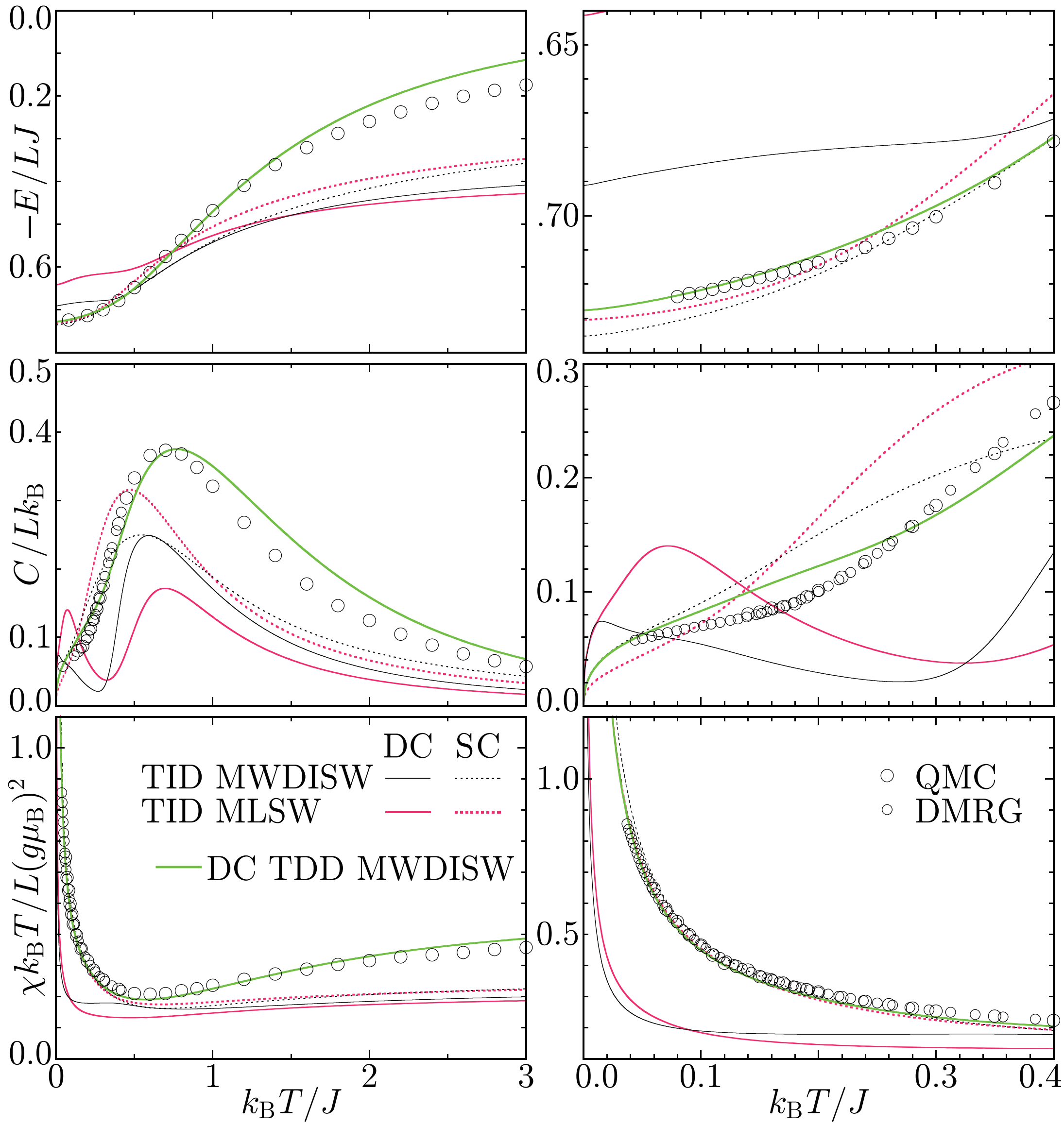

Fig. 3.8: TID-MSW calculations of the internal energy E, specific heat C, and uniform susceptibility χ as functions of temperature for the Hamiltonian (2.1) on the single-chain lattice with $(S,s)=(1,\frac{1}{2})$, the former two of which are defined with the up-to-$O(S^0)$ Hamiltonian. The findings with various approximation schemes are compared with QMC and DMRG calculations.[47)]

and the renormalized temperature t

$$\begin{aligned} t \equiv& \frac{k_{\mathrm{B}}T}{zJ\langle\!\langle \mathcal{S}\rangle\!\rangle}\frac{\tilde{q}_{\mathrm{csw}}}{2\tilde{q}_{\mathrm{csw}}-\tilde{p}'_{\mathrm{csw}}}\left[1+\frac{1}{2\tilde{q}_{\mathrm{csw}}-\tilde{p}'_{\mathrm{csw}}}\left(\frac{\tilde{p}_{\mathrm{csw}}}{\tilde{q}_{\mathrm{csw}}}\frac{\mu_{\mathrm{A}}-\mu_{\mathrm{B}}}{2zJ\langle\!\langle \mathcal{S}\rangle\!\rangle}+\tilde{p}'_{\mathrm{csw}}-\tilde{q}_{\mathrm{csw}}\right)\right]^{-1} \\ =& \frac{k_{\mathrm{B}}T}{zJ\langle\!\langle \mathcal{S}\rangle\!\rangle}\left(1+\frac{\tilde{p}_{\mathrm{csw}}}{\tilde{q}^2_{\mathrm{csw}}}\frac{\mu_{\mathrm{A}}-\mu_{\mathrm{B}}}{2zJ\langle\!\langle \mathcal{S}\rangle\!\rangle}\right)^{-1} = \frac{k_{\mathrm{B}}T}{zJ\langle\!\langle \mathcal{S}\rangle\!\rangle}\frac{\tilde{q}_{\mathrm{csw}}}{2\tilde{q}_{\mathrm{csw}}-\tilde{p}'_{\mathrm{csw}}}\left[1+O(T^2)\right], \end{aligned} \tag{3.109}$$

with scheme-dependent average

$$\langle\!\langle \mathcal{S}\rangle\!\rangle = \begin{cases} \sqrt{Ss} & \text{(SC TID MLSW)}, \\ \sqrt{Ss}+\epsilon\left(\tilde{p}_{\mathrm{csw}}\right)+(\tilde{p}_{\mathrm{csw}}-p)\tau\left(\tilde{p}_{\mathrm{csw}}\right) & \text{(SC TID MWDISW)}. \end{cases} \tag{3.110}$$

Table 3.6: Leading coefficients of the up-to-$O(S^0)$ internal energy E/NzJ expanded in powers of $(k_{\mathrm{B}}T/J)^{\frac{1}{2}}$ in the SC-TID-MSW theory for the Hamiltonian (2.1) on the single-chain lattice with various S and s [cf. Eq. (3.114)].

(S,s)	Scheme	$-\varphi(\tilde{p}_{\mathrm{csw}})^2$ $+\varphi'(\tilde{p}_{\mathrm{csw}})^2$	$\tilde{e}_{\frac{3}{2}}\left(\frac{\tilde{q}_{\mathrm{CSW}}}{2\varsigma}\right)^{\frac{3}{2}}$	$\tilde{e}_2\left(\frac{\tilde{q}_{\mathrm{CSW}}}{2\varsigma}\right)^{2}$	$\tilde{e}_{\frac{5}{2}}\left(\frac{\tilde{q}_{\mathrm{CSW}}}{2\varsigma}\right)^{\frac{5}{2}}$
$(1,\frac{1}{2})$	SC TID MLSW	-0.73042	0.19825	-0.64104	2.3386
	SC TID MWDISW	-0.73518	0.29979	-0.71805	1.8140
$(\frac{3}{2},\frac{1}{2})$	SC TID MLSW	-0.98491	0.27200	-0.37043	0.74403
	SC TID MWDISW	-0.98921	0.33410	-0.39605	0.63978
$(\frac{3}{2},1)$	SC TID MLSW	-1.9338	0.11352	-0.19902	0.54508
	SC TID MWDISW	-1.9371	0.17984	-0.24911	0.44624
$(2,1)$	SC TID MLSW	-2.4486	0.16221	-0.13813	0.24891
	SC TID MWDISW	-2.4526	0.20958	-0.15566	0.20728

The SC-TID-MSW theory indeed expands the thermodynamic quantities into low-temperature series similar to Eqs. (3.101) and (3.102),

$$\sum_{l=0}^{2}\frac{\langle\mathcal{H}^{(l)}\rangle_T}{NzJ}=-\varphi\left(\tilde{p}_{\mathrm{csw}}\right)^2+\varphi'\left(\tilde{p}_{\mathrm{csw}}\right)^2+\sum_{l=3}^{5}e_{\frac{l}{2}}(\tilde{q}_{\mathrm{csw}}t)^{\frac{l}{2}}+O(t^3), \tag{3.111}$$

$$e_{\frac{3}{2}}=\frac{(2\tilde{q}_{\mathrm{csw}}-q)\varphi\left(\tilde{p}_{\mathrm{csw}}\right)-p\varphi'\left(\tilde{p}_{\mathrm{csw}}\right)}{\tilde{q}_{\mathrm{csw}}^2}\frac{\zeta(\frac{3}{2})}{\sqrt{2\pi}},$$

$$e_2=-\frac{2[(2\tilde{q}_{\mathrm{csw}}-q)\varphi\left(\tilde{p}_{\mathrm{csw}}\right)-p\varphi'\left(\tilde{p}_{\mathrm{csw}}\right)]}{\tilde{q}_{\mathrm{csw}}^2}\left(\frac{\tilde{q}_{\mathrm{csw}}[S+s-2\tau\left(\tilde{p}_{\mathrm{csw}}\right)]}{\tilde{p}_{\mathrm{csw}}}\right)^{-1},$$

$$e_{\frac{5}{2}}=-\frac{3[(2\tilde{q}_{\mathrm{csw}}-q)\varphi\left(\tilde{p}_{\mathrm{csw}}\right)-p\varphi'\left(\tilde{p}_{\mathrm{csw}}\right)]}{2\tilde{q}_{\mathrm{csw}}^2}\Bigg\{4\left(\frac{\tilde{q}_{\mathrm{csw}}[S+s-2\tau\left(\tilde{p}_{\mathrm{csw}}\right)]}{\tilde{p}_{\mathrm{csw}}}\right)^{-2}\frac{\zeta(\frac{1}{2})}{\sqrt{2\pi}}$$
$$-\left[1+\frac{3}{4\tilde{q}_{\mathrm{csw}}^2}-\frac{1}{\tilde{q}_{\mathrm{csw}}^2}\frac{(\tilde{q}_{\mathrm{csw}}-q)\varphi\left(\tilde{p}_{\mathrm{csw}}\right)-p\varphi'\left(\tilde{p}_{\mathrm{csw}}\right)}{(2\tilde{q}_{\mathrm{csw}}-q)\varphi\left(\tilde{p}_{\mathrm{csw}}\right)-p\varphi'\left(\tilde{p}_{\mathrm{csw}}\right)}-\frac{5}{2}\frac{1}{\tilde{q}_{\mathrm{csw}}^2}\frac{\tilde{p}'_{\mathrm{csw}}-\tilde{q}_{\mathrm{csw}}}{2\tilde{q}_{\mathrm{csw}}-\tilde{p}'_{\mathrm{csw}}}\right]\frac{\zeta(\frac{5}{2})}{\sqrt{2\pi}}\Bigg\},$$

$$\frac{1}{3}\frac{\chi^{\lambda\lambda}k_{\mathrm{B}}T}{L(g\mu_{\mathrm{B}})^2}=\sum_{l=-2}^{0}c_{\frac{l}{2}}^{\lambda\lambda}(\tilde{q}_{\mathrm{csw}}t)^{\frac{l}{2}}+O(t^{\frac{1}{2}})\qquad(\lambda=x,y,z), \tag{3.112}$$

$$c_{-1}^{xx}=c_{-1}^{yy}=\frac{1}{12}\left[\frac{\tilde{q}_{\mathrm{csw}}+q}{2\tilde{q}_{\mathrm{csw}}}\left(S-s-\frac{\tilde{q}_{\mathrm{csw}}[S+s-2\tau\left(\tilde{p}_{\mathrm{csw}}\right)]}{\tilde{p}_{\mathrm{csw}}}\right)\right]\left(\frac{\tilde{q}_{\mathrm{csw}}[S+s-2\tau\left(\tilde{p}_{\mathrm{csw}}\right)]}{\tilde{p}_{\mathrm{csw}}}\right)^2,$$

$$c_{-\frac{1}{2}}^{xx}=c_{-\frac{1}{2}}^{yy}=-\frac{1}{3}\left[\frac{\tilde{q}_{\mathrm{csw}}+q}{2\tilde{q}_{\mathrm{csw}}}\left(S-s-\frac{\tilde{q}_{\mathrm{csw}}[S+s-2\tau\left(\tilde{p}_{\mathrm{csw}}\right)]}{\tilde{p}_{\mathrm{csw}}}\right)\right]$$
$$\times\left(\frac{\tilde{q}_{\mathrm{csw}}[S+s-2\tau\left(\tilde{p}_{\mathrm{csw}}\right)]}{\tilde{p}_{\mathrm{csw}}}\right)\frac{\zeta(\frac{1}{2})}{\sqrt{2\pi}},$$

$$c_0^{xx}=c_0^{yy}=\frac{1}{6}\left[\frac{\tilde{q}_{\mathrm{csw}}+q}{2\tilde{q}_{\mathrm{csw}}}\left(S-s-\frac{\tilde{q}_{\mathrm{csw}}[S+s-2\tau\left(\tilde{p}_{\mathrm{csw}}\right)]}{\tilde{p}_{\mathrm{csw}}}\right)\right]\left\{2\left[\frac{\zeta(\frac{1}{2})}{\sqrt{2\pi}}\right]^2-\frac{1}{2}\frac{\tilde{q}_{\mathrm{csw}}-q}{\tilde{q}_{\mathrm{csw}}+q}\right\},$$

Table 3.7: Leading coefficients of susceptibility-temperature product $\chi k_{\mathrm{B}}T/L(g\mu_{\mathrm{B}})^2$ expanded in powers of $(k_{\mathrm{B}}T/J)^{\frac{1}{2}}$ in the SC-TID-MSW theory for the Hamiltonian (2.1) on the single-chain lattice with various S and s [cf. Eq. (3.115)].

(S,s)	Scheme	$\tilde{c}_{-1}\left(\frac{\tilde{q}_{\mathrm{CSW}}}{2\varsigma}\right)^{-1}$	$\tilde{c}_{-\frac{1}{2}}\left(\frac{\tilde{q}_{\mathrm{CSW}}}{2\varsigma}\right)^{-\frac{1}{2}}$	$\tilde{c}_{0}\left(\frac{\tilde{q}_{\mathrm{CSW}}}{2\varsigma}\right)^{0}$
$(1,\frac{1}{2})$	SC TID MLSW	0.016287	0.072503	0.096353
	SC TID MWDISW	0.019274	0.072178	0.086127
$(\frac{3}{2},\frac{1}{2})$	SC TID MLSW	0.12901	0.26901	0.18026
	SC TID MWDISW	0.12527	0.25466	0.17124
$(\frac{3}{2},1)$	SC TID MLSW	0.052520	0.12861	0.095265
	SC TID MWDISW	0.055386	0.12180	0.086074
$(2,1)$	SC TID MLSW	0.34063	0.43942	0.18121
	SC TID MWDISW	0.32187	0.40848	0.17136

$$c_{-1}^{zz}=\frac{1}{24}\left\{\frac{\tilde{q}_{\mathrm{csw}}[S+s-2\tau(\tilde{p}_{\mathrm{csw}})]}{\tilde{p}_{\mathrm{csw}}}\right\}^3,\quad c_{-\frac{1}{2}}^{zz}=-\frac{1}{4}\left\{\frac{\tilde{q}_{\mathrm{csw}}[S+s-2\tau(\tilde{p}_{\mathrm{csw}})]}{\tilde{p}_{\mathrm{csw}}}\right\}^2\frac{\zeta(\frac{1}{2})}{\sqrt{2\pi}},$$
$$c_{0}^{zz}=\frac{1}{2}\left\{\frac{\tilde{q}_{\mathrm{csw}}[S+s-2\tau(\tilde{p}_{\mathrm{csw}})]}{\tilde{p}_{\mathrm{csw}}}\right\}\left[\frac{\zeta(\frac{1}{2})}{\sqrt{2\pi}}\right]^2.$$

The renormalized temperature t depends on the formulation

$$t=\frac{k_{\mathrm{B}}T}{zJ\varsigma}\left[1+O(T^2)\right];\qquad \varsigma\equiv\langle\!\langle\mathcal{S}\rangle\!\rangle\frac{2\tilde{q}_{\mathrm{csw}}-\tilde{p}'_{\mathrm{csw}}}{\tilde{q}_{\mathrm{csw}}}. \tag{3.113}$$

We eventually have

$$\sum_{l=0}^{2}\frac{\langle\mathcal{H}^{(l)}\rangle_T}{NzJ}=-\varphi(\tilde{p}_{\mathrm{csw}})^2+\varphi'(\tilde{p}_{\mathrm{csw}})^2+\sum_{l=3}^{5}e_{\frac{l}{2}}\left(\frac{\tilde{q}_{\mathrm{csw}}}{z\varsigma}\frac{k_{\mathrm{B}}T}{J}\right)^{\frac{l}{2}}+O(T^3), \tag{3.114}$$
$$\frac{1}{3}\frac{\chi^{\lambda\lambda}k_{\mathrm{B}}T}{L(g\mu_{\mathrm{B}})^2}=\sum_{l=-2}^{0}c_{\frac{l}{2}}^{\lambda\lambda}\left(\frac{\tilde{q}_{\mathrm{csw}}}{z\varsigma}\frac{k_{\mathrm{B}}T}{J}\right)^{\frac{l}{2}}+O(T^{\frac{1}{2}})\qquad(\lambda=x,y,z). \tag{3.115}$$

Numerical calculations of the low-temperature series expansion coefficients are listed in Tables 3.6 and 3.7. Comparing Tables 3.6 and 3.7 with Tables 3.4 and 3.5, we are fully convinced that the SC-TID-MWDISW and DC-TDD-MWDISW findings for C and χT are fairly close to each other at sufficiently low temperatures, as was shown in Fig. 3.8. We find that the SC condition works better than the DC condition in the TID-MSW theory.

Chapter 4

Renormalization

4.1 Magnetic Raman Scattering

We discuss the Raman spectrum of the square-lattice antiferromagnets at zero temperature. The $B_{1\mathrm{g}}$ mode is Raman active, and the Loudon–Fleury (LF)[71] operator has the form

$$\mathcal{R} = \sum_{m=1}^{N}\sum_{l=1}^{z} \Lambda_{\boldsymbol{\delta}_l} \boldsymbol{S}_{\boldsymbol{r}_m} \cdot \boldsymbol{S}_{\boldsymbol{r}_m+\boldsymbol{\delta}_l}, \qquad \Lambda_{\boldsymbol{\delta}_l} = \begin{cases} \Lambda & (\boldsymbol{\delta}_l = \pm\boldsymbol{x}), \\ -\Lambda & (\boldsymbol{\delta}_l = \pm\boldsymbol{y}), \end{cases} \tag{4.1}$$

where $\boldsymbol{x}$ and $\boldsymbol{y}$ are vectors connecting nearest neighbors of x and y directions, respectively. The scattering intensity is given by

$$I(\omega) = \frac{J}{2\pi\hbar}\int_{-\infty}^{\infty} \frac{1}{L}\left\langle \mathcal{R}(t)\mathcal{R}(0)\right\rangle \mathrm{e}^{\mathrm{i}\omega t}\mathrm{d}t, \tag{4.2}$$

where $\mathcal{R}(t) = \mathrm{e}^{\mathrm{i}\mathcal{H}t/\hbar}\mathcal{R}\mathrm{e}^{-\mathrm{i}\mathcal{H}t/\hbar}$ is a time-dependent operator in the Heisenberg picture and $\langle\cdots\rangle$ is a quantum average in the true ground state.

Via the HP transformation (2.2), the LF operator (4.1) is expanded into the series

$$\mathcal{R} = \mathcal{R}^{(2)} + \mathcal{R}^{(1)} + \mathcal{R}^{(0)} + O(S^{-1}), \tag{4.3}$$

where $\mathcal{R}^{(l)}$, on the order of S^l, reads

$$\mathcal{R}^{(2)} = 0, \tag{4.4}$$

$$\mathcal{R}^{(1)} = S\sum_{m=1}^{N}\sum_{l=1}^{z}\Lambda_{\boldsymbol{\delta}_l}\left(a_{\boldsymbol{r}_m}^{\dagger}a_{\boldsymbol{r}_m} + b_{\boldsymbol{r}_m+\boldsymbol{\delta}_l}^{\dagger}b_{\boldsymbol{r}_m+\boldsymbol{\delta}_l} + a_{\boldsymbol{r}_m}^{\dagger}b_{\boldsymbol{r}_m+\boldsymbol{\delta}_l}^{\dagger} + a_{\boldsymbol{r}_m}b_{\boldsymbol{r}_m+\boldsymbol{\delta}_l}\right), \tag{4.5}$$

$$\begin{aligned}\mathcal{R}^{(0)} = -\frac{1}{4}\sum_{m=1}^{N}\sum_{l=1}^{z}\Lambda_{\boldsymbol{\delta}_l}\Big[& a_{\boldsymbol{r}_m}^{\dagger}\left(a_{\boldsymbol{r}_m} + b_{\boldsymbol{r}_m+\boldsymbol{\delta}_l}^{\dagger}\right)^2 b_{\boldsymbol{r}_m+\boldsymbol{\delta}_l} \\ &+ b_{\boldsymbol{r}_m+\boldsymbol{\delta}_l}^{\dagger}\left(a_{\boldsymbol{r}_m}^{\dagger} + b_{\boldsymbol{r}_m+\boldsymbol{\delta}_l}\right)^2 a_{\boldsymbol{r}_m}\Big].\end{aligned} \tag{4.6}$$

Using the Wick theorem, the $O(S^0)$ quartic LF operator (4.6) is decomposed into quadratic terms,

$$\mathcal{R}^{(0)} = :\mathcal{R}^{(0)}: + \mathcal{R}_{\mathrm{BL}}^{(0)}, \tag{4.7}$$

where we introduce the $O(S^0)$ bilinear LF operator

$$\mathcal{R}^{(0)}_{\mathrm{BL}} \equiv \left(\langle \mathcal{S}\rangle_0 - S\right) \sum_{m=1}^{N}\sum_{l=1}^{z} \Lambda_{\boldsymbol{\delta}_l} \left(a^\dagger_{\boldsymbol{r}_m} a_{\boldsymbol{r}_m} + b^\dagger_{\boldsymbol{r}_m+\boldsymbol{\delta}_l} b_{\boldsymbol{r}_m+\boldsymbol{\delta}_l} + a^\dagger_{\boldsymbol{r}_m} b^\dagger_{\boldsymbol{r}_m+\boldsymbol{\delta}_l} + a_{\boldsymbol{r}_m} b_{\boldsymbol{r}_m+\boldsymbol{\delta}_l} \right). \tag{4.8}$$

The bosonic LF operator (4.3) is decomposed into the quadratic LF operator

$$\begin{aligned} \mathcal{R}_{\mathrm{BL}} &\equiv \mathcal{R}^{(2)} + \mathcal{R}^{(1)} + \mathcal{R}^{(0)}_{\mathrm{BL}} \qquad (4.9)\\ &= z\Lambda \langle \mathcal{S}\rangle_0 \sum_{\nu=1}^{N} \widetilde{\gamma}_{\boldsymbol{\kappa}_\nu} \cosh 2\theta_{\boldsymbol{\kappa}_\nu} \Bigg[-\frac{\gamma_{\boldsymbol{\kappa}_\nu}}{|\gamma_{\boldsymbol{\kappa}_\nu}|} \tanh 2\theta_{\boldsymbol{\kappa}_\nu} \left(\alpha^{-\dagger}_{\boldsymbol{\kappa}_\nu} \alpha^{-}_{\boldsymbol{\kappa}_\nu} + \alpha^{+\dagger}_{\boldsymbol{\kappa}_\nu} \alpha^{+}_{\boldsymbol{\kappa}_\nu} \right) \\ &\qquad + \left(\alpha^{-\dagger}_{\boldsymbol{\kappa}_\nu} \alpha^{+\dagger}_{\boldsymbol{\kappa}_\nu} + \alpha^{-}_{\boldsymbol{\kappa}_\nu} \alpha^{+}_{\boldsymbol{\kappa}_\nu} \right) \Bigg], \end{aligned}$$

where we introduce function of $\boldsymbol{\kappa}_\nu$

$$\widetilde{\gamma}_{\boldsymbol{\kappa}_\nu} \equiv \frac{1}{z} \sum_{\sigma=\pm} \left(\mathrm{e}^{\sigma \mathrm{i} \boldsymbol{\kappa}_\nu \cdot \boldsymbol{x}} - \mathrm{e}^{\sigma \mathrm{i} \boldsymbol{\kappa}_\nu \cdot \boldsymbol{y}} \right). \tag{4.10}$$

Finally, the bosonic LF operator (4.3) becomes

$$\mathcal{R} = \mathcal{R}_{\mathrm{BL}} + :\mathcal{R}^{(0)}: + O(S^{-1}). \tag{4.11}$$

4.2 Magnon Green's Function

The Green's functions are defined as

$$\mathrm{i}\hbar G_2(\tfrac{\mathbf{12}}{\mathbf{\bar{1}\bar{2}}}, t-\bar{t}) = \langle \mathcal{T}\{ \alpha^{+}_{\mathbf{1}}(t) \alpha^{-}_{\mathbf{2}}(t) \alpha^{+\dagger}_{\mathbf{\bar{1}}}(\bar{t}) \alpha^{-\dagger}_{\mathbf{\bar{2}}}(\bar{t}) \} \rangle, \tag{4.12}$$

$$\mathrm{i}\hbar G_3(\tfrac{\mathbf{123}}{\mathbf{\bar{1}\bar{2}\bar{3}}}; t-\bar{t}) = \langle \mathcal{T}\{ \alpha^{+}_{\mathbf{1}}(t) \alpha^{+}_{\mathbf{2}}(t) \alpha^{-}_{\mathbf{3}}(t) \alpha^{+\dagger}_{\mathbf{\bar{1}}}(\bar{t}) \alpha^{+\dagger}_{\mathbf{\bar{2}}}(\bar{t}) \alpha^{-\dagger}_{\mathbf{\bar{3}}}(\bar{t}) \} \rangle, \tag{4.13}$$

$$\mathrm{i}\hbar G_4(\tfrac{\mathbf{1234}}{\mathbf{\bar{1}\bar{2}\bar{3}\bar{4}}}; t-\bar{t}) = \langle \mathcal{T}\{ \alpha^{+}_{\mathbf{1}}(t) \alpha^{+}_{\mathbf{2}}(t) \alpha^{-}_{\mathbf{3}}(t) \alpha^{-}_{\mathbf{4}}(t) \alpha^{+\dagger}_{\mathbf{\bar{1}}}(\bar{t}) \alpha^{+\dagger}_{\mathbf{\bar{2}}}(\bar{t}) \alpha^{-\dagger}_{\mathbf{\bar{3}}}(\bar{t}) \alpha^{-\dagger}_{\mathbf{\bar{4}}}(\bar{t}) \} \rangle, \tag{4.14}$$

where $\mathcal{T}\{\cdots\}$ is the time-ordered product of operators.

We introduce the Fourier representations according to

$$G_2(\tfrac{\mathbf{12}}{\mathbf{\bar{1}\bar{2}}}, t) = \frac{1}{2\pi} \int_{-\infty}^{\infty} G_2(\tfrac{\mathbf{12}}{\mathbf{\bar{1}\bar{2}}}, \omega) \mathrm{e}^{-\mathrm{i}\omega t} \mathrm{d}\omega, \tag{4.15}$$

$$G_3(\tfrac{\mathbf{123}}{\mathbf{\bar{1}\bar{2}\bar{3}}}; t) = \frac{1}{2\pi} \int_{-\infty}^{\infty} G_3(\tfrac{\mathbf{123}}{\mathbf{\bar{1}\bar{2}\bar{3}}}; \omega) \mathrm{e}^{-\mathrm{i}\omega t} \mathrm{d}\omega, \tag{4.16}$$

$$G_4(\tfrac{\mathbf{1234}}{\mathbf{\bar{1}\bar{2}\bar{3}\bar{4}}}; t) = \frac{1}{2\pi} \int_{-\infty}^{\infty} G_4(\tfrac{\mathbf{1234}}{\mathbf{\bar{1}\bar{2}\bar{3}\bar{4}}}; \omega) \mathrm{e}^{-\mathrm{i}\omega t} \mathrm{d}\omega, \tag{4.17}$$

or equivalently

$$G_2(\tfrac{\mathbf{12}}{\mathbf{\bar{1}\bar{2}}}, \omega) = \int_{-\infty}^{\infty} G_2(\tfrac{\mathbf{12}}{\mathbf{\bar{1}\bar{2}}}, t) \mathrm{e}^{\mathrm{i}\omega t} \mathrm{d}t, \tag{4.18}$$

$$G_3(\tfrac{\mathbf{123}}{\mathbf{\bar{1}\bar{2}\bar{3}}}; \omega) = \int_{-\infty}^{\infty} G_3(\tfrac{\mathbf{123}}{\mathbf{\bar{1}\bar{2}\bar{3}}}; t) \mathrm{e}^{\mathrm{i}\omega t} \mathrm{d}t, \tag{4.19}$$

$$G_4(\tfrac{\mathbf{1234}}{\mathbf{\bar{1}\bar{2}\bar{3}\bar{4}}}; \omega) = \int_{-\infty}^{\infty} G_4(\tfrac{\mathbf{1234}}{\mathbf{\bar{1}\bar{2}\bar{3}\bar{4}}}; t) \mathrm{e}^{\mathrm{i}\omega t} \mathrm{d}t. \tag{4.20}$$

We have the relation

$$I(\omega) = I_2(\omega) + I_4(\omega) + \cdots, \tag{4.21}$$

$$\begin{aligned} I_2(\omega) &= \frac{J}{2\pi\hbar}\int_{-\infty}^{\infty}\frac{1}{L}\left\langle \mathcal{R}_{\mathrm{BL}}(t)\mathcal{R}_{\mathrm{BL}}(0)\right\rangle \mathrm{e}^{\mathrm{i}\omega t}\mathrm{d}t \\ &\approx -\frac{J}{\pi}\mathrm{Im}\left[\frac{1}{L}\sum_{\substack{\mathbf{12}\\ \bar{\mathbf{1}}\bar{\mathbf{2}}}}\widetilde{v}_{\mathbf{12}}\widetilde{v}_{\bar{\mathbf{1}}\bar{\mathbf{2}}}G_2(\tfrac{\mathbf{12}}{\bar{\mathbf{1}}\bar{\mathbf{2}}},\omega)\right], \end{aligned} \tag{4.22}$$

$$\begin{aligned} I_4(\omega) &= \frac{J}{2\pi\hbar}\int_{-\infty}^{\infty}\frac{1}{L}\left\langle : \mathcal{R}^{(0)} : (t) : \mathcal{R}^{(0)} : (0)\right\rangle \mathrm{e}^{\mathrm{i}\omega t}\mathrm{d}t \\ &\approx -\frac{J}{\pi}\mathrm{Im}\left[\frac{1}{L}\sum_{\substack{\mathbf{1234}\\ \bar{\mathbf{1}}\bar{\mathbf{2}}\bar{\mathbf{3}}\bar{\mathbf{4}}}}\widetilde{V}_{\mathbf{1234}}\widetilde{V}_{\bar{\mathbf{1}}\bar{\mathbf{2}}\bar{\mathbf{3}}\bar{\mathbf{4}}}G_4(\tfrac{\mathbf{1234}}{\bar{\mathbf{1}}\bar{\mathbf{2}}\bar{\mathbf{3}}\bar{\mathbf{4}}},\omega)\right], \end{aligned} \tag{4.23}$$

$$\widetilde{v}_{\boldsymbol{\kappa}_\nu\boldsymbol{\kappa}_{\nu'}} \equiv z\Lambda\left\langle \mathcal{S}\right\rangle_0 \widetilde{\gamma}_{\boldsymbol{\kappa}_\nu}\cosh 2\theta_{\boldsymbol{\kappa}_\nu}\delta_{\nu,\nu'}, \tag{4.24}$$

where the function $\widetilde{V}_{\mathbf{1234}}$ is given explicitly in Appendix A.

The unperturbed Green's functions are

$$G_2^{(0)}(\tfrac{\mathbf{12}}{\bar{\mathbf{1}}\bar{\mathbf{2}}},\omega) = \frac{\delta_{\mathbf{1},\bar{\mathbf{1}}}\delta_{\mathbf{2},\bar{\mathbf{2}}}}{\hbar\omega - \varepsilon_{\mathbf{1}}(\tilde{p}) - \varepsilon_{\mathbf{2}}(\tilde{p}) + \mathrm{i}\eta}, \tag{4.25}$$

$$G_3^{(0)}(\tfrac{\mathbf{123}}{\bar{\mathbf{1}}\bar{\mathbf{2}}\bar{\mathbf{3}}};\omega) = \frac{(\delta_{\mathbf{1},\bar{\mathbf{1}}}\delta_{\mathbf{2},\bar{\mathbf{2}}} + \delta_{\mathbf{1},\bar{\mathbf{2}}}\delta_{\mathbf{2},\bar{\mathbf{1}}})\delta_{\mathbf{3},\bar{\mathbf{3}}}}{\hbar\omega - \varepsilon_{\mathbf{1}}(\tilde{p}) - \varepsilon_{\mathbf{2}}(\tilde{p}) - \varepsilon_{\mathbf{3}}(\tilde{p}) + \mathrm{i}\eta}, \tag{4.26}$$

$$G_4^{(0)}(\tfrac{\mathbf{1234}}{\bar{\mathbf{1}}\bar{\mathbf{2}}\bar{\mathbf{3}}\bar{\mathbf{4}}};\omega) = \frac{(\delta_{\mathbf{1},\bar{\mathbf{1}}}\delta_{\mathbf{2},\bar{\mathbf{2}}} + \delta_{\mathbf{1},\bar{\mathbf{2}}}\delta_{\mathbf{2},\bar{\mathbf{1}}})(\delta_{\mathbf{3},\bar{\mathbf{3}}}\delta_{\mathbf{4},\bar{\mathbf{4}}} + \delta_{\mathbf{3},\bar{\mathbf{4}}}\delta_{\mathbf{4},\bar{\mathbf{3}}})}{\hbar\omega - \varepsilon_{\mathbf{1}}(\tilde{p}) - \varepsilon_{\mathbf{2}}(\tilde{p}) - \varepsilon_{\mathbf{3}}(\tilde{p}) - \varepsilon_{\mathbf{4}}(\tilde{p}) + \mathrm{i}\eta}, \tag{4.27}$$

where $\mathrm{i}\eta$ is a small imaginary part added to give a finite damping of the Dirac delta function. If we neglect the residual normal-ordered interaction $:\mathcal{H}^{(0)}:$, the scattering intensity is given by

$$I^{(0)}(\omega) = I_2^{(0)}(\omega) + I_4^{(0)}(\omega) + \cdots, \tag{4.28}$$

$$I_2^{(0)}(\omega) = -\frac{J}{\pi}\mathrm{Im}\left[\frac{1}{L}\sum_{\substack{\mathbf{12}\\ \bar{\mathbf{1}}\bar{\mathbf{2}}}}\widetilde{v}_{\mathbf{12}}\widetilde{v}_{\bar{\mathbf{1}}\bar{\mathbf{2}}}G_2^{(0)}(\tfrac{\mathbf{12}}{\bar{\mathbf{1}}\bar{\mathbf{2}}},\omega)\right], \tag{4.29}$$

$$I_4^{(0)}(\omega) = -\frac{J}{\pi}\mathrm{Im}\left[\frac{1}{L}\sum_{\substack{\mathbf{1234}\\ \bar{\mathbf{1}}\bar{\mathbf{2}}\bar{\mathbf{3}}\bar{\mathbf{4}}}}\widetilde{V}_{\mathbf{1234}}\widetilde{V}_{\bar{\mathbf{1}}\bar{\mathbf{2}}\bar{\mathbf{3}}\bar{\mathbf{4}}}G_4^{(0)}(\tfrac{\mathbf{1234}}{\bar{\mathbf{1}}\bar{\mathbf{2}}\bar{\mathbf{3}}\bar{\mathbf{4}}},\omega)\right]. \tag{4.30}$$

It is well known that this result is strongly modified when takes into account the residual normal-ordered interaction.[72–74]

4.3 Residual Normal-Ordered Interaction

Via the Fourier Transformation (2.23) and the Bogoliubov Transformation (2.24), the residual normal-ordered interaction $:\mathcal{H}^{(0)}:$ becomes

$$
\begin{aligned}
:\mathcal{H}^{(0)}: = \sum_{\mathbf{1}\mathbf{2}\bar{\mathbf{1}}\bar{\mathbf{2}}} \Big\{ & V_{+-+-}\tbinom{\mathbf{1}\mathbf{2}}{\bar{\mathbf{1}}\bar{\mathbf{2}}}\, \alpha_{\mathbf{1}}^{+\dagger}\alpha_{\mathbf{2}}^{-\dagger}\alpha_{\bar{\mathbf{1}}}^{+}\alpha_{\bar{\mathbf{2}}}^{-} + \frac{1}{2}V_{++++}\tbinom{\mathbf{1}\mathbf{2}}{\bar{\mathbf{1}}\bar{\mathbf{2}}}\, \alpha_{\mathbf{1}}^{+\dagger}\alpha_{\mathbf{2}}^{+\dagger}\alpha_{\bar{\mathbf{1}}}^{+}\alpha_{\bar{\mathbf{2}}}^{+} \\
& + \frac{1}{2}V_{----}\tbinom{\mathbf{1}\mathbf{2}}{\bar{\mathbf{1}}\bar{\mathbf{2}}}\, \alpha_{\mathbf{1}}^{-\dagger}\alpha_{\mathbf{2}}^{-\dagger}\alpha_{\bar{\mathbf{1}}}^{-}\alpha_{\bar{\mathbf{2}}}^{-} \Big\} \\
+ \sum_{\mathbf{1}\bar{\mathbf{1}}\bar{\mathbf{2}}\bar{\mathbf{3}}} \Big\{ & \frac{1}{2}V_{+--+}\tbinom{\mathbf{1}}{\bar{\mathbf{1}}\bar{\mathbf{2}}\bar{\mathbf{3}}}\, \alpha_{\mathbf{1}}^{+\dagger}\alpha_{\bar{\mathbf{1}}}^{-\dagger}\alpha_{\bar{\mathbf{2}}}^{-\dagger}\alpha_{\bar{\mathbf{3}}}^{+\dagger} + \frac{1}{2}V_{+--+}^{\dagger}\tbinom{\bar{\mathbf{1}}\bar{\mathbf{2}}\bar{\mathbf{3}}}{\mathbf{1}}\, \alpha_{\mathbf{1}}^{+}\alpha_{\bar{\mathbf{1}}}^{-}\alpha_{\bar{\mathbf{2}}}^{-}\alpha_{\bar{\mathbf{3}}}^{+} \\
& + V_{+++-}\tbinom{\mathbf{1}}{\bar{\mathbf{1}}\bar{\mathbf{2}}\bar{\mathbf{3}}}\, \alpha_{\mathbf{1}}^{+\dagger}\alpha_{\bar{\mathbf{1}}}^{+}\alpha_{\bar{\mathbf{2}}}^{+}\alpha_{\bar{\mathbf{3}}}^{-} + V_{+++-}^{\dagger}\tbinom{\bar{\mathbf{1}}\bar{\mathbf{2}}\bar{\mathbf{3}}}{\mathbf{1}}\, \alpha_{\bar{\mathbf{1}}}^{+\dagger}\alpha_{\bar{\mathbf{2}}}^{+\dagger}\alpha_{\bar{\mathbf{3}}}^{-\dagger}\alpha_{\mathbf{1}}^{+} \\
& + V_{---+}\tbinom{\mathbf{1}}{\bar{\mathbf{1}}\bar{\mathbf{2}}\bar{\mathbf{3}}}\, \alpha_{\mathbf{1}}^{-\dagger}\alpha_{\bar{\mathbf{1}}}^{-}\alpha_{\bar{\mathbf{2}}}^{-}\alpha_{\bar{\mathbf{3}}}^{+} + V_{---+}^{\dagger}\tbinom{\bar{\mathbf{1}}\bar{\mathbf{2}}\bar{\mathbf{3}}}{\mathbf{1}}\, \alpha_{\bar{\mathbf{1}}}^{-\dagger}\alpha_{\bar{\mathbf{2}}}^{-\dagger}\alpha_{\bar{\mathbf{3}}}^{+\dagger}\alpha_{\mathbf{1}}^{-} \Big\},
\end{aligned}
\tag{4.31}
$$

where the nine vertex functions are given explicitly in Appendix A.

4.3.1 2-Particle Green's Function

In order to take into account the residual normal-ordered interaction, we consider the ladder approximation Bethe–Salpeter equation

$$
G_2\big(\tbinom{\mathbf{1}\mathbf{2}}{\bar{\mathbf{1}}\bar{\mathbf{2}}};\omega\big) = G_2^{(0)}\big(\tbinom{\mathbf{1}\mathbf{2}}{\bar{\mathbf{1}}\bar{\mathbf{2}}};\omega\big) + \sum_{\hat{\mathbf{1}}\hat{\mathbf{2}}} G_2^{(0)}\big(\tbinom{\mathbf{1}\mathbf{2}}{\hat{\mathbf{1}}\hat{\mathbf{2}}};\omega\big) \sum_{\tilde{\mathbf{1}}\tilde{\mathbf{2}}} V_{+-+-}\tbinom{\hat{\mathbf{1}}\hat{\mathbf{2}}}{\tilde{\mathbf{1}}\tilde{\mathbf{2}}} G_2\big(\tbinom{\tilde{\mathbf{1}}\tilde{\mathbf{2}}}{\bar{\mathbf{1}}\bar{\mathbf{2}}};\omega\big). \tag{4.32}
$$

In the Lehmann representation, this solution has the form

$$
G_2\big(\tbinom{\mathbf{1}\mathbf{2}}{\bar{\mathbf{1}}\bar{\mathbf{2}}};\omega\big) = \sum_m \frac{\mathcal{X}_2\tbinom{\mathbf{1}\mathbf{2}}{m}\mathcal{X}_2^{\dagger}\tbinom{m}{\bar{\mathbf{1}}\bar{\mathbf{2}}}}{\hbar\omega - \varepsilon_m^{(2)} + \mathrm{i}\eta}, \tag{4.33}
$$

where $\varepsilon_m^{(2)}$ and $\mathcal{X}_2\tbinom{\mathbf{1}\mathbf{2}}{m}$ are eigenvalues and eigenvectors of the eigenvalue equation

$$
\varepsilon_m^{(2)}\mathcal{X}_2\tbinom{\mathbf{1}\mathbf{2}}{m} = \sum_{\bar{\mathbf{1}}\bar{\mathbf{2}}} \left\{ \delta_{\mathbf{1},\bar{\mathbf{1}}}\delta_{\mathbf{2},\bar{\mathbf{2}}}\left[\varepsilon_{\mathbf{1}}(\tilde{p}) + \varepsilon_{\mathbf{2}}(\tilde{p})\right] + V_{+-+-}\tbinom{\mathbf{1}\mathbf{2}}{\bar{\mathbf{1}}\bar{\mathbf{2}}} \right\} \mathcal{X}_2\tbinom{\bar{\mathbf{1}}\bar{\mathbf{2}}}{m}, \tag{4.34}
$$

$$
\sum_{\bar{\mathbf{1}}\bar{\mathbf{2}}} \mathcal{X}_2^{\dagger}\tbinom{m}{\bar{\mathbf{1}}\bar{\mathbf{2}}}\mathcal{X}_2\tbinom{\bar{\mathbf{1}}\bar{\mathbf{2}}}{m} = 1. \tag{4.35}
$$

The 2-magnon scattering intensity (4.22) with (4.33) reproduces the spectrum in the low-energy region (cf. Fig. 4.1).

4.3.2 4-Particle Green's Function

In order to evaluate 4-magnon scattering intensity $I_4(\omega)$, we consider the Bethe–Salpeter-like equation

$$G_4(\begin{smallmatrix}\mathbf{1234}\\ \mathbf{\bar{1}\bar{2}\bar{3}\bar{4}}\end{smallmatrix};\omega) = \left(\frac{\mathrm{i}\hbar}{2\pi}\right)^3 \int_{-\infty}^{\infty} \mathrm{d}\omega_1 \mathrm{d}\omega_2 \mathrm{d}\omega_3 \mathrm{d}\omega_4 \delta(\omega-\omega_1-\omega_2-\omega_3-\omega_4) R(\begin{smallmatrix}\mathbf{1234}\\ \mathbf{\bar{1}\bar{2}\bar{3}\bar{4}}\end{smallmatrix};\omega_1,\omega_2,\omega_3,\omega_4),$$

$$\begin{aligned}
&R(\begin{smallmatrix}\mathbf{1234}\\ \mathbf{\bar{1}\bar{2}\bar{3}\bar{4}}\end{smallmatrix};\omega_1,\omega_2,\omega_3,\omega_4) \\
&\quad = G_1^{(0)}(\begin{smallmatrix}\mathbf{1}\\ \mathbf{1}\end{smallmatrix},\omega_1) G_1^{(0)}(\begin{smallmatrix}\mathbf{2}\\ \mathbf{2}\end{smallmatrix},\omega_2) G_1^{(0)}(\begin{smallmatrix}\mathbf{3}\\ \mathbf{3}\end{smallmatrix},\omega_3) G_1^{(0)}(\begin{smallmatrix}\mathbf{4}\\ \mathbf{4}\end{smallmatrix},\omega_4) (\delta_{\mathbf{1},\mathbf{\bar{1}}}\delta_{\mathbf{2},\mathbf{\bar{2}}} + \delta_{\mathbf{1},\mathbf{\bar{2}}}\delta_{\mathbf{2},\mathbf{\bar{1}}})(\delta_{\mathbf{3},\mathbf{\bar{3}}}\delta_{\mathbf{4},\mathbf{\bar{4}}} + \delta_{\mathbf{3},\mathbf{\bar{4}}}\delta_{\mathbf{4},\mathbf{\bar{3}}}) \\
&\quad + G_1^{(0)}(\begin{smallmatrix}\mathbf{1}\\ \mathbf{1}\end{smallmatrix},\omega_1) G_1^{(0)}(\begin{smallmatrix}\mathbf{2}\\ \mathbf{2}\end{smallmatrix},\omega_2) G_1^{(0)}(\begin{smallmatrix}\mathbf{3}\\ \mathbf{3}\end{smallmatrix},\omega_3) G_1^{(0)}(\begin{smallmatrix}\mathbf{4}\\ \mathbf{4}\end{smallmatrix},\omega_4) \\
&\qquad \times \sum_{\mathbf{\hat{1}\hat{2}\hat{3}\hat{4}}} \frac{\mathrm{i}\hbar}{2\pi} \int_{-\infty}^{\infty} \mathrm{d}\hat{\omega}_1 \mathrm{d}\hat{\omega}_2 \mathrm{d}\hat{\omega}_3 \mathrm{d}\hat{\omega}_4 \sum_{i=1}^{6} \Gamma^{(i)}(\begin{smallmatrix}\mathbf{1234}\\ \mathbf{\hat{1}\hat{2}\hat{3}\hat{4}}\end{smallmatrix};\begin{smallmatrix}\omega_1,\omega_2,\omega_3,\omega_4\\ \hat{\omega}_1,\hat{\omega}_2,\hat{\omega}_3,\hat{\omega}_4\end{smallmatrix}) R(\begin{smallmatrix}\mathbf{\hat{1}\hat{2}\hat{3}\hat{4}}\\ \mathbf{\bar{1}\bar{2}\bar{3}\bar{4}}\end{smallmatrix};\hat{\omega}_1,\hat{\omega}_2,\hat{\omega}_3,\hat{\omega}_4),
\end{aligned} \tag{4.36}$$

where we introduce

$$\begin{aligned}
&\Gamma^{(1)}(\begin{smallmatrix}\mathbf{1234}\\ \mathbf{\hat{1}\hat{2}\hat{3}\hat{4}}\end{smallmatrix};\begin{smallmatrix}\omega_1,\omega_2,\omega_3,\omega_4\\ \hat{\omega}_1,\hat{\omega}_2,\hat{\omega}_3,\hat{\omega}_4\end{smallmatrix}) \equiv \delta_{\mathbf{3},\mathbf{\hat{3}}}\delta_{\mathbf{4},\mathbf{\hat{4}}}\delta(\omega_3-\hat{\omega}_3)\delta(\omega_4-\hat{\omega}_4)\left[G_1^{(0)}(\begin{smallmatrix}\mathbf{3}\\ \mathbf{3}\end{smallmatrix},\omega_3) G_1^{(0)}(\begin{smallmatrix}\mathbf{4}\\ \mathbf{4}\end{smallmatrix},\omega_4)\right]^{-1} \\
&\qquad\qquad V_{++++}(\begin{smallmatrix}\mathbf{12}\\ \mathbf{\hat{1}\hat{2}}\end{smallmatrix})\delta(\omega_1+\omega_2-\hat{\omega}_1-\hat{\omega}_2), \\
&\Gamma^{(2)}(\begin{smallmatrix}\mathbf{1234}\\ \mathbf{\hat{1}\hat{2}\hat{3}\hat{4}}\end{smallmatrix};\begin{smallmatrix}\omega_1,\omega_2,\omega_3,\omega_4\\ \hat{\omega}_1,\hat{\omega}_2,\hat{\omega}_3,\hat{\omega}_4\end{smallmatrix}) \equiv \delta_{\mathbf{1},\mathbf{\hat{1}}}\delta_{\mathbf{2},\mathbf{\hat{2}}}\delta(\omega_1-\hat{\omega}_1)\delta(\omega_2-\hat{\omega}_2)\left[G_1^{(0)}(\begin{smallmatrix}\mathbf{1}\\ \mathbf{1}\end{smallmatrix},\omega_1) G_1^{(0)}(\begin{smallmatrix}\mathbf{2}\\ \mathbf{2}\end{smallmatrix},\omega_2)\right]^{-1} \\
&\qquad\qquad V_{----}(\begin{smallmatrix}\mathbf{34}\\ \mathbf{\hat{3}\hat{4}}\end{smallmatrix})\delta(\omega_3+\omega_4-\hat{\omega}_3-\hat{\omega}_4), \\
&\Gamma^{(3)}(\begin{smallmatrix}\mathbf{1234}\\ \mathbf{\hat{1}\hat{2}\hat{3}\hat{4}}\end{smallmatrix};\begin{smallmatrix}\omega_1,\omega_2,\omega_3,\omega_4\\ \hat{\omega}_1,\hat{\omega}_2,\hat{\omega}_3,\hat{\omega}_4\end{smallmatrix}) \equiv \delta_{\mathbf{2},\mathbf{\hat{2}}}\delta_{\mathbf{4},\mathbf{\hat{4}}}\delta(\omega_2-\hat{\omega}_2)\delta(\omega_4-\hat{\omega}_4)\left[G_1^{(0)}(\begin{smallmatrix}\mathbf{2}\\ \mathbf{2}\end{smallmatrix},\omega_2) G_1^{(0)}(\begin{smallmatrix}\mathbf{4}\\ \mathbf{4}\end{smallmatrix},\omega_4)\right]^{-1} \\
&\qquad\qquad V_{+-+-}(\begin{smallmatrix}\mathbf{13}\\ \mathbf{\hat{1}\hat{3}}\end{smallmatrix})\delta(\omega_1+\omega_3-\hat{\omega}_1-\hat{\omega}_3), \\
&\Gamma^{(4)}(\begin{smallmatrix}\mathbf{1234}\\ \mathbf{\hat{1}\hat{2}\hat{3}\hat{4}}\end{smallmatrix};\begin{smallmatrix}\omega_1,\omega_2,\omega_3,\omega_4\\ \hat{\omega}_1,\hat{\omega}_2,\hat{\omega}_3,\hat{\omega}_4\end{smallmatrix}) \equiv \Gamma^{(3)}(\begin{smallmatrix}\mathbf{1243}\\ \mathbf{\hat{1}\hat{2}\hat{4}\hat{3}}\end{smallmatrix};\begin{smallmatrix}\omega_1,\omega_2,\omega_4,\omega_3\\ \hat{\omega}_1,\hat{\omega}_2,\hat{\omega}_4,\hat{\omega}_3\end{smallmatrix}), \\
&\Gamma^{(5)}(\begin{smallmatrix}\mathbf{1234}\\ \mathbf{\hat{1}\hat{2}\hat{3}\hat{4}}\end{smallmatrix};\begin{smallmatrix}\omega_1,\omega_2,\omega_3,\omega_4\\ \hat{\omega}_1,\hat{\omega}_2,\hat{\omega}_3,\hat{\omega}_4\end{smallmatrix}) \equiv \Gamma^{(3)}(\begin{smallmatrix}\mathbf{2134}\\ \mathbf{\hat{2}\hat{1}\hat{3}\hat{4}}\end{smallmatrix};\begin{smallmatrix}\omega_2,\omega_1,\omega_3,\omega_4\\ \hat{\omega}_2,\hat{\omega}_1,\hat{\omega}_3,\hat{\omega}_4\end{smallmatrix}), \quad G_1^{(0)}(\begin{smallmatrix}\mathbf{1}\\ \mathbf{\bar{1}}\end{smallmatrix},\omega) = \frac{\delta_{\mathbf{1},\mathbf{\bar{1}}}}{\hbar\omega-\varepsilon_{\mathbf{1}}(\tilde{p})+\mathrm{i}\eta}. \\
&\Gamma^{(6)}(\begin{smallmatrix}\mathbf{1234}\\ \mathbf{\hat{1}\hat{2}\hat{3}\hat{4}}\end{smallmatrix};\begin{smallmatrix}\omega_1,\omega_2,\omega_3,\omega_4\\ \hat{\omega}_1,\hat{\omega}_2,\hat{\omega}_3,\hat{\omega}_4\end{smallmatrix}) \equiv \Gamma^{(3)}(\begin{smallmatrix}\mathbf{2143}\\ \mathbf{\hat{2}\hat{1}\hat{4}\hat{3}}\end{smallmatrix};\begin{smallmatrix}\omega_2,\omega_1,\omega_4,\omega_3\\ \hat{\omega}_2,\hat{\omega}_1,\hat{\omega}_4,\hat{\omega}_3\end{smallmatrix}),
\end{aligned} \tag{4.37}$$

However, the solution of this equation appears beyond reach of the present day computers and one needs to avoid dealing directly with multiple-frequency integrals. The strategy used is to first decompose 4-particle Green's function into the product of 3-particle Green's function and 1-particle Green's function:

$$\begin{aligned}
\mathrm{i}\hbar G_4(\begin{smallmatrix}\mathbf{1234}\\ \mathbf{\bar{1}\bar{2}\bar{3}\bar{4}}\end{smallmatrix};t-\bar{t}) &= \langle \mathcal{T}\{\alpha_{\mathbf{1}}^{+}(t)\alpha_{\mathbf{2}}^{+}(t)\alpha_{\mathbf{3}}^{-}(t)\alpha_{\mathbf{4}}^{-}(t)\alpha_{\mathbf{\bar{1}}}^{+\dagger}(\bar{t})\alpha_{\mathbf{\bar{2}}}^{+\dagger}(\bar{t})\alpha_{\mathbf{\bar{3}}}^{-\dagger}(\bar{t})\alpha_{\mathbf{\bar{4}}}^{-\dagger}(\bar{t})\}\rangle \\
&\approx \langle \mathcal{T}\{\alpha_{\mathbf{1}}^{+}(t)\alpha_{\mathbf{2}}^{+}(t)\alpha_{\mathbf{3}}^{-}(t)\alpha_{\mathbf{\bar{1}}}^{+\dagger}(\bar{t})\alpha_{\mathbf{\bar{2}}}^{+\dagger}(\bar{t})\alpha_{\mathbf{\bar{3}}}^{-\dagger}(\bar{t})\}\rangle \langle \mathcal{T}\{\alpha_{\mathbf{4}}^{-}(t)\alpha_{\mathbf{\bar{4}}}^{-\dagger}(\bar{t})\}\rangle \\
&+ \langle \mathcal{T}\{\alpha_{\mathbf{1}}^{+}(t)\alpha_{\mathbf{2}}^{+}(t)\alpha_{\mathbf{3}}^{-}(t)\alpha_{\mathbf{\bar{1}}}^{+\dagger}(\bar{t})\alpha_{\mathbf{\bar{2}}}^{+\dagger}(\bar{t})\alpha_{\mathbf{\bar{4}}}^{-\dagger}(\bar{t})\}\rangle \langle \mathcal{T}\{\alpha_{\mathbf{4}}^{-}(t)\alpha_{\mathbf{\bar{3}}}^{-\dagger}(\bar{t})\}\rangle \\
&= \mathrm{i}\hbar G_3(\begin{smallmatrix}\mathbf{123}\\ \mathbf{\bar{1}\bar{2}\bar{3}}\end{smallmatrix};t-\bar{t})\mathrm{i}\hbar G_1(\begin{smallmatrix}\mathbf{4}\\ \mathbf{\bar{4}}\end{smallmatrix},t-\bar{t}) + \mathrm{i}\hbar G_3(\begin{smallmatrix}\mathbf{123}\\ \mathbf{\bar{1}\bar{2}\bar{4}}\end{smallmatrix};t-\bar{t})\mathrm{i}\hbar G_1(\begin{smallmatrix}\mathbf{4}\\ \mathbf{\bar{3}}\end{smallmatrix},t-\bar{t}).
\end{aligned} \tag{4.38}$$

This decomposition becomes exact when the quantum average is evaluated in the magnon vacuum.

The 3-particle Green's function is obtained as the solution of the following Bethe–Salpeter-like equation

$$
\begin{aligned}
G_3(\tbinom{\mathbf{123}}{\bar{\mathbf{1}}\bar{\mathbf{2}}\bar{\mathbf{3}}};\omega) = G_3^{(0)}(\tbinom{\mathbf{123}}{\bar{\mathbf{1}}\bar{\mathbf{2}}\bar{\mathbf{3}}};\omega) &+ \sum_{\hat{\mathbf{1}}\hat{\mathbf{2}}\hat{\mathbf{3}}} \widetilde{G}_3^{(0)}(\tbinom{\mathbf{123}}{\hat{\mathbf{1}}\hat{\mathbf{2}}\hat{\mathbf{3}}};\omega) \sum_{\tilde{\mathbf{1}}\tilde{\mathbf{2}}\tilde{\mathbf{3}}} \delta_{\hat{\mathbf{1}},\tilde{\mathbf{1}}} V_{+-+-}(\tbinom{\hat{\mathbf{2}}\hat{\mathbf{3}}}{\tilde{\mathbf{2}}\tilde{\mathbf{3}}}) G_3(\tbinom{\tilde{\mathbf{1}}\tilde{\mathbf{2}}\tilde{\mathbf{3}}}{\bar{\mathbf{1}}\bar{\mathbf{2}}\bar{\mathbf{3}}};\omega) \\
&+ \sum_{\hat{\mathbf{1}}\hat{\mathbf{2}}\hat{\mathbf{3}}} \widetilde{G}_3^{(0)}(\tbinom{\mathbf{123}}{\hat{\mathbf{1}}\hat{\mathbf{2}}\hat{\mathbf{3}}};\omega) \sum_{\tilde{\mathbf{1}}\tilde{\mathbf{2}}\tilde{\mathbf{3}}} \delta_{\hat{\mathbf{2}},\tilde{\mathbf{2}}} V_{+-+-}(\tbinom{\hat{\mathbf{1}}\hat{\mathbf{3}}}{\tilde{\mathbf{1}}\tilde{\mathbf{3}}}) G_3(\tbinom{\tilde{\mathbf{1}}\tilde{\mathbf{2}}\tilde{\mathbf{3}}}{\bar{\mathbf{1}}\bar{\mathbf{2}}\bar{\mathbf{3}}};\omega) \\
&+ \sum_{\hat{\mathbf{1}}\hat{\mathbf{2}}\hat{\mathbf{3}}} \widetilde{G}_3^{(0)}(\tbinom{\mathbf{123}}{\hat{\mathbf{1}}\hat{\mathbf{2}}\hat{\mathbf{3}}};\omega) \sum_{\tilde{\mathbf{1}}\tilde{\mathbf{2}}\tilde{\mathbf{3}}} \delta_{\hat{\mathbf{3}},\tilde{\mathbf{3}}} V_{++++}(\tbinom{\hat{\mathbf{1}}\hat{\mathbf{2}}}{\tilde{\mathbf{1}}\tilde{\mathbf{2}}}) G_3(\tbinom{\tilde{\mathbf{1}}\tilde{\mathbf{2}}\tilde{\mathbf{3}}}{\bar{\mathbf{1}}\bar{\mathbf{2}}\bar{\mathbf{3}}};\omega),
\end{aligned}
\tag{4.39}
$$

where we introduce

$$
\widetilde{G}_3^{(0)}(\tbinom{\mathbf{123}}{\bar{\mathbf{1}}\bar{\mathbf{2}}\bar{\mathbf{3}}};\omega) = \frac{\delta_{\mathbf{1},\bar{\mathbf{1}}}\delta_{\mathbf{2},\bar{\mathbf{2}}}\delta_{\mathbf{3},\bar{\mathbf{3}}}}{\hbar\omega - \varepsilon_{\mathbf{1}}(\tilde{p}) - \varepsilon_{\mathbf{2}}(\tilde{p}) - \varepsilon_{\mathbf{3}}(\tilde{p}) + \mathrm{i}\eta}. \tag{4.40}
$$

In the Lehmann representation, this solution has the form

$$
G_3(\tbinom{\mathbf{123}}{\bar{\mathbf{1}}\bar{\mathbf{2}}\bar{\mathbf{3}}};\omega) = \sum_l \frac{\mathcal{X}_3(\tbinom{\mathbf{123}}{l})\mathcal{X}_3^\dagger(\tbinom{l}{\bar{\mathbf{1}}\bar{\mathbf{2}}\bar{\mathbf{3}}})}{\hbar\omega - \varepsilon_l^{(3)} + \mathrm{i}\eta}, \tag{4.41}
$$

where $\varepsilon_l^{(3)}$ and $\mathcal{X}_3(\tbinom{\mathbf{123}}{l})$ are eigenvalues and eigenvectors of the eigenvalue equation

$$
\begin{aligned}
\varepsilon_l^{(3)}\mathcal{X}_3(\tbinom{\mathbf{123}}{l}) = \sum_{\bar{\mathbf{1}}\bar{\mathbf{2}}\bar{\mathbf{3}}} \Big\{ \delta_{\mathbf{1},\bar{\mathbf{1}}}\delta_{\mathbf{2},\bar{\mathbf{2}}}\delta_{\mathbf{3},\bar{\mathbf{3}}}\left[\varepsilon_{\mathbf{1}}(\tilde{p}) + \varepsilon_{\mathbf{2}}(\tilde{p}) + \varepsilon_{\mathbf{3}}(\tilde{p})\right] &+ \delta_{\mathbf{1},\bar{\mathbf{1}}} V_{+-+-}(\tbinom{\mathbf{23}}{\bar{\mathbf{2}}\bar{\mathbf{3}}}) \\
&+ \delta_{\mathbf{2},\bar{\mathbf{2}}} V_{+-+-}(\tbinom{\mathbf{13}}{\bar{\mathbf{1}}\bar{\mathbf{3}}}) \\
&+ \delta_{\mathbf{3},\bar{\mathbf{3}}} V_{++++}(\tbinom{\mathbf{12}}{\bar{\mathbf{1}}\bar{\mathbf{2}}}) \Big\} \mathcal{X}_3(\tbinom{\bar{\mathbf{1}}\bar{\mathbf{2}}\bar{\mathbf{3}}}{l}),
\end{aligned}
\tag{4.42}
$$

$$
\sum_{\bar{\mathbf{1}}\bar{\mathbf{2}}\bar{\mathbf{3}}} \mathcal{X}_3^\dagger(\tbinom{l}{\bar{\mathbf{1}}\bar{\mathbf{2}}\bar{\mathbf{3}}})\mathcal{X}_3(\tbinom{\bar{\mathbf{1}}\bar{\mathbf{2}}\bar{\mathbf{3}}}{l}) = 2. \tag{4.43}
$$

The decomposed 4-particle Green's function (4.38) becomes

$$
G_4(\tbinom{\mathbf{1234}}{\bar{\mathbf{1}}\bar{\mathbf{2}}\bar{\mathbf{3}}\bar{\mathbf{4}}};\omega) = \sum_l \frac{\mathcal{X}_3(\tbinom{\mathbf{123}}{l})\mathcal{X}_3^\dagger(\tbinom{l}{\bar{\mathbf{1}}\bar{\mathbf{2}}\bar{\mathbf{3}}})}{\hbar\omega - \varepsilon_l^{(3)} - \varepsilon_{\mathbf{4}}(\tilde{p}) + \mathrm{i}\eta}\delta_{\mathbf{4},\bar{\mathbf{4}}} + \sum_l \frac{\mathcal{X}_3(\tbinom{\mathbf{123}}{l})\mathcal{X}_3^\dagger(\tbinom{l}{\bar{\mathbf{1}}\bar{\mathbf{2}}\bar{\mathbf{4}}})}{\hbar\omega - \varepsilon_l^{(3)} - \varepsilon_{\mathbf{4}}(\tilde{p}) + \mathrm{i}\eta}\delta_{\mathbf{4},\bar{\mathbf{3}}}. \tag{4.44}
$$

The 4-magnon scattering intensity (4.23) with (4.44) reproduces the spectrum in the high-energy region (cf. Fig. 4.1).

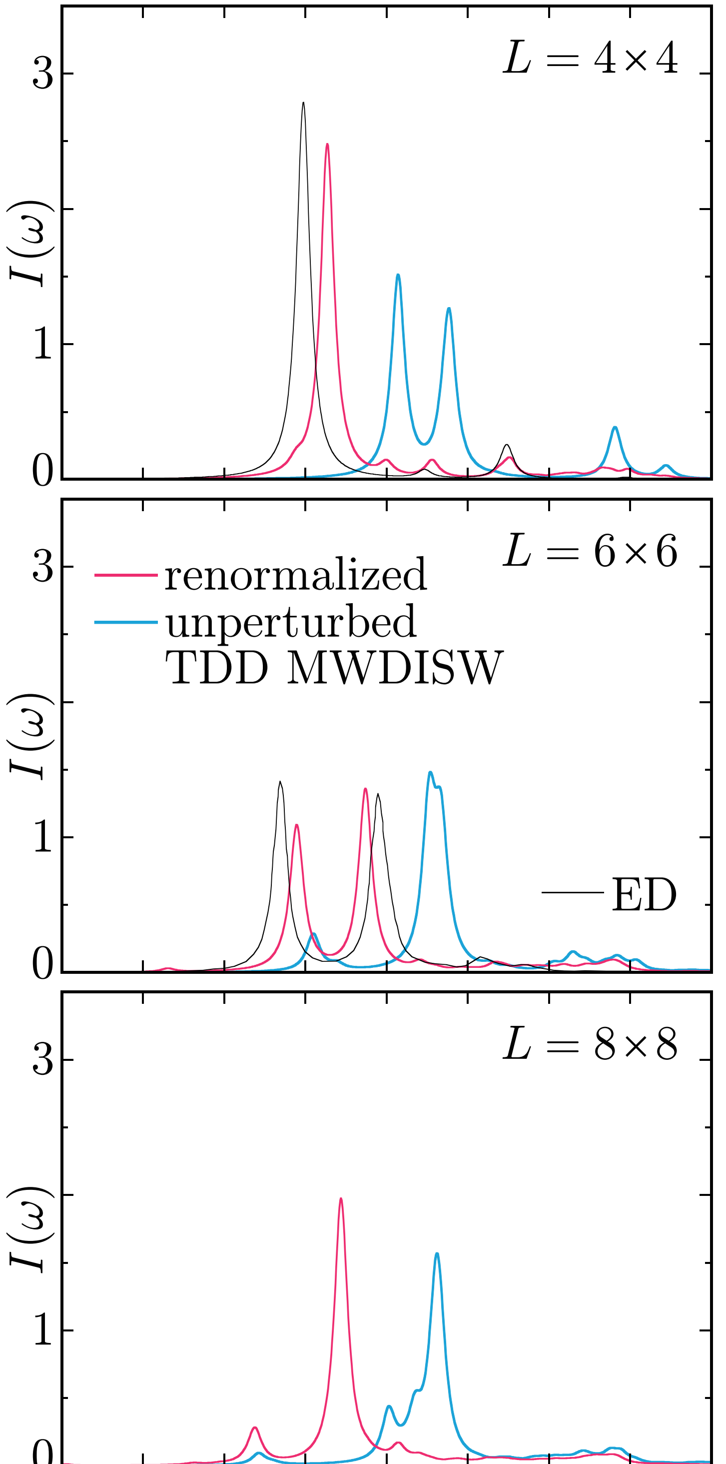

Fig. 4.1: TDD-MWDISW calculations of the B_{1g} Raman-scattering intensity $I(\omega)$ at $T = 0$ as functions of ω for the Hamiltonian (2.1) on the square lattice with $(S, s) = (\frac{1}{2}, \frac{1}{2})$. The findings with various number of sites L are compared with ED calculations.[74)] Red lines represent the renormalized case, Eq. (4.21) with (4.33) and (4.44); blue lines represent the unperturbed case, Eq. (4.28).

Chapter 5

Summary and Discussion

We have fully demonstrated that the DC-TDD-MWDISW description describes thermodynamic properties over the whole temperature range. Further, by taking into account the residual normal-ordered interaction, the description also describes dynamic properties over the whole energy region. The DC-TDD-MHFISW description cannot avoid an artificial phase transition to the paramagnetic noncorrelated state at a certain finite temperature.

The DC-TDD-MWDISW formulation is elaborate yet robust. Why is the DC-TDD-MHFISW formulation, on the other hand, so fragile? In order to gain a deeper understanding of their difference, we show the scheme-dependent self-consistent fields $\langle\!\langle \mathcal{S} \rangle\!\rangle$ and $\langle\!\langle \mathcal{S}' \rangle\!\rangle$ in Figs. 5.1(c) and 5.1(c$'$). The DC-TDD-MHFISW thermodynamics is characterized by $\langle \mathcal{S} \rangle_T$ and $\langle \mathcal{S}' \rangle_T$, while the DC-TDD-MWDISW thermodynamics is characterized by $\langle \mathcal{S} \rangle_0$ and $\langle \mathcal{S}' \rangle_0$. The double-constraint condition $\langle \mathcal{M}_{\mathrm{A}}^z \rangle_T = \langle \mathcal{M}_{\mathrm{B}}^z \rangle_T = 0$ so strongly affects the Hartree-Fock fields as to reduce them to

$$\langle \mathcal{S} \rangle_T = -\langle a_{\boldsymbol{r}_m} b_{\boldsymbol{r}_m + \boldsymbol{\delta}_l} \rangle_T, \qquad \langle \mathcal{S}' \rangle_T = 0. \tag{5.1}$$

With increasing temperature, the bond amplitude $\langle \mathcal{S} \rangle_T$ also vanishes in two steps. With both $\langle \mathcal{S} \rangle_T$ and $\langle \mathcal{S}' \rangle_T$ vanishing, the Hartree-Fock Hamiltonian (2.17) becomes null, resulting in uncorrelated HP bosons. The WD fields, on the other hand, consist of both bond and site variables,

$$\begin{aligned} \langle \mathcal{S} \rangle_0 &= \sqrt{Ss} - \langle a_{\boldsymbol{r}_m} b_{\boldsymbol{r}_m + \boldsymbol{\delta}_l} \rangle_0 - \frac{S \langle b_{\boldsymbol{r}_n}^\dagger b_{\boldsymbol{r}_n} \rangle_0 + s \langle a_{\boldsymbol{r}_m}^\dagger a_{\boldsymbol{r}_m} \rangle_0}{2\sqrt{Ss}}, \\ \langle \mathcal{S}' \rangle_0 &= \frac{S \langle b_{\boldsymbol{r}_n}^\dagger b_{\boldsymbol{r}_n} \rangle_0 - s \langle a_{\boldsymbol{r}_m}^\dagger a_{\boldsymbol{r}_m} \rangle_0}{2\sqrt{Ss}}. \end{aligned} \tag{5.2}$$

They are also influenced by the "number constraint" on the HP bosons, $\langle \mathcal{M}_{\mathrm{A}}^z \rangle_T = \langle \mathcal{M}_{\mathrm{B}}^z \rangle_T = 0$, but the effect of the "thermal condition" on the magnon-vacuum "quantum averages" is moderate and indirect. It should, however, be noted that the WD fields also depend on temperature through the chemical potentials [cf. Eqs. (2.18) and (3.75)]. It is the modification of CSWs that causes the thermal variation of the WD fields. Unless $T \to \infty$, $\langle a_{\boldsymbol{r}_m}^\dagger a_{\boldsymbol{r}_m} \rangle_0$, $\langle b_{\boldsymbol{r}_n}^\dagger b_{\boldsymbol{r}_n} \rangle_0$, and $\langle a_{\boldsymbol{r}_m} b_{\boldsymbol{r}_m + \boldsymbol{\delta}_l} \rangle_0$ all remain finite so that the WD Hamiltonian (2.17) can reasonably bring the two sublattices into interaction. In the $T \to \infty$ limit, they all vanish to reproduce the paramagnetic behavior correctly.

We hope that this new modified-spin-wave formulation will stimulate further exploration, measurement, and characterization of novel magnetic substances.

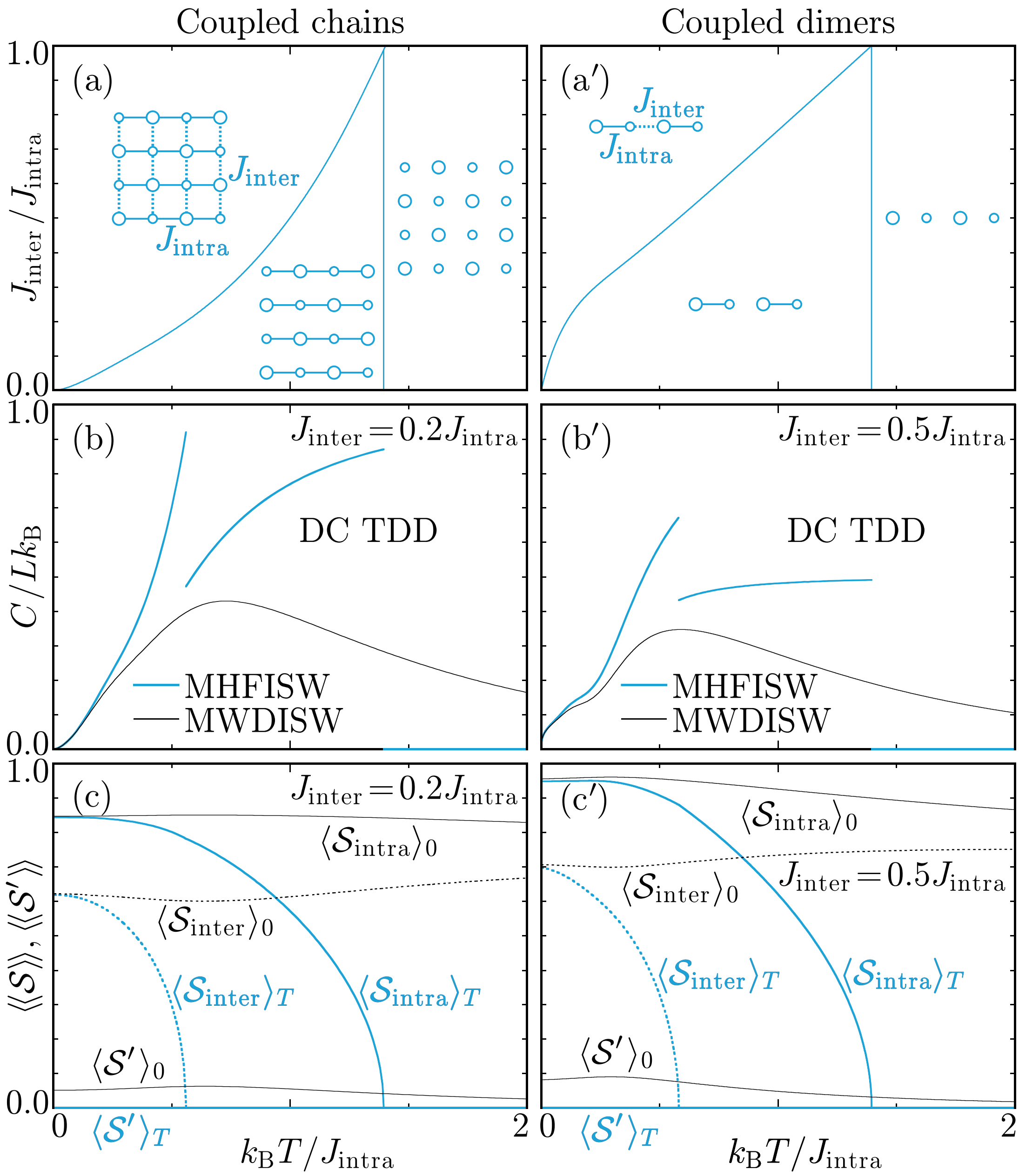

Fig. 5.1: DC-TDD-MHFISW versus DC-TDD-MWDISW descriptions of $(S, s) = (1, \frac{1}{2})$ coupled-chain [(a), (b), and (c)] and coupled-dimer [(a′), (b′), and (c′)] ferrimagnets whose Hamiltonians are given by Eq. (2.1) but with varying interchain or interdimer coupling J_{inter} against fixed intrachain or intradimer coupling J_{intra} as illustrated in (a) and (a′). (a) and (a′) Artificial thermal phase boundaries as functions of $J_{\mathrm{inter}}/J_{\mathrm{intra}}$ in the DC-TDD-MHFISW theory, where in (a), every transition between the decoupled-chain and noncorrelated states is of the second order, but all other transitions are of the first order, while in (a′), every transition is of the second order. (b) and (b′) DC-TDD-MSW calculations of the specific heat C as a function of temperature with $J_{\mathrm{inter}}/J_{\mathrm{intra}}$ set to 0.2 (b) and 0.5 (b′). (c) and (c′) DC-TDD-MSW calculations of the self-consistent fields (3.74) and (3.75) as functions of temperature with $J_{\mathrm{inter}}/J_{\mathrm{intra}}$ set to 0.2 (c) and 0.5 (c′). Since $\mathcal{S}$ includes bond operators such as $a_{\boldsymbol{r}_m} b_{\boldsymbol{r}_m+\boldsymbol{\delta}_l}$, $\langle\langle\mathcal{S}\rangle\rangle$ is inhomogeneous. We denote $\mathcal{S}$ by $\mathcal{S}_{\mathrm{intra}}$ ($\mathcal{S}_{\mathrm{inter}}$) when $\boldsymbol{\delta}_l$ connects J_{intra} (J_{inter})-correlated neighbors. Since $\mathcal{S}'$ includes no such bond operator, $\langle\langle\mathcal{S}'\rangle\rangle$ is uniform.

Bibliography

[1] F. Bloch, Z. Physik **61**, 206 (1930).
[2] F. Keffer, H. Kaplan, and Y. Yafet, Am. J. Phys. **21**, 250 (1953).
[3] R. Kubo, Rev. Mod. Phys. **25**, 344 (1953).
[4] J. Van Kranendonk and J. H. Van Vleck, Rev. Mod. Phys. **30**, 1 (1958).
[5] H. Kaplan, Phys. Rev. **86**, 121 (1952).
[6] P. W. Anderson, Phys. Rev. **86**, 694 (1952).
[7] R. Kubo, Phys. Rev. **87**, 568 (1952).
[8] C. Møller, Z. Physik **82**, 559 (1933).
[9] M. Fallot, Ann. Phys. **6**, 305 (1936).
[10] J. Van Kranendonk and M. Bloom, Physica **22**, 545 (1956).
[11] T. Moriya, Prog. Theor. Phys. **16**, 23 (1956).
[12] T. Moriya, Prog. Theor. Phys. **16**, 641 (1956).
[13] T. Oguchi and F. Keffer, J. Phys. Chem. Solids **25**, 405 (1964).
[14] P. Pincus, Phys. Rev. Lett. **16**, 398 (1966).
[15] D. Beeman and P. Pincus, Phys. Rev. **166**, 359 (1968).
[16] A. Narath and A. T. Fromhold, Jr., Phys. Rev. Lett. **17**, 354 (1966).
[17] E. Rastelli and A. Tassi, Phys. Lett. **48A**, 119 (1974).
[18] N. Karchev, J. Phys.: Condens. Matter **20**, 325219 (2008).
[19] N. Karchev, J. Phys.: Condens. Matter **21**, 216003 (2009).
[20] M. Takahashi, Prog. Theor. Phys. Suppl. **87**, 233 (1986).
[21] M. Takahashi, Phys. Rev. Lett. **58**, 168 (1987).
[22] M. Takahashi, Phys. Rev. B **36**, 3791 (1987).
[23] M. Takahashi, Phys. Rev. B **42**, 766 (1990).
[24] J. E. Hirsch and S. Tang, Phys. Rev. B **40**, 4769 (1989).
[25] S. Tang, M. E. Lazzouni, and J. E. Hirsch, Phys. Rev. B **40**, 5000 (1989).
[26] M. Takahashi, Phys. Rev. B **40**, 2494 (1989).
[27] M. Takahashi, Prog. Theor. Phys. Suppl. **101**, 487 (1990).
[28] J.-K. Kim and M. Troyer, Phys. Rev. Lett. **80**, 2705 (1998).
[29] K. Ohara and K. Yosida, J. Phys. Soc. Jpn. **58**, 2521 (1989).
[30] K. Ohara and K. Yosida, J. Phys. Soc. Jpn. **59**, 3340 (1990).
[31] J. E. Hirsch and S. Tang, Phys. Rev. B **39**, R2887 (1989).
[32] J. H. Xu and C. S. Ting, Phys. Rev. B **42**, R6861 (1990).
[33] H. Nishimori and Y. Saika, J. Phys. Soc. Jpn. **59**, 4454 (1990).
[34] J. H. Xu and C. S. Ting, Phys. Rev. B **43**, 6177 (1991).
[35] H. A. Ceccatto, C. J. Gazza, and A. E. Trumper, Phys. Rev. B **45**, 7832 (1992).
[36] N. B. Ivanov and P. Ch. Ivanov, Phys. Rev. B **46**, 8206 (1992).
[37] A. V. Dotsenko and O. P. Sushkov, Phys. Rev. B **50**, 13821 (1994).
[38] J. Yang, J.-L. Shen, and H.-Q. Lin, J. Phys. Soc. Jpn. **68**, 2384 (1999).
[39] Y. Wu and Y. Chen, Int. J. Mod. Phys. B **27**, 1350021 (2013).

[40] S. M. Rezende, Phys. Rev. B **42**, 2589 (1990).
[41] S. Yamamoto and H. Hori, J. Phys. Soc. Jpn. **72**, 769 (2003).
[42] H. Hori. and S. Yamamoto, J. Phys. Soc. Jpn. **73**, 549 (2004).
[43] S. Yamamoto and H. Hori, J. Phys. Soc. Jpn. **73**, 822 (2004).
[44] S. Yamamoto and K. Funase, Low Temp. Phys. **31**, 740 (2005).
[45] S. Yamamoto and T. Fukui, Phys. Rev. B **57**, R14008 (1998).
[46] A. S. Ovchinnikov, I. G. Bostrem, V. E. Sinitsyn, A. S. Boyarchenkov, N. V. Baranov, and K. Inoue, J. Phys.: Condens. Matter **14**, 8067 (2002).
[47] S. Yamamoto, T. Fukui, K. Maisinger, and U. Schollwöck, J. Phys.: Condens. Matter **10**, 11033 (1998).
[48] S. Yamamoto, T. Fukui, and T. Sakai, Eur. Phys. J. B **15**, 211 (2000).
[49] S. Yamamoto, J. Phys. Soc. Jpn. **69**, 2324 (2000).
[50] H. Hori and S. Yamamoto, Phys. Rev. B **68**, 054409 (2003).
[51] S. Yamamoto and T. Nakanishi, Phys. Rev. Lett. **89**, 157603 (2002).
[52] H. Hori and S. Yamamoto, J. Phys.: Condens. Matter **16**, 9023 (2004).
[53] S. Yamamoto, H. Hori, Y. Furukawa, Y. Nishisaka, Y. Sumida, K. Yamada, K. Kumagai, T. Asano, and Y. Inagaki, J. Phys. Soc. Jpn. **75**, 074703 (2006).
[54] S. Yamamoto, Phys. Rev. B **69**, 064426 (2004).
[55] T. Holstein and H. Primakoff, Phys. Rev. **58**, 1098 (1940).
[56] M. S. Makivić and H.-Q. Ding, Phys. Rev. B **43**, 3562 (1991).
[57] ALPS Collaboration, A. F. Albuquerque *et al.*, J. Magn. Magn. Mater. **310**, 1187 (2007); B. Bauer *et al.*, J. Stat. Mech. (2011) P05001.
[58] D. P. Arovas and A. Auerbach, Phys. Rev. B **38**, 316 (1988).
[59] A. Auerbach and D. P. Arovas, Phys. Rev. Lett. **61**, 617 (1988).
[60] C.-X. Chen and H.-B. Schüttler, Phys. Rev. B **40**, 239 (1989).
[61] Y. Noriki and S. Yamamoto, J. Phys. Soc. Jpn. **86**, 034714 (2017).
[62] S. Yamamoto, S. Brehmer, and H.-J. Mikeska, Phys. Rev. B **57**, 13610 (1998).
[63] M. Takahashi and M. Yamada, J. Phys. Soc. Jpn. **54**, 2808 (1985).
[64] M. Yamada and M. Takahashi, J. Phys. Soc. Jpn. **55**, 2024 (1986).
[65] S. Yamamoto, Phys. Rev. B **59**, 1024 (1999).
[66] A. W. Sandvik, Phys. Rev. B **56**, 11678 (1997).
[67] S. Yamamoto and H. Hori, Phys. Rev. B **72**, 054423 (2005).
[68] X. Wan, K. Yang, and R. N. Bhatt, Phys. Rev. B **66**, 014429 (2002).
[69] A. Langari and M. A. Martin-Delgado, Phys. Rev. B **63**, 054432 (2001).
[70] T. Nakanishi, S. Yamamoto, and T. Sakai, J. Phys. Soc. Jpn. **70**, 1380 (2001).
[71] P. A. Fleury and R. Loudon, Phys. Rev. **166**, 514 (1968).
[72] C. M. Canali and S. M. Girvin, Phys. Rev. B **45**, 7127 (1992).
[73] A. V. Chubukov and D. M. Frenkel, Phys. Rev. B **52**, 9760 (1995).
[74] A. W. Sandvik, S. Capponi, D. Poilblanc, and E. Dagotto, Phys. Rev. B **57**, 8478 (1998).

Appendix A

Holstein–Primakoff Vertices

In the square-lattice antiferromagnets, the residual normal-ordered interaction becomes

$$
\begin{aligned}
:\mathcal{H}^{(0)}: = \sum_{\mathbf{1}\mathbf{2}\bar{\mathbf{1}}\bar{\mathbf{2}}} \Big\{ & V_{+-+-}\left(\begin{smallmatrix}\mathbf{1}\mathbf{2}\\ \bar{\mathbf{1}}\bar{\mathbf{2}}\end{smallmatrix}\right) \alpha_{\mathbf{1}}^{+\dagger}\alpha_{\mathbf{2}}^{-\dagger}\alpha_{\bar{\mathbf{1}}}^{+}\alpha_{\bar{\mathbf{2}}}^{-} + \frac{1}{2}V_{++++}\left(\begin{smallmatrix}\mathbf{1}\mathbf{2}\\ \bar{\mathbf{1}}\bar{\mathbf{2}}\end{smallmatrix}\right) \alpha_{\mathbf{1}}^{+\dagger}\alpha_{\mathbf{2}}^{+\dagger}\alpha_{\bar{\mathbf{1}}}^{+}\alpha_{\bar{\mathbf{2}}}^{+} \\
& + \frac{1}{2}V_{----}\left(\begin{smallmatrix}\mathbf{1}\mathbf{2}\\ \bar{\mathbf{1}}\bar{\mathbf{2}}\end{smallmatrix}\right) \alpha_{\mathbf{1}}^{-\dagger}\alpha_{\mathbf{2}}^{-\dagger}\alpha_{\bar{\mathbf{1}}}^{-}\alpha_{\bar{\mathbf{2}}}^{-} \Big\} \\
+ \sum_{\mathbf{1}\bar{\mathbf{1}}\bar{\mathbf{2}}\bar{\mathbf{3}}} \Big\{ & \frac{1}{2}V_{+--+}\left(\begin{smallmatrix}\mathbf{1}\\ \bar{\mathbf{1}}\bar{\mathbf{2}}\bar{\mathbf{3}}\end{smallmatrix}\right) \alpha_{\mathbf{1}}^{+\dagger}\alpha_{\bar{\mathbf{1}}}^{-\dagger}\alpha_{\bar{\mathbf{2}}}^{-\dagger}\alpha_{\bar{\mathbf{3}}}^{+\dagger} + \frac{1}{2}V_{+--+}^{\dagger}\left(\begin{smallmatrix}\bar{\mathbf{1}}\bar{\mathbf{2}}\bar{\mathbf{3}}\\ \mathbf{1}\end{smallmatrix}\right) \alpha_{\mathbf{1}}^{+}\alpha_{\bar{\mathbf{1}}}^{-}\alpha_{\bar{\mathbf{2}}}^{-}\alpha_{\bar{\mathbf{3}}}^{+} \\
& + V_{+++-}\left(\begin{smallmatrix}\mathbf{1}\\ \bar{\mathbf{1}}\bar{\mathbf{2}}\bar{\mathbf{3}}\end{smallmatrix}\right) \alpha_{\mathbf{1}}^{+\dagger}\alpha_{\bar{\mathbf{1}}}^{+}\alpha_{\bar{\mathbf{2}}}^{+}\alpha_{\bar{\mathbf{3}}}^{-} + V_{+++-}^{\dagger}\left(\begin{smallmatrix}\bar{\mathbf{1}}\bar{\mathbf{2}}\bar{\mathbf{3}}\\ \mathbf{1}\end{smallmatrix}\right) \alpha_{\bar{\mathbf{1}}}^{+\dagger}\alpha_{\bar{\mathbf{2}}}^{+\dagger}\alpha_{\bar{\mathbf{3}}}^{-\dagger}\alpha_{\mathbf{1}}^{+} \\
& + V_{---+}\left(\begin{smallmatrix}\mathbf{1}\\ \bar{\mathbf{1}}\bar{\mathbf{2}}\bar{\mathbf{3}}\end{smallmatrix}\right) \alpha_{\mathbf{1}}^{-\dagger}\alpha_{\bar{\mathbf{1}}}^{-}\alpha_{\bar{\mathbf{2}}}^{-}\alpha_{\bar{\mathbf{3}}}^{+} + V_{---+}^{\dagger}\left(\begin{smallmatrix}\bar{\mathbf{1}}\bar{\mathbf{2}}\bar{\mathbf{3}}\\ \mathbf{1}\end{smallmatrix}\right) \alpha_{\bar{\mathbf{1}}}^{-\dagger}\alpha_{\bar{\mathbf{2}}}^{-\dagger}\alpha_{\bar{\mathbf{3}}}^{+\dagger}\alpha_{\mathbf{1}}^{-} \Big\},
\end{aligned}
\tag{4.31}
$$

where the nine vertex functions are given by

$$
\begin{aligned}
& V_{+-+-}\left(\begin{smallmatrix}\mathbf{1}\mathbf{2}\\ \bar{\mathbf{1}}\bar{\mathbf{2}}\end{smallmatrix}\right) \\
& \equiv -2\frac{zJ}{4N}\delta(\mathbf{1}-\mathbf{2}-\bar{\mathbf{1}}+\bar{\mathbf{2}})u_{\mathbf{1}}u_{\mathbf{2}}u_{\bar{\mathbf{1}}}u_{\bar{\mathbf{2}}}\Big[x_{\mathbf{1}}x_{\bar{\mathbf{2}}}\left(\gamma_{\bar{\mathbf{2}}}x_{\bar{\mathbf{1}}}+\gamma_{\bar{\mathbf{2}}-\bar{\mathbf{1}}}+\gamma_{\bar{\mathbf{2}}-\mathbf{2}}x_{\mathbf{2}}x_{\bar{\mathbf{1}}}+\gamma_{\bar{\mathbf{2}}-\mathbf{2}-\bar{\mathbf{1}}}x_{\mathbf{2}}\right) \\
& \qquad +\left(\gamma_{\mathbf{1}}x_{\bar{\mathbf{1}}}+\gamma_{\mathbf{1}-\bar{\mathbf{1}}}+\gamma_{\mathbf{1}-\mathbf{2}}x_{\mathbf{2}}x_{\bar{\mathbf{1}}}+\gamma_{\mathbf{1}-\mathbf{2}-\bar{\mathbf{1}}}x_{\mathbf{2}}\right) \\
& \qquad +x_{\bar{\mathbf{1}}}x_{\mathbf{2}}\left(\gamma_{\mathbf{2}}x_{\mathbf{1}}+\gamma_{\mathbf{2}-\mathbf{1}}+\gamma_{\mathbf{2}-\bar{\mathbf{2}}}x_{\bar{\mathbf{2}}}x_{\mathbf{1}}+\gamma_{\mathbf{2}-\bar{\mathbf{2}}-\mathbf{1}}x_{\bar{\mathbf{2}}}\right) \\
& \qquad +\left(\gamma_{\bar{\mathbf{1}}}x_{\mathbf{1}}+\gamma_{\bar{\mathbf{1}}-\mathbf{1}}+\gamma_{\bar{\mathbf{1}}-\bar{\mathbf{2}}}x_{\bar{\mathbf{2}}}x_{\mathbf{1}}+\gamma_{\bar{\mathbf{1}}-\bar{\mathbf{2}}-\mathbf{1}}x_{\bar{\mathbf{2}}}\right)\Big],
\end{aligned}
\tag{A.1}
$$

$$
\begin{aligned}
& V_{++++}\left(\begin{smallmatrix}\mathbf{1}\mathbf{2}\\ \bar{\mathbf{1}}\bar{\mathbf{2}}\end{smallmatrix}\right) \\
& \equiv -\frac{zJ}{4N}\delta(\mathbf{1}+\mathbf{2}-\bar{\mathbf{1}}-\bar{\mathbf{2}})u_{\mathbf{1}}u_{\mathbf{2}}u_{\bar{\mathbf{1}}}u_{\bar{\mathbf{2}}}\Big[x_{\mathbf{1}}\left(\gamma_{\mathbf{2}}x_{\bar{\mathbf{1}}}x_{\bar{\mathbf{2}}}+\gamma_{\mathbf{2}-\bar{\mathbf{2}}}x_{\bar{\mathbf{1}}}+\gamma_{\mathbf{2}-\bar{\mathbf{1}}}x_{\bar{\mathbf{2}}}+\gamma_{\mathbf{2}-\bar{\mathbf{1}}-\bar{\mathbf{2}}}\right) \\
& \qquad +x_{\mathbf{2}}\left(\gamma_{\mathbf{1}}x_{\bar{\mathbf{1}}}x_{\bar{\mathbf{2}}}+\gamma_{\mathbf{1}-\bar{\mathbf{2}}}x_{\bar{\mathbf{1}}}+\gamma_{\mathbf{1}-\bar{\mathbf{1}}}x_{\bar{\mathbf{2}}}+\gamma_{\mathbf{1}-\bar{\mathbf{1}}-\bar{\mathbf{2}}}\right) \\
& \qquad +x_{\bar{\mathbf{1}}}\left(\gamma_{\bar{\mathbf{2}}}x_{\mathbf{1}}x_{\mathbf{2}}+\gamma_{\bar{\mathbf{2}}-\mathbf{2}}x_{\mathbf{1}}+\gamma_{\bar{\mathbf{2}}-\mathbf{1}}x_{\mathbf{2}}+\gamma_{\bar{\mathbf{2}}-\mathbf{1}-\mathbf{2}}\right) \\
& \qquad +x_{\bar{\mathbf{2}}}\left(\gamma_{\bar{\mathbf{1}}}x_{\mathbf{1}}x_{\mathbf{2}}+\gamma_{\bar{\mathbf{1}}-\mathbf{2}}x_{\mathbf{1}}+\gamma_{\bar{\mathbf{1}}-\mathbf{1}}x_{\mathbf{2}}+\gamma_{\bar{\mathbf{1}}-\mathbf{1}-\mathbf{2}}\right)\Big],
\end{aligned}
\tag{A.2}
$$

$$
\begin{aligned}
& V_{----}\left(\begin{smallmatrix}\mathbf{1}\mathbf{2}\\ \bar{\mathbf{1}}\bar{\mathbf{2}}\end{smallmatrix}\right) \\
& \equiv -\frac{zJ}{4N}\delta(\mathbf{1}+\mathbf{2}-\bar{\mathbf{1}}-\bar{\mathbf{2}})u_{\mathbf{1}}u_{\mathbf{2}}u_{\bar{\mathbf{1}}}u_{\bar{\mathbf{2}}}\Big[x_{\mathbf{1}}\left(\gamma_{\mathbf{1}}+\gamma_{\mathbf{1}-\bar{\mathbf{1}}}x_{\bar{\mathbf{1}}}+\gamma_{\mathbf{1}-\bar{\mathbf{2}}}x_{\bar{\mathbf{2}}}+\gamma_{\mathbf{1}-\bar{\mathbf{1}}-\bar{\mathbf{2}}}x_{\bar{\mathbf{1}}}x_{\bar{\mathbf{2}}}\right) \\
& \qquad +x_{\mathbf{2}}\left(\gamma_{\mathbf{2}}+\gamma_{\mathbf{2}-\bar{\mathbf{1}}}x_{\bar{\mathbf{1}}}+\gamma_{\mathbf{2}-\bar{\mathbf{2}}}x_{\bar{\mathbf{2}}}+\gamma_{\mathbf{2}-\bar{\mathbf{1}}-\bar{\mathbf{2}}}x_{\bar{\mathbf{1}}}x_{\bar{\mathbf{2}}}\right) \\
& \qquad +x_{\bar{\mathbf{1}}}\left(\gamma_{\bar{\mathbf{1}}}+\gamma_{\bar{\mathbf{1}}-\mathbf{1}}x_{\mathbf{1}}+\gamma_{\bar{\mathbf{1}}-\mathbf{2}}x_{\mathbf{2}}+\gamma_{\bar{\mathbf{1}}-\mathbf{1}-\mathbf{2}}x_{\mathbf{1}}x_{\mathbf{2}}\right) \\
& \qquad +x_{\bar{\mathbf{2}}}\left(\gamma_{\bar{\mathbf{2}}}+\gamma_{\bar{\mathbf{2}}-\mathbf{1}}x_{\mathbf{1}}+\gamma_{\bar{\mathbf{2}}-\mathbf{2}}x_{\mathbf{2}}+\gamma_{\bar{\mathbf{2}}-\mathbf{1}-\mathbf{2}}x_{\mathbf{1}}x_{\mathbf{2}}\right)\Big],
\end{aligned}
\tag{A.3}
$$

$$
\begin{aligned}
V_{+--+}\left(\begin{smallmatrix}\mathbf{1}\\ \bar{\mathbf{1}}\bar{\mathbf{2}}\bar{\mathbf{3}}\end{smallmatrix}\right) &= V^{\dagger}_{+--+}\left(\begin{smallmatrix}\bar{\mathbf{1}}\bar{\mathbf{2}}\bar{\mathbf{3}}\\ \mathbf{1}\end{smallmatrix}\right) \qquad \text{(A.4)}\\
&\equiv -\frac{zJ}{4N}\delta(\mathbf{1}-\bar{\mathbf{1}}-\bar{\mathbf{2}}+\bar{\mathbf{3}})u_{\mathbf{1}}u_{\bar{\mathbf{3}}}u_{\bar{\mathbf{2}}}u_{\bar{\mathbf{1}}}\Big[x_{\mathbf{1}}\left(\gamma_{\bar{\mathbf{3}}}+\gamma_{\bar{\mathbf{3}}-\bar{\mathbf{1}}}x_{\bar{\mathbf{1}}}+\gamma_{\bar{\mathbf{3}}-\bar{\mathbf{2}}}x_{\bar{\mathbf{2}}}+\gamma_{\bar{\mathbf{3}}-\bar{\mathbf{2}}-\bar{\mathbf{1}}}x_{\bar{\mathbf{2}}}x_{\bar{\mathbf{1}}}\right)\\
&\qquad +x_{\bar{\mathbf{3}}}\left(\gamma_{\mathbf{1}}+\gamma_{\mathbf{1}-\bar{\mathbf{1}}}x_{\bar{\mathbf{1}}}+\gamma_{\mathbf{1}-\bar{\mathbf{2}}}x_{\bar{\mathbf{2}}}+\gamma_{\mathbf{1}-\bar{\mathbf{2}}-\bar{\mathbf{1}}}x_{\bar{\mathbf{2}}}x_{\bar{\mathbf{1}}}\right)\\
&\qquad +x_{\bar{\mathbf{2}}}\left(\gamma_{\bar{\mathbf{2}}}x_{\bar{\mathbf{3}}}x_{\mathbf{1}}+\gamma_{\bar{\mathbf{2}}-\mathbf{1}}x_{\bar{\mathbf{3}}}+\gamma_{\bar{\mathbf{2}}-\bar{\mathbf{3}}}x_{\mathbf{1}}+\gamma_{\bar{\mathbf{2}}-\bar{\mathbf{3}}-\mathbf{1}}\right)\\
&\qquad +x_{\bar{\mathbf{1}}}\left(\gamma_{\bar{\mathbf{1}}}x_{\bar{\mathbf{3}}}x_{\mathbf{1}}+\gamma_{\bar{\mathbf{1}}-\mathbf{1}}x_{\bar{\mathbf{3}}}+\gamma_{\bar{\mathbf{1}}-\bar{\mathbf{3}}}x_{\mathbf{1}}+\gamma_{\bar{\mathbf{1}}-\bar{\mathbf{3}}-\mathbf{1}}\right)\Big],\\
V_{+++-}\left(\begin{smallmatrix}\mathbf{1}\\ \bar{\mathbf{1}}\bar{\mathbf{2}}\bar{\mathbf{3}}\end{smallmatrix}\right) &= V^{\dagger}_{+++-}\left(\begin{smallmatrix}\bar{\mathbf{1}}\bar{\mathbf{2}}\bar{\mathbf{3}}\\ \mathbf{1}\end{smallmatrix}\right) \qquad \text{(A.5)}\\
&\equiv -\frac{zJ}{4N}\delta(\mathbf{1}-\bar{\mathbf{1}}-\bar{\mathbf{2}}+\bar{\mathbf{3}})u_{\mathbf{1}}u_{\bar{\mathbf{1}}}u_{\bar{\mathbf{2}}}u_{\bar{\mathbf{3}}}\Big[x_{\mathbf{1}}x_{\bar{\mathbf{3}}}\left(\gamma_{\bar{\mathbf{3}}}x_{\bar{\mathbf{2}}}x_{\bar{\mathbf{1}}}+\gamma_{\bar{\mathbf{3}}-\bar{\mathbf{1}}}x_{\bar{\mathbf{2}}}+\gamma_{\bar{\mathbf{3}}-\bar{\mathbf{2}}}x_{\bar{\mathbf{1}}}+\gamma_{\bar{\mathbf{3}}-\bar{\mathbf{2}}-\bar{\mathbf{1}}}\right)\\
&\qquad +\left(\gamma_{\mathbf{1}}x_{\bar{\mathbf{2}}}x_{\bar{\mathbf{1}}}+\gamma_{\mathbf{1}-\bar{\mathbf{1}}}x_{\bar{\mathbf{2}}}+\gamma_{\mathbf{1}-\bar{\mathbf{2}}}x_{\bar{\mathbf{1}}}+\gamma_{\mathbf{1}-\bar{\mathbf{2}}-\bar{\mathbf{1}}}\right)\\
&\qquad +x_{\bar{\mathbf{1}}}\left(\gamma_{\bar{\mathbf{2}}}x_{\mathbf{1}}+\gamma_{\bar{\mathbf{2}}-\mathbf{1}}+\gamma_{\bar{\mathbf{2}}-\bar{\mathbf{3}}}x_{\bar{\mathbf{3}}}x_{\mathbf{1}}+\gamma_{\bar{\mathbf{2}}-\bar{\mathbf{3}}-\mathbf{1}}x_{\bar{\mathbf{3}}}\right)\\
&\qquad +x_{\bar{\mathbf{2}}}\left(\gamma_{\bar{\mathbf{1}}}x_{\mathbf{1}}+\gamma_{\bar{\mathbf{1}}-\mathbf{1}}+\gamma_{\bar{\mathbf{1}}-\bar{\mathbf{3}}}x_{\bar{\mathbf{3}}}x_{\mathbf{1}}+\gamma_{\bar{\mathbf{1}}-\bar{\mathbf{3}}-\mathbf{1}}x_{\bar{\mathbf{3}}}\right)\Big],\\
V_{---+}\left(\begin{smallmatrix}\mathbf{1}\\ \bar{\mathbf{1}}\bar{\mathbf{2}}\bar{\mathbf{3}}\end{smallmatrix}\right) &= V^{\dagger}_{---+}\left(\begin{smallmatrix}\bar{\mathbf{1}}\bar{\mathbf{2}}\bar{\mathbf{3}}\\ \mathbf{1}\end{smallmatrix}\right) \qquad \text{(A.6)}\\
&\equiv -\frac{zJ}{4N}\delta(\mathbf{1}-\bar{\mathbf{1}}-\bar{\mathbf{2}}+\bar{\mathbf{3}})u_{\mathbf{1}}u_{\bar{\mathbf{1}}}u_{\bar{\mathbf{2}}}u_{\bar{\mathbf{3}}}\Big[x_{\mathbf{1}}x_{\bar{\mathbf{3}}}\left(\gamma_{\mathbf{1}}+\gamma_{\mathbf{1}-\bar{\mathbf{2}}}x_{\bar{\mathbf{2}}}+\gamma_{\mathbf{1}-\bar{\mathbf{1}}}x_{\bar{\mathbf{1}}}+\gamma_{\mathbf{1}-\bar{\mathbf{1}}-\bar{\mathbf{2}}}x_{\bar{\mathbf{1}}}x_{\bar{\mathbf{2}}}\right)\\
&\qquad +\left(\gamma_{\bar{\mathbf{3}}}+\gamma_{\bar{\mathbf{3}}-\bar{\mathbf{2}}}x_{\bar{\mathbf{2}}}+\gamma_{\bar{\mathbf{3}}-\bar{\mathbf{1}}}x_{\bar{\mathbf{1}}}+\gamma_{\bar{\mathbf{3}}-\bar{\mathbf{1}}-\bar{\mathbf{2}}}x_{\bar{\mathbf{1}}}x_{\bar{\mathbf{2}}}\right)\\
&\qquad +x_{\bar{\mathbf{1}}}\left(\gamma_{\bar{\mathbf{1}}}x_{\bar{\mathbf{3}}}+\gamma_{\bar{\mathbf{1}}-\bar{\mathbf{3}}}+\gamma_{\bar{\mathbf{1}}-\mathbf{1}}x_{\bar{\mathbf{3}}}x_{\mathbf{1}}+\gamma_{\bar{\mathbf{1}}-\bar{\mathbf{3}}-\mathbf{1}}x_{\mathbf{1}}\right)\\
&\qquad +x_{\bar{\mathbf{2}}}\left(\gamma_{\bar{\mathbf{2}}}x_{\bar{\mathbf{3}}}+\gamma_{\bar{\mathbf{2}}-\bar{\mathbf{3}}}+\gamma_{\bar{\mathbf{2}}-\mathbf{1}}x_{\bar{\mathbf{3}}}x_{\mathbf{1}}+\gamma_{\bar{\mathbf{2}}-\bar{\mathbf{3}}-\mathbf{1}}x_{\mathbf{1}}\right)\Big],
\end{aligned}
$$

and we introduce

$$
u_{\boldsymbol{\kappa}_\nu}\equiv\cosh\theta_{\boldsymbol{\kappa}_\nu},\qquad v_{\boldsymbol{\kappa}_\nu}\equiv-\frac{\gamma_{\boldsymbol{\kappa}_\nu}}{|\gamma_{\boldsymbol{\kappa}_\nu}|}\sinh\theta_{\boldsymbol{\kappa}_\nu},\qquad x_{\boldsymbol{\kappa}_\nu}\equiv\frac{v_{\boldsymbol{\kappa}_\nu}}{u_{\boldsymbol{\kappa}_\nu}}. \tag{A.7}
$$

$\gamma_{\boldsymbol{\kappa}_\nu}$ is real in the square lattice. The quartic LF operator $:\mathcal{R}^{(0)}:$ also becomes

$$
\begin{aligned}
:\mathcal{R}^{(0)}: = &\sum_{\mathbf{1}\mathbf{2}\bar{\mathbf{1}}\bar{\mathbf{2}}}\Big\{\widetilde{V}_{+-+-}\left(\begin{smallmatrix}\mathbf{1}\mathbf{2}\\ \bar{\mathbf{1}}\bar{\mathbf{2}}\end{smallmatrix}\right)\alpha^{+\dagger}_{\mathbf{1}}\alpha^{-\dagger}_{\mathbf{2}}\alpha^{+}_{\bar{\mathbf{1}}}\alpha^{-}_{\bar{\mathbf{2}}}+\frac{1}{2}\widetilde{V}_{++++}\left(\begin{smallmatrix}\mathbf{1}\mathbf{2}\\ \bar{\mathbf{1}}\bar{\mathbf{2}}\end{smallmatrix}\right)\alpha^{+\dagger}_{\mathbf{1}}\alpha^{+\dagger}_{\mathbf{2}}\alpha^{+}_{\bar{\mathbf{1}}}\alpha^{+}_{\bar{\mathbf{2}}}\\
&\qquad +\frac{1}{2}\widetilde{V}_{----}\left(\begin{smallmatrix}\mathbf{1}\mathbf{2}\\ \bar{\mathbf{1}}\bar{\mathbf{2}}\end{smallmatrix}\right)\alpha^{-\dagger}_{\mathbf{1}}\alpha^{-\dagger}_{\mathbf{2}}\alpha^{-}_{\bar{\mathbf{1}}}\alpha^{-}_{\bar{\mathbf{2}}}\Big\}\\
&+\sum_{\mathbf{1}\bar{\mathbf{1}}\bar{\mathbf{2}}\bar{\mathbf{3}}}\Big\{\frac{1}{2}\widetilde{V}_{+--+}\left(\begin{smallmatrix}\mathbf{1}\\ \bar{\mathbf{1}}\bar{\mathbf{2}}\bar{\mathbf{3}}\end{smallmatrix}\right)\alpha^{+\dagger}_{\mathbf{1}}\alpha^{-\dagger}_{\bar{\mathbf{1}}}\alpha^{-\dagger}_{\bar{\mathbf{2}}}\alpha^{+\dagger}_{\bar{\mathbf{3}}}+\frac{1}{2}\widetilde{V}^{\dagger}_{+--+}\left(\begin{smallmatrix}\bar{\mathbf{1}}\bar{\mathbf{2}}\bar{\mathbf{3}}\\ \mathbf{1}\end{smallmatrix}\right)\alpha^{+}_{\mathbf{1}}\alpha^{-}_{\bar{\mathbf{1}}}\alpha^{-}_{\bar{\mathbf{2}}}\alpha^{+}_{\bar{\mathbf{3}}}\\
&\qquad +\widetilde{V}_{+++-}\left(\begin{smallmatrix}\mathbf{1}\\ \bar{\mathbf{1}}\bar{\mathbf{2}}\bar{\mathbf{3}}\end{smallmatrix}\right)\alpha^{+\dagger}_{\mathbf{1}}\alpha^{+}_{\bar{\mathbf{1}}}\alpha^{+}_{\bar{\mathbf{2}}}\alpha^{-}_{\bar{\mathbf{3}}}+\widetilde{V}^{\dagger}_{+++-}\left(\begin{smallmatrix}\bar{\mathbf{1}}\bar{\mathbf{2}}\bar{\mathbf{3}}\\ \mathbf{1}\end{smallmatrix}\right)\alpha^{+\dagger}_{\bar{\mathbf{1}}}\alpha^{+\dagger}_{\bar{\mathbf{2}}}\alpha^{-\dagger}_{\bar{\mathbf{3}}}\alpha^{+}_{\mathbf{1}}\\
&\qquad +\widetilde{V}_{---+}\left(\begin{smallmatrix}\mathbf{1}\\ \bar{\mathbf{1}}\bar{\mathbf{2}}\bar{\mathbf{3}}\end{smallmatrix}\right)\alpha^{-\dagger}_{\mathbf{1}}\alpha^{-}_{\bar{\mathbf{1}}}\alpha^{-}_{\bar{\mathbf{2}}}\alpha^{+}_{\bar{\mathbf{3}}}+\widetilde{V}^{\dagger}_{---+}\left(\begin{smallmatrix}\bar{\mathbf{1}}\bar{\mathbf{2}}\bar{\mathbf{3}}\\ \mathbf{1}\end{smallmatrix}\right)\alpha^{-\dagger}_{\bar{\mathbf{1}}}\alpha^{-\dagger}_{\bar{\mathbf{2}}}\alpha^{+\dagger}_{\bar{\mathbf{3}}}\alpha^{-}_{\mathbf{1}}\Big\},
\end{aligned} \tag{A.8}
$$

where the nine vertex functions are given by Eqs. (A.1)–(A.6), provided that J and $\gamma_{\boldsymbol{\kappa}_\nu}$ are replaced by Λ and $\widetilde{\gamma}_{\boldsymbol{\kappa}_\nu}$, respectively. We define $\widetilde{V}_{\mathbf{1234}}\equiv\frac{1}{2}\widetilde{V}_{+--+}\left(\begin{smallmatrix}\mathbf{1}\\ \mathbf{432}\end{smallmatrix}\right)$ for convenience.